의 학 박 사 학 위 논 문

Development of serotonin metabolism PET imaging agents using ^{18}F-labeled tryptophan derivatives

^{18}F-표지 트립토판 유도체를 이용한 세로토닌 대사 PET 영상제 개발

2019년 7월

서울대학교 대학원
의학과 핵의학전공

김 호 영

ABSTRACT

Development of serotonin metabolism PET imaging agents using ^{18}F-labeled tryptophan derivatives

Ho Young Kim

Department of Nuclear Medicine, College of Medicine

The Graduate School

Seoul National University

Purpose:

The serotonergic system is related to various dysfunctions in the central nervous system, such as depression, social anxiety disorder, and epilepsy. Thus, the development of a radioactive probe for imaging serotonin synthesis is important for the diagnosis of such diseases. α-[^{11}C]Methyltryptophan ([^{11}C]AMT) is available for the imaging of serotonin synthesis. However, the brain uptake of [^{11}C]AMT reflects

both serotonin and kynurenine metabolism. In addition, since tryptophan is rapidly cleared from the brain, α-methylation would be needed to prolong the retention time in the brain and reduce the metabolism by monoamine oxidase (MAO). In the present study, we designed and synthesized ^{18}F- labeled [^{18}F]trifluoromethyl-L-tryptophan ([^{18}F]CF_3-L-Trp) and [^{18}F]trifluoromethyl-L-α-methyl tryptophan ([^{18}F]CF_3-L-AMT) which might be metabolized to serotonin only. To evaluate the feasibility of labeled tryptophan derivatives for imaging the serotonergic system, the distribution and metabolism were investigated in rat brain.

Methods:

Precursor of [^{18}F]CF_3-L-Trp or [^{18}F]CF_3-L-AMT was prepared by regio-selective iodination using palladium or mercury catalyst, respectively. [^{18}F]Trifluromethyl group was introduced by copper-catalyzed coupling using methyl chlorodifluoroacetate and tetramethylenediamine at 150°C for 15 min. Protecting groups were removed by 1 N HCl at 100°C for 10 min. The reaction mixture was purified by HPLC and radiochemical and enantiomeric purities were measured by HPLC. Biodistribution was performed in normal BALB/c mice at 10, 60 and 120 min post injection. For the autoradiography, [^{18}F]CF_3-L-Trp and [^{18}F]CF_3-L-AMT were injected into rats by tail vein injections without anesthesia. PET studies were performed in SD rat by intravenous administration of [^{18}F]CF_3-L-Trp. Metabolite study was performed in BALB/c mice using non-radioactive CF_3-L-Trp and brain, blood, and urine samples were analyzed by HPLC and LC/MS. To evaluate brain

distribution of [^{18}F]CF_3-L-AMT in serotonin metabolism enhanced SD rat, lithium chloride was administered to rats 2 times per day for 5 days (85 mg/kg, i.p.).

Results:

Protected L-Trp and its bromo and iodo derivatives were tested for [^{18}F]trifluoromethylation and iodo derivative showed the highest labeling efficiency. Radiochemical yield was 6±1.5% based on the isolated product and radiochemical purity was over 99%. The molar activity of [^{18}F]CF_3-L-Trp was 0.44–0.76 GBq/μmol and [^{18}F]CF_3-L-AMT was 0.94–1.44 GBq/μmol which are enough for *in vivo* application. Enantiomeric purity was measured by chiral HPLC and no racemic form was found. In the biodistribution, at 10 min, the brain uptakes of [^{18}F]CF_3-L-AMT and [^{18}F]CF_3-L-Trp were 2.27 ± 0.14%ID/g and 2.06 ± 0.22%ID/g, respectively and the brain uptake of [^{18}F]CF_3-L-AMT (0.73 ± 0.08%ID/g) at 60 min was significantly higher than that of [^{18}F]CF_3-L-Trp (0.43 ± 0.08%ID/g). This result indicated that α-methylation increased the retention in the brain by reducing metabolism by MAO. The bone uptake of [^{18}F]CF_3-L-AMT at 60 min (4.50 ± 0.47%ID/g) was significantly lower than that of [^{18}F]CF_3-L-Trp (9.34 ± 0.62%ID/g), suggesting the lower *in vivo* defluorination of [^{18}F]CF_3-L-AMT. Both of the tracers showed high uptakes in the kidney. In PET and autoradiography measurements, the uptake of raphe nucleus (dorsal and medial) was comparatively very low. Instead, pineal gland, thalamus, hypothalamus and midbrain showed particularly high uptake. [^{18}F]CF_3-L-Trp penetrated the blood-brain barrier via the L-type amino acid transporter, while

[^{18}F]CF_3-D-Trp did not. In the metabolism study, CF_3-serotonin peak was found in brain and blood at 60 min, and the mass value of the CF_3-serotonin peak was confirmed by LC-MS. The distribution pattern of [^{18}F]CF_3-L-AMT in Li-treated SD rat brains was similar to that detected in normal SD rat brains. However, the brain uptake rate of [^{18}F]CF_3-L-AMT in Li-treated SD rats was faster than normal SD rats and the brain uptake in Li-treated SD rats lasted longer than that in normal SD rats.

Conclusion:

[^{18}F]CF_3-L-Trp could be successfully synthesized by [^{18}F]trifluoromethylation, but fast washout from the brain and high *in vivo* defluorination showed that [^{18}F]CF_3-L-Trp was not suitable for imaging the serotonergic system. α-Methylation of tryptophan increased the retention in the brain by reducing metabolism and might decrease the *in vivo* defluorination. However, it is not clear that the PET imaging of [^{18}F]CF_3-L-Trp reflect serotonin metabolism due to the low uptake in raphe nucleus. A large unmetabolized form in the brain also makes it difficult to obtain the absolute serotonin synthesis rate. Nevertheless, experimental data suggest that the distribution patterns of [^{18}F]CF_3-L-AMT in normal and Li-treated SD rats were related with serotonergic activity and metabolism. Therefore, [^{18}F]CF_3-L-AMT could be used as an feasible imaging agent representing serotonergic system.

Key Words: [^{18}F]trifluoromethylation; CF_3-L-Trp; Serotonin; 5-HT; Tryptophan; amino acid; monoamine oxidase; α-methyltryptophan

Student number: 2011-31118

Contents

List of SCHEMES, FIGURES and TABLES

List of Abbreviations

Full name	Abbreviation
5-hydroxytryptamine	5-HT
central nervous system	CNS
Social anxiety disease	SAD
Alzheimer's disease	AD
tryptophan	Trp
5-hydroxytryptophan	5-HTP
aromatic amino acid decarboxylase	AAAD
Nicotinamide adenine dinucleotide	NAD
α-methyl- L-tryptophan	AMT
indole 2,3,-dioxygenase	IDO
tryptophan 2,3-dioxygenase	TDO

serotonin transporter	**SERT**
***tert*-butoxycarbonyl**	**Boc**
trifluoroacetic acid	**TFA**
N-bromosuccinimide	**NBS**
high performance liquid chromatography	**HPLC**
radiochemical yield	**RCY**
radiochemical conversion	**RCC**
instant thin-layer chromatography	**ITLC**
thin-layer chromatography	**TLC**
methyl chlorodifluoroacetate	**MCDFA**
tetramethylethylenediamine	**TMEDA**
tetrabutylammonium bicarbonate	**TBAB**

2-amno-2-norbornanecarboxylic acid	**BCH**
Blood-brain barrier	**BBB**
L-type amino acid transporter	**LAT**
positron emission tomography	**PET**
magnetic resonance imaging	**MR**
5-hydroxyindoleacetic acid	**5-HIAA**
Sprague-Dawley	**SD**
dimethylformamide	**DMF**
diethylenetriaminepentaacetic acid	**DTPA**
ethylenediaminetetraacetic acid	**EDTA**

1 INTRODUCTION

Serotonin (5-hydroxytryptamine (5-HT)) is a major neurotransmitter in the serotonergic system, and contains an indole ring in its structure. The serotonergic system of the central nervous system (CNS) originates from the raphe nuclei and projects throughout the whole brain. This widespread system controls a variety of psychological functions. Studies have investigated whether altered levels of serotonin synthesis could be used as diagnostic tools for depression,[1] social anxiety disorder (SAD),[2] epilepsy,[3] attention deficit hyperactivity disorder (ADHD),[4] Alzheimer's disease (AD),[5] or brain cancers[6-8] and found that the increased or decreased synthesis of serotonin is associated with those diseases.

Serotonin is synthesized from the essential amino acid L-tryptophan (Trp) by serotonin neurons, mainly in synaptic endings. As the cell bodies of serotonin neurons are located in the raphe nuclei and protect into the almost every region of the brain[9]. The biosynthetic precursor of serotonin is Trp, which is metabolized to serotonin by a two-step enzymatic process (Figure 1): 5-hydroxylation of L-Trp and decarboxylation of 5-hydroxytryptophan (5-HTP). The first 5-hydroxylation step is the rate-limiting step,[10] and the enzyme for this process is located only in the serotonergic neurons.[11] The second decarboxylation step by aromatic amino acid decarboxylase (AAAD) is fast and less specific.[12]

Alternatively, L-Trp can also be metabolized by Trp dioxygenase at the 2- and 3-positions of the indole ring and enter the kynurenine pathway (Figure 1), which is a

biosynthetic pathway for nicotinamide adenine dinucleotide (NAD) and is highly activated in inflammatory conditions.[13]

Tryptophan derivatives labeled with positron emitters have been developed for the imaging of serotonin synthesis in the brain. Among them, α-[^{11}C]methyl- L-tryptophan ([^{11}C]AMT) is the most widely studied PET agent.[14-16] Autoradiograms in rats demonstrated that [^{11}C]AMT is highly accumulated in dorsal raphe nuclei in which serotonergic cell bodies are located[14]. The metabolism of AMT into α-methyl-serotonin was also confirmed by HPLC[17]. [^{3}H]AMT was located to serotonergic neurons in raphe nucleus and confirmed by tryptophan hydroxylase immunocytochemistry simultaneously at the electron microscopic level[18]. Despite of these studies, there are still disadvantages of the presence of a large unmetabolized pool and entering the kynurenine pathway as well (Figure 2).[7,19] Especially, [^{11}C]AMT can be metabolized via both serotonin and kynurenine pathway by the action of serotonin hydroxylase and indole 2,3-dioxygenase (IDO), respectively. Serotonin pathway is major in normal condition, and kynurenine pathway is major in certain pathologic condition, such as ischemic brain injury or immune activation by the increased activity of IDO[20,21]. So the uptake of [^{11}C]AMT may not accurately represent serotonin synthesis especially in an inflammation condition. Furthermore, short half-life of ^{11}C (20 min) restricts its use to facilities equipped with a cyclotron and automatic synthesis module. 5-Hydroxy-[β-^{11}C]- L-tryptophan ([^{11}C]HTP) was also used for measuring of serotonin synthesis rate. Although it was metabolized in

the exact same way as endogenous 5-HTP, it was metabolized not only to [^{11}C]5-HT but also to [^{11}C]HIAA and rapidly excreted from the brain in rodent[22].

Recently, 4-, 5-, 6-, and 7-[^{18}F]fluorotryptophan derivatives have been tested for imaging serotonin synthesis *in vivo*.[23] Among them, 4-, 5-, and 6-[^{18}F]fluorotryptophan are metabolized by IDO or tryptophan 2,3-dioxygenase (TDO) and show rapid defluorination and high bone uptake.[24,25] Only 7-[^{18}F]fluorotryptophan exhibited slow defluorination and high uptake in the melatonin-producing pineal gland and serotonergic areas of the rat brain.[23] However, the possibility of these compounds entering the kynurenine pathway still remains, because the 2-position of their indole rings is not protected from dioxygenation.

To develop a novel ^{18}F-labeled Trp derivative that reflects only the serotonin pathway and not the kynurenine pathway, we first attempted to synthesize 2-[^{18}F]fluorotryptophan, which might be resistant to indole dioxygenase. Since indole dioxygenase oxidizes the 2- and 3-positions of the indole ring, we expected that substituting a fluorine atom at the 2-position might protect it from oxidation due to its electron-withdrawing effect. Even if [^{18}F]fluorine was able to be labeled at 5-position, there was still a possibility that 5-[^{18}F]fluorotryptophan could be metabolized to kynurenine analog. Moreover, since tryptophan hydroxylase which exists in serotonin neuron specifically acts on position-5, [^{18}F]fluorine prevent the enzymatic process of 5-hydroxylation.

2-Halotryptophan derivatives can be synthesized by electrophilic substitution, and we supposed that 2-fluorotryptophan could also be synthesized.[26,27] However, its

synthesis by the introduction of [^{18}F]fluoride at the 2-position of the indole ring via nucleophilic substitution was not successful due to the electron-rich ene-amine structure (Figure 3A). We succeeded in synthesizing a 2-fluorotryptophan derivative protected with Boc and a methyl group at the amino and carboxyl groups, respectively, using a tributyltin-functionalized precursor purged with 0.1% F_2 gas in Ne by electrophilic substitution. However, when we attempted to label tributyltin-functionalized precursor with ^{18}F, the indole ring moiety was easily degraded in acid, and we failed to obtain the 2-[^{18}F]fluorotryptophan derivative (Figure 3B). 2-Chlorotryptophan has been reported to be less stable than 2-bromotryptophan to acid treatment, which is an essential step in ^{18}F-labeling.[28] Thus, 2-[^{18}F]fluorotryptophan was supposed to be even less stable and more susceptible to acid than 2-chlorotryptophan, and thus could not be obtained. Another attempt to prepare 2-trimethylammoniumtryptophan protected with trifluoroacetyl residue as a precursor for 2-[^{18}F]fluorotryptophan was unsuccessful, as the intermediate 2-aminotryptophan was unstable and rapidly oxidized in air (Figure 3C).[29]

We then tried to synthesize [^{18}F]trifluoromethyltryptophan ([^{18}F]CF_3- L-Trp), which might be stable in acidic condition for hydrolysis. Previous reports indicated that [^{18}F]CF_3 could be introduced into electron-rich arenes or heteroarenes functionalized with halogen atoms via a copper(I)-mediated cross-coupling reaction (Figure 4).[30,31] We treated the 2-chloro, 2-bromo, 2-iodo, and 2-trifluorotryptophan derivatives with a TFA solution, and found that only the 2-trifluoromethyl tryptophan derivative was stable in acid. The 2-chloro and 2-bromotryptophan derivatives

rapidly decomposed, and the 2-iodotryptophan derivative was rapidly deiodinated into L-Trp.

However, there was still challenge for measuring *in vivo* serotonin synthesis using radiolabeled tryptophan derivative. As serotonin is rapidly metabolized into 5-hydroxyindoleacetic acid (HIAA) by monoamine oxidase (MAO) and released from the brain, the brain radioactivity cannot reflect the ongoing synthesis of serotonin. Although pharmacological treatment was tried to inhibit MAO or AADC and to accumulate endogenous serotonin, the effect of the drugs distorted the data making interpretation of data and quantitative conclusions more difficult. To enhance the metabolic characteristic, α-methyl group was introduced into tryptophan. α-Substituted tryptophan derivatives may be resistant to monoamine oxidase (MAO) and accumulated in the tissue (probably in the neurons)[32] because α-substitution dramatically increase the resistance to hydrolysis[33,34]. Hence, α-substituted tryptophan derivatives don't require the intervention of a serotonin metabolism inhibitor like NSD-1095 to increase nerve cell retention[35].

In the present study, we tried to develop [^{18}F]CF_3-L-Trp for serotonin metabolism PET imaging. Protected L-Trp and its bromo and iodo derivatives at the 2-position of Trp were tested for [^{18}F]trifluoro methylation as precursors. The serum stability and protein binding of [^{18}F]CF_3- L-Trp were examined *in vitro*. To evaluate the feasibility of [^{18}F]CF_3-L-Trp for imaging serotonin metabolism, a biodistribution, autoradiography, PET, and metabolism studies were performed in rodents. [^{18}F]Trifluoromethyl-L-α-methyltryptophan ([^{18}F]CF_3-L-AMT) was also developed

to prolong the brain retention and reduce the metabolism. Even if the α-methyl modification on tryptophan may affect the transport into the brain through the blood-brain barrier (BBB) or serotonin neurons, it can exhibit better metabolic properties than tryptophan.

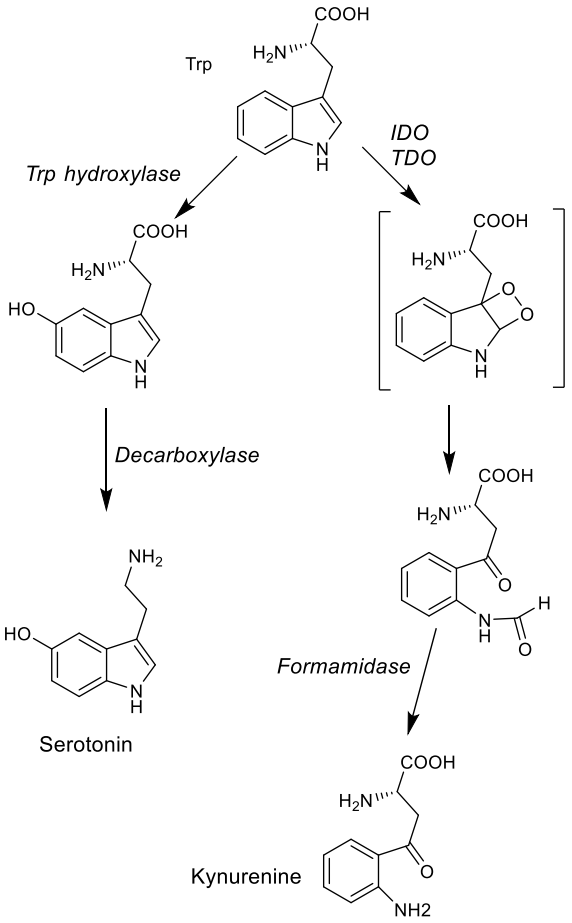

FIGURE 1. Metabolism of Trp. Trp is metabolized to serotonin by 5-hydroxylation and subsequent decarboxylation (left). However, it also is metabolized to kynurenine after 2,3-dioxygenation by IDO or TDO (right). A Trp derivative having substituent at the 5-position may proceed to the kynurenine pathway, while one substituted at the 2-position may proceed to the serotonin pathway.

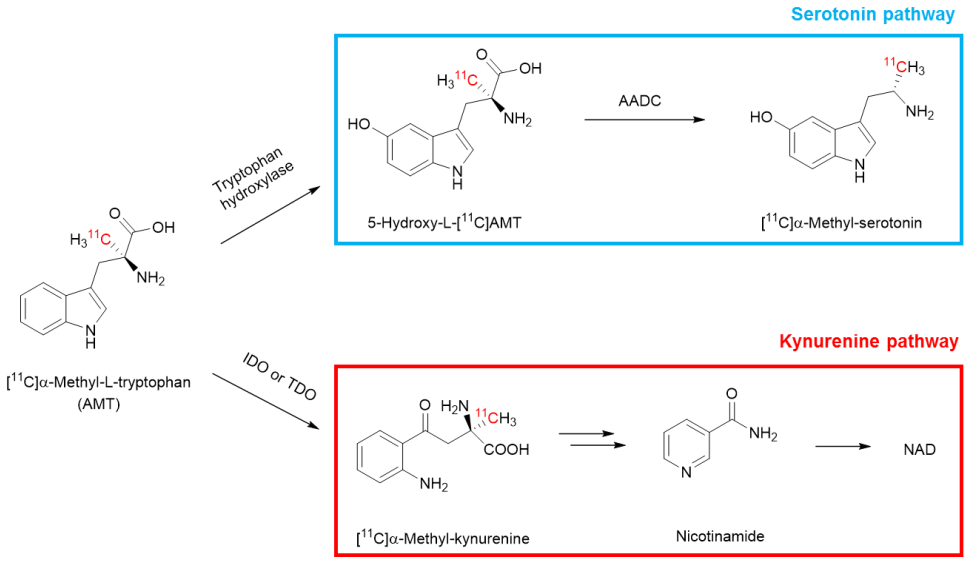

FIGURE 2. Limitation of AMT for imaging of serotonin metabolism. IDO, indole 2,3-dioxygenase; TDO, tryptophan 2,3-dioxygenase; NAD, nicotinamide adenine dinucleotide.

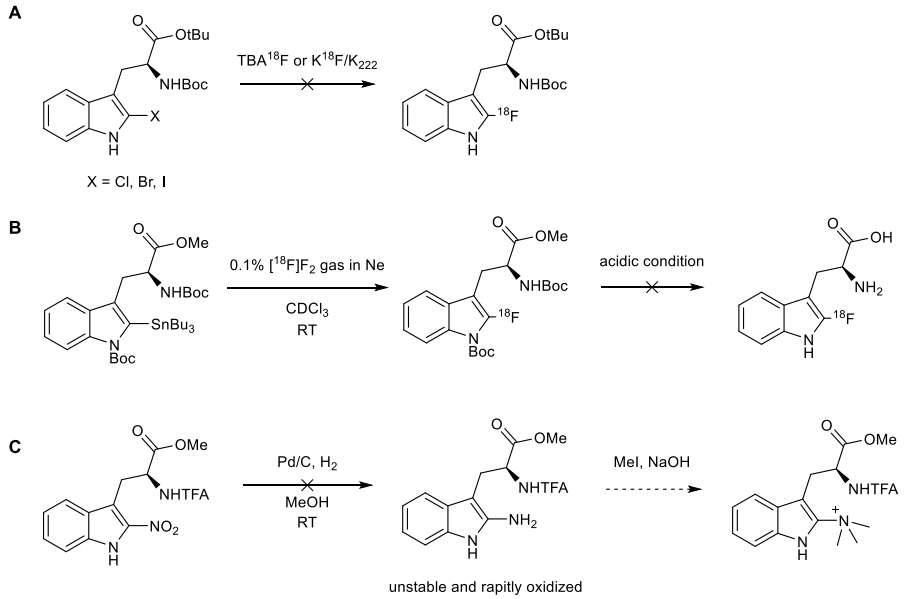

FIGURE 3. Trials for the labeling the 2-position of tryptophan with [^{18}F]fluorine. [^{18}F]Fluorination was attempted by (A) nucleophilic substitution using 2-halotryptophan, (B) electrophilic substitution using 2-tributyltintryptophan, and (C) introduction of trimethylammonium after the synthesis of 2-aminotryptophan, which could be used as a precursor for [^{18}F]fluorine labeling.

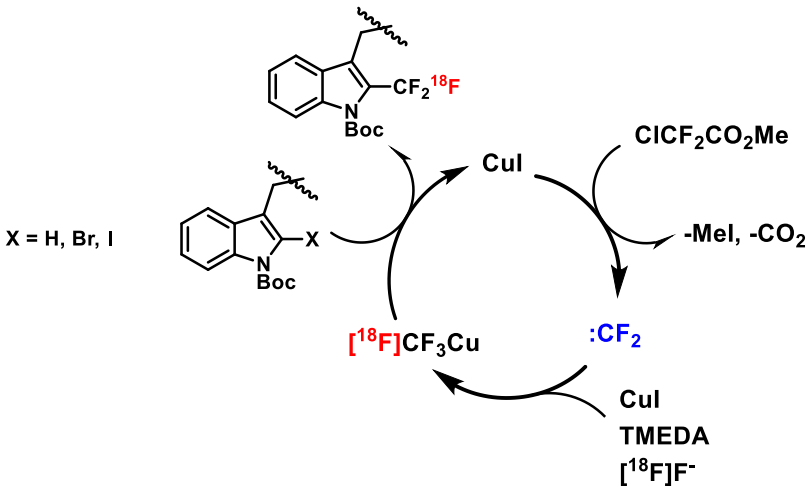

FIGURE 4. Proposed mechanism of [^{18}F]trifluoromethylation. [^{18}F]CF_3 can be introduced into tryptophan via copper(I)-mediated cross coupled [^{18}F]trifluoromethylation at 2-position of indole ring.

2 MATERIALS AND METHODS

2.1 General

L-Trp methyl ester hydrochloride was purchased from TCI (Tokyo, Japan) and used without further purification. 2-Bromo-L-Trp methyl ester[26] and 2-iodo-L-Trp methyl ester[27] were prepared according to previously published procedures. AMT racemic mixture was purchased from Chemi-Impex International (IL, USA). The other reagents and solvents were purchased from Acros organics (Thermo Fisher Scientific, MA, U.S.A.), TCI (Tokyo, Japan) or Sigma-Aldrich (MO, U.S.A.) and were used as received. All non-aqueous reactions were performed under an inert atmosphere of dry argon or N_2 gas. Reactions were monitored by thin layer chromatography (TLC) using Merck Kieselgel 60 F_{254} plates or high performance liquid chromatography (HPLC) (Gilson Inc., WI, U.S.A.). The spots were detected under UV light (254 nm) and developed using ninhydrin or anisaldehyde. Flash column chromatography was carried out on silica gel 60 (230-400 mesh), and all chromatographic solvents were of HPLC grade. ^{1}H and ^{13}C nuclear magnetic resonance (NMR) spectra were obtained using a 300-MHz Al-300 FTNMR spectrometer (JEOL Ltd., Tokyo, Japan) and ^{19}F NMR spectra were obtained using 600 MHz High Resolution NMR spectrometer (AVANCE 600, Bruker, Germany). Chemical shifts (δ) were recorded in parts per million (ppm) relative to tetramethylsilane (TMS) using the deuterated solvent as an internal reference, and coupling constants (J) were reported in unit of hertz (Hz). The following

abbreviations are used to describe multiplicities: s (singlet), d (doublet), t (triplet), q (quartet), and m (multiplet). Mass spectra (*m/z*) were recorded on a LTQ velos spectrometer (Thermo Fisher Scientific, MA, U.S.A.) or a Waters 3100 liquid chromatography-mass spectroscopy (LC-MS) (Waters Corporation, MA, U.S.A.) using positive electrospray ionization (ESI^+). High resolution mass spectra (HRMS, *m/z*) were acquired on a LTQ-Orbitrap Velos ion trap spectrometer (Thermo Scientific, France)

[^{18}F]Fluoride was produced via the $^{18}O(p,n)^{18}F$ reaction with ^{18}O-enriched (98%) water using a 16.5-MeV proton beam generated by a PETtrace 10 cyclotron (GE Healthcare, Uppsala, Sweden). Automated radiosyntheses for animal studies were performed in a TRACERLab Fx-F_N module (GE Medical Systems, Germany) equipped with preparative HPLC with a Geiger-Mueller detector. The radiochemical purity, specific activity, and chiral purity were measured using analytical HPLC connected to a Gabi Star flow-through gamma radioactivity detector (Raytest GmbH, Germany). The dose calibrator (Atomlab 100; Biodex Medical Systems, Inc., New York, NY, U.S.A.) was used for measuring the level of radioactivity. *In vivo* metabolites of unlabeled CF_3-L-Trp were analyzed using HPLC and mass spectrometry (MS). All animal studies were carried out with the approval of Institutional Animal Care and Use Committee of Clinical Research Institute, Seoul National University Hospital. This facility was accredited by the Association for the Assessment and Accreditation of Laboratory Animal Care International. In addition,

National Research Council guidelines for the care and use of laboratory animals (revised in 1996) were observed throughout.

2.2 [^{18}F]Trifluoromethyl- L-tryptophan ([^{18}F]CF_3- L-Trp)

2.2.1 Chemistry

2.2.1.1 Synthesis of the protected L-Trp derivatives as precursor

2.2.1.1.1 (tert-Butoxycarbonyl)-L-tryptophan (1)

Di-*tert*-butyl dicarbonate (4.3 mL, 18.9 mmol) and triethylamine (2.6 mL, 18.9 mmol) were added to a solution of L-Trp (2.6 g, 12.6 mmol) in MeOH (63 mL) successively using syringes, and the mixture was stirred at room temperature under an argon atmosphere overnight. The solvent was removed under reduced pressure using a rotary evaporator at 30-35°C. The colorless oily residue was dissolved in EtOAc and washed with water and brine. The reaction mixture was dried over anhydrous magnesium sulfate, filtered, and concentrated *in vacuo*. The crude product (3.8 g, 100% yield) was obtained as a colorless oil and used for the next step of the synthesis without further purification. (^{1}H NMR, 300 MHz, Acetone-d): δ = 10.04 (s, N*H*), 7.59 (d, *J* = 6 Hz, 1H), 7.34 (d, *J* = 6 Hz, 1H), 7.18 (s, 1H), 7.09-6.96 (m, 2H), 5.91 (d, *J* = 6 Hz, N*H*), 4.49 (q, J = 6 Hz, 1H), 3.36-3.13 (m, 2H), 1.33 (s, 9H); (^{13}C

NMR, 75 MHz, Acetone-d): δ = 206.43, 174.05, 156.22, 137.47, 128.65, 124.31, 122.11, 119.54, 119.23, 112.13, 111.05, 79.20, 55.14, 28.47, 28.17. ESI-MS *m/z* calculated for $C_{16}H_{21}N_2O_4^+$ $[M+H]^+$ 305.15; found 305.35.

2.2.1.1.2 tert-Butyl (tert-butoxycarbonyl)-L-tryptophan (2)

Benzyltriethylammonium chloride (2.8 g, 12.2 mmol) and anhydrous potassium carbonate (8.4 g, 60.8 mmol) were added to crude **1** (3.7 g, 12.2 mmol) in $AcNMe_2$ (15 mL), and then 2-bromo-2-methylpropane (14 mL, 122 mmol) was added slowly with vigorous stirring at room temperature. The mixture was reacted at 55 °C with stirring for 2.5 h and checked by TLC (EtOAc/hexane = 1:4, R_f = 0.3). The reaction mixture was quenched by adding chilled water. The precipitate was extracted with EtOAc and the organic layer was washed with water two times and with brine one time. The organic layer was then dried over anhydrous sodium sulfate, filtered, and concentrated *in vacuo*. The crude product was purified by flash column chromatography on silica gel (EtOAc/hexane = 1:7) to afford **2** (2.1 g, 49% yield) as a white waxy solid. (^{1}H NMR, 300 MHz, Acetone-d): δ = 10.04 (s, N*H*), 7.57 (d, *J* = 9 Hz, 1H), 7.34 (d, *J* = 6 Hz, 1H), 7.17-6.97 (m, 2H), 5.90 (d, *J* = 9 Hz, N*H*), 4.34 (q, *J* = 6 Hz, 1H), 3.25-3.06 (m, 2H), 1.34 (s, 18H); (^{13}C NMR, 75 MHz, Acetone-d): δ = 206.22, 172.25, 156.11, 137.46, 128.63, 124.26, 122.09, 119.46, 119.30, 112.10, 111.10, 81.28, 79.05, 56.04, 54.96, 28.47, 28.02. ESI-MS *m/z* calculated for $C_{25}H_{36}N_2O_6^+$ $[M+H]^+$ 361.21; found 361.41.

2.2.1.1.3 tert-Butyl (S)-3-(3-((tert-butoxy)-2-((tert-butoxycarbonyl)amino)-3-oxopropyl)-1H-indol-1-carboxylate (3)

To a solution of **2** (100 mg, 0.28 mmol) in Me_2Cl_2 (2.8 mL), di-*tert*-butyl dicarbonate (0.06 mL, 0.28 mmol) and 4-dimethylaminopyridine (3.4 mg, 0.03 mmol) were added at room temperature. The reaction mixture was stirred for 10 min and the completion of the reaction was checked by TLC (EtOAc/hexane = 1:7, R_f = 0.3). The solvent was removed under reduced pressure and the residue was dissolved in EtOAc. The organic layer was washed with 1 N HCl and water twice each, dried over anhydrous magnesium sulfate, filtered, and concentrated *in vacuo*. The crude product was purified by flash column chromatography on silica gel (EtOAc/hexane = 1:10) to afford **3** (128 mg, 99% yield) as a white waxy solid. (^{1}H NMR, 300 MHz, Acetone-d): δ = 8.01 (d, *J* = 9 Hz, 1H), 7.50 (d, *J* = 9 Hz, 1H), 7.40 (s, 1H), 7.21-7.09 (m, 2H), 5.94 (d, *J* = 9 Hz, N*H*), 4.28 (q, *J* = 6 Hz, 1H), 3.13-2.94 (m, 2H), 1.52 (s, 9H), 1.29 (s, 9H), 1.25 (s, 9H); (^{13}C NMR, 75 MHz, Acetone-d): δ = 206.11, 171.75, 156.07, 150.11, 136.20, 131.47, 125.05, 124.81, 123.23, 119.90, 117.13, 115.79, 84.02, 81.71, 79.17, 55.22, 28.46, 28.16, 28.03. ESI-MS *m/z* calculated for $C_{25}H_{37}N_2O_6^+$ $[M+H]^+$ 461.26; found 461.51 HRMS (ESI) for $C_{25}H_{36}N_2NaO_6^+$ $[M+Na]^+$ requires 483.2466; found 483.2461

2.2.1.2 Synthesis of bromo L-Trp derivatives as precursor

2.2.1.2.1 Methyl (S)-3-(2-bromo-1H-indole-3-yl)-2-((tert-butoxycarbonyl)amino)propanoate (5)

To a solution of 2-bromo L-tryptophan methyl ester **4** (3.6 g, 9.4 mmol) in MeOH (50 mL), di-*tert*-butyl dicarbonate (5.4 mL, 23.6 mmol) and triethylamine (4.3 mL, 30.6) were added slowly at room temperature. The solution was stirred at room temperature under an argon atmosphere overnight. The solvent was removed under reduced pressure, and the residue was dissolved in EtOAc. The organic layer was washed with water and brine, dried over anhydrous sodium sulfate, filtered, and concentrated *in vacuo*. The crude product was purified by flash column chromatography on silica gel (EtOAc/hexane = 1 : 4) to afford **5** (3.4 g, 46% yield, 2 steps) as a white solid. (^{1}H NMR, 300 MHz, Acetone-d): δ = 10.69 (s, N*H*), 7.56 (d, *J* = 6 Hz, 1H), 7.33 (d, *J* = 6 Hz, 1H), 7.14-7.03 (m, 2H), 6.05 (d, *J* = 6 Hz, N*H*), 4.46 (q, *J* = 9 Hz, 1H), 3.14 (s, 3H), 3.28-3.12 (m, 2H), 1.34 (s, 9H); (^{13}C NMR, 75 MHz, Acetone-d): δ = 206.27, 172.97, 155.89, 137.36, 128.71, 122.69, 120.42, 118.83, 111.51, 79.35, 54.83, 28.34. ESI-MS *m/z* calculated for $C_{17}H_{22}BrN_2O_4^+$ $[M+H]^+$ 397.08; found 397.33.

2.2.1.2.2 tert-Butyl (S)-2-bromo-3-(2-((tert-butoxycarbonyl)amino)-3-methoxy-3-oxopro pyl)-1H-indol-1-carboxylate (6)

To a solution of **5** (3.4 g, 8.7 mmol) in Me_2Cl_2 (30 mL), di-*tert*-butyl dicarbonate (2 mL, 8.7 mmol) and 4-dimethylaminopyridine (106 mg, 0.87 mmol) were added at

room temperature. The solution was stirred for 10 min and the completion of the reaction was checked by TLC (EtOAc/hexane = 1:7, R_f = 0.3). The solvent was removed under reduced pressure and the residue was dissolved in EtOAc. The organic layer was washed with 1 N HCl and water twice each, dried over anhydrous sodium sulfate, filtered, and concentrated *in vacuo*. The crude product was purified by flash column chromatography on silica gel (EtOAc/hexane = 1:10) to afford **6** (4 g, 92% yield) as a white waxy solid. (^{1}H NMR, 300 MHz, Acetone-d): δ = 8.03 (d, *J* = 9 Hz, 1H), 7.58 (d, *J* = 6 Hz, 1H), 7.30-7.18 (m, 2H), 6.20 (d, *J* = 9 Hz, N*H*), 4.45 (q, *J* = 9 Hz, 1H), 3.59 (s, 3H), 3.27-3.12 (m, 2H), 1.66 (s, 9H), 1.28 (s, 9H); (^{13}C NMR, 75 MHz, Acetone-d): δ = 206.12, 172.62, 164.28, 155.86, 149.49, 137.17, 129.77, 125.27, 123.66, 119.66, 119.23, 115.78, 110.82, 85.60, 79.32, 53.99, 52.41, 28.36, 28.17. ESI-MS *m/z* calculated for $C_{22}H_{30}BrN_2O_6^+$ $[M+H]^+$ 497.1; found 497.3.

2.2.1.2.3 (S)-3-(2-Bromo-1-(tert-butoxycarbonyl)-1H-indol-3-yl)-2-((tert-butoxycarbonyl) amino)propanoic acid (7)

6 (1 g, 2 mmol) was dissolved in a mixture of tetrahydrofuran (THF)/MeOH/water (21 mL, 1:1:1) and the solution was cooled to 0 °C in an ice bath. To the solution, lithium hydroxide monohydrate (337 mg, 8 mmol) was added slowly, and the reaction mixture was warmed to room temperature. The reaction mixture was stirred for 20 min, and the completion of the reaction was checked by TLC (Me_2Cl_2/MeOH = 10:1, R_f = 0.1). The solvent was removed under reduced pressure until a precipitate began to form, and the residue was dissolved in EtOAc. The organic

layer was washed with 1 N HCl and water twice each, dried over anhydrous sodium sulfate, filtered, and concentrated *in vacuo*. **7** (860 mg, 89%) was obtained as a white waxy solid. ESI-MS *m/z* calculated for $C_{21}H_{28}BrN_2O_6^+$ $[M+H]^+$ 483.11; found 483.25.

2.2.1.2.4 tert-Butyl (S)-2-bromo-3-(3-(tert-butoxy)-2-((tert-butoxycarbonyl)amino)-3-oxopropyl)-1H-indol-1-carboxylate (8)

Benzyltriethylammonium chloride (0.3 g, 1.3 mmol) and anhydrous potassium carbonate (1 g, 7.5 mmol) were added to crude **7** (620 mg, 1.3 mmol) in $AcNMe_2$ (4.3 mL), and then 2-methyl-2-bromopropane (1.5 mL, 13 mmol) was added slowly with vigorous stirring at room temperature. The mixture was heated at 55 °C for 2.5 h, and the reaction was checked by TLC (EtOAc/hexane = 1:7, R_f = 0.4). When the reaction was completed, the reaction mixture was quenched by adding chilled water. The precipitate was extracted with EtOAc, and the organic layer was washed with water and brine. The organic layer was dried over anhydrous sodium sulfate, filtered, and concentrated *in vacuo*. The crude product was purified by flash column chromatography on silica gel (EtOAc/hexane = 1:10) to afford **8** (300 mg, 43% yield) as a white waxy solid. (^{1}H NMR, 300 MHz, Acetone-d): δ = 8.04 (d, *J* = 6 Hz, 1H), 7.64 (d, *J* = 6 Hz, 1H), 7.31-7.19 (m, 2H), 6.12 (d, *J* = 6 Hz, N*H*), 4.36 (q, *J* = 9 Hz, 1H), 3.23-3.08 (m, 2H), 1.66 (s, 9H), 1.31 (s, 9H), 1.29 (s, 9H); (^{13}C NMR, 75 MHz, Acetone-d): δ = 206.14, 171.40, 156.00, 149.61, 137.32, 129.92, 125.25, 123.69, 120.24, 119.55, 115.76, 85.61, 81.54, 79.19, 54.71, 28.43, 28.21, 27.97. ESI-MS *m/z*

calculated for $C_{25}H_{36}BrN_2O_6^+$ $[M+H]^+$ 539.18; found 539.25. HRMS (ESI) for $C_{25}H_{35}BrN_2NaO_6^+$ $[M+Na]^+$ requires 561.1571; found 561.1566.

2.2.1.3 Synthesis of iodo L-Trp derivatives as precursor

2.2.1.3.1 Methyl (S)-2-((tert-butoxycarbonylamino)-3-(2-iodo-1H-indole-3-yl)propanoate (12)

To a solution of 2-iodo L-tryptophan methyl ester **11** (3 g, 8.9 mmol) in MeOH (88 mL) at room temperature, di-*tert*-butyl dicarbonate (2 mL, 8.9 mmol) and triethylamine (1.2 mL, 8.9) were added slowly. The solution was stirred at room temperature under an argon atmosphere overnight. The solvent was removed under reduced pressure, and the colorless residue was dissolved in EtOAc. The organic layer was washed with 1 N HCl and water twice each, dried over anhydrous sodium sulfate, filtered, and concentrated *in vacuo*. The crude product was purified by flash column chromatography on silica gel (EtOAc/hexane = 1:4) to afford **12** (2.6 g, 66% yield) as a white solid. (^{1}H NMR, 300 MHz, Acetonitrile-d): δ = 10.51 (s, N*H*), 7.56 (d, *J* = 9 Hz, 1H), 7.32 (d, *J* = 9 Hz, 1H), 7.07-6.97 (m, 2H), 6.05 (d, *J* = 9 Hz, N*H*), 4.48 (q, *J* = 9 Hz, 1H), 3.56 (s, 3H), 3.25-3.11 (m, 2H), 1.33 (s, 9H); (^{13}C NMR, 75 MHz, Acetonitrile-d): δ = 206.54, 173.15, 156.00, 140.13, 128.67, 122.67, 120.25, 118.67, 111.56, 79.56, 55.16, 28.65. ESI-MS *m/z* calculated for $C_{17}H_{22}IN_2O_4^+$ $[M+H]^+$ 445.06; found 445.17.

2.2.1.3.2 tert-Butyl (S)-3-(2-((tert-butoxycarbonyl)amino)-3-methoxy-3-oxopropyl)-2-iodo-1H-indol-1-carboxylate (13)

To a solution of **12** (2.6 g, 5.9 mmol) in Me_2Cl_2 (60 mL), di-*tert*-butyl dicarbonate (1.4 mL, 5.9 mmol) and 4-dimethylaminopyridine (71 mg, 0.59 mmol) were added at room temperature. The solution was stirred for 10 min, and the completion of the reaction was checked by TLC (EtOAc/hexane = 1:7, R_f = 0.3). The solvent was removed under reduced pressure and the residue was dissolved in EtOAc. The organic layer was washed with 1 N HCl and water twice each, dried over anhydrous sodium sulfate, filtered, and concentrated *in vacuo*. The crude product was purified by flash column chromatography on silica gel (EtOAc/hexane = 1:10) to afford **13** (3.1 g, 97% yield) as a white waxy solid. (^{1}H NMR, 300 MHz, Acetonitrile-d): δ = 8.02 (d, *J* = 9 Hz, 1H), 7.51 (d, *J* = 9 Hz, 1H), 7.26-7.16 (m, 2H), 5.60 (d, *J* = 9 Hz, N*H*), 4.43 (q, *J* = 9 Hz, 1H), 3.62 (s, 3H), 3.22-3.04 (m, 2H), 1.67 (s, 9H), 1.28 (s, 9H); (^{13}C NMR, 75 MHz, Acetonitrile-d): δ = 206.52, 183.70, 172.38, 164.28, 159.53, 158.92, 157.21, 152.88, 151.77, 149.90, 119.79, 86.50, 62.04. ESI-MS *m/z* calculated for $C_{22}H_{30}IN_2O_6^+$ $[M+H]^+$ 545.11; found 545.17.

2.2.1.3.3 (S)-3-(1-(tert-butoxycarbonyl)-2-iodo-1H-indol-3-yl)-2-((tert-butoxycarbonyl) amino)propanoic acid (14)

13 (3.1 g, 5.7 mmol) was dissolved in a mixture of THF/MeOH/water (30 mL, 1:1:1) and the solution was cooled to 0 °C in an ice bath. To the solution, lithium hydroxide monohydrate (1.6 g, 38.1 mmol) was added slowly and the reaction

mixture was warmed to room temperature. The reaction mixture was stirred for 20 min and the completion of the reaction was checked by TLC (Me_2Cl_2/MeOH = 10:1, R_f = 0.1). The solvent was removed under reduced pressure until a precipitate began to form, and the residue was dissolved in EtOAc. The organic layer was washed with 1 N HCl and water twice each, dried over anhydrous sodium sulfate, filtered, and concentrated *in vacuo*. **14** (3 g, 99%) was obtained as a white waxy solid. ESI-MS *m/z* calculated for $C_{21}H_{28}IN_2O_6^+$ $[M+H]^+$ 531.1; found 531.3.

2.2.1.3.4 tert-Butyl (S)-3-(3-(tert-butoxy)-2-((tert-butoxycarbonylamino)-3-oxopropyl)-2-iodo-1H-indol-1-carboxylate (15)

Benzyltriethylammonium chloride (1.4 g, 6 mmol) and dried potassium carbonate (4.1 g, 30 mmol) were added to crude **14** (3.2 g, 6 mmol) in $AcNMe_2$ (20 mL) and then, 2-bromo-2-methylpropane (6.8 mL, 60 mmol) was added slowly with vigorous stirring at room temperature. The mixture was heated at 55 °C and stirred for 2.5 h. The reaction was checked by TLC (EtOAc /hexane = 1:7, R_f = 0.4) and quenched by adding chilled water. The precipitate was extracted with EtOAc and the organic layer was washed with water and brine. The organic layer was dried over anhydrous sodium sulfate, filtered, and concentrated *in vacuo*. The crude product was purified by flash column chromatography on silica gel (EtOAc /hexane = 1:10) to afford **15** (2 g, 58% yield) as a white waxy solid. The enantiomeric purity was measured by HPLC using a chiral column (Chiralpak ID®prep 5 μm, 10 × 250 mm, eluent: isocratic 5% isopropyl alcohol in hexane, wavelength: 280 nm, flow rate: 5 mL/min, retention

time : 8.9 min (retention time of D-form : 7.2 min)). (^{1}H NMR, 300 MHz, Acetone-d): δ = 8.04 (d, *J* = 9 Hz, 1H), 7.64 (d, *J* = 9 Hz, 1H), 7.24-7.15 (m, 2H), 6.13 (d, *J* = 9 Hz, N*H*), 4.37 (q, *J* = 9 Hz, 1H), 3.25-3.10 (m, 2H), 1.67 (s, 9H), 1.31 (s, 9H), 1.27 (s, 9H); (^{13}C NMR, 75 MHz, Acetone-d): δ = 206.14, 171.40, 155.94, 149.89, 138.82, 130.86, 126.54, 125.02, 123.36, 119.52, 115.92, 85.67, 81.44, 79.12, 54.96, 28.39, 28.28, 27.98. ESI-MS *m/z* calculated for $C_{25}H_{36}N_2O_6^+$ [M+H]+ 587.16; found 587.19. HRMS (ESI) for $C_{25}H_{35}IN_2NaO_6^+$ [M+Na]$^+$ requires 609.1432; found 609.1430.

2.2.1.4 Synthesis of non-radioactive standard

2.2.1.4.1 tert-Butyl (S)-2-((tert-butoxycarbonyl)amino)-3-(2-(trifluoromethyl)-1H-indol-3-yl)propanoate (16)

To a solution of **2** (145 mg, 0.4 mmol) in MeOH (2 mL), copper iodide (9.1 mg, 0.048 mmol) and 40% 1-trifluoromethyl-1,2-benziodoxol-3(1*H*)-one (Togni's reagent, contains 60% diatomaceous earth) (381 mg, 0.48 mmol) were added at room temperature under argon atmosphere. The mixture was heated at 70 °C and stirred for 2 h. When the reaction was completed, EtOAc (2 mL) and saturated $NaHCO_3$ (5 mL) were added, and the mixture was extracted with EtOAc. The organic layer was washed with water and brine, dried over anhydrous magnesium sulfate, and filtered. After the solvent was removed under reduced pressure, the crude product was purified by silica gel column chromatography (EtOAc/hexane = 1:10) to afford **16** as a white waxy solid. (86 mg, 50%) (^{1}H NMR, 300 MHz, Acetone-d): δ = 11.00 (s, N*H*), 7.76 (d, *J* = 9 Hz, 1H), 7.42 (d, *J* = 9 Hz, 1H), 7.25 (t, *J* = 9 Hz, 1H), 7.11 (t, *J* = 9 Hz, 1H),

6.11 (s, N*H*), 4.32 (q, *J* = 9 Hz, 1H) 3.41-3.21 (m, 2H), 1.45 (s, 9H), 1.43 (s, 9H), 1.26 (s, 9H), 1.25 (s, 9H); (^{13}C NMR, 75 MHz, Acetone-d): δ = 206.18, 171.66, 156.03, 136.94, 128.51, 121.37, 121.02, 112.89, 81.46, 79.15, 56.31, 28.42, 27.93. ESI-MS *m/z* calculated for $C_{22}H_{30}F_3N_2O_4^+$ $[M+H]^+$ 443.48; found 443.40

2.2.1.4.2 (S)-2-amino-3-(2-(trifluoromethyl)-1H-indol-3-yl)propanoic acid (17)

In a 25 mL round bottom flask, **16** (66 mg, 0.15 mmol) was dissolved in Me_2Cl_2 (1.5 mL) under an argon atmosphere. Dimethyl sulfide (1.5 mL, 20.8 mmol) and 1,2-ethanedithiol (0.155 mL, 1.85 mmol) were added, and the solution was cooled to 0 °C using an ice-water bath. Trifluoroacetic acid (1.5 mL, 20 mmol) was added slowly, and the solution was allowed to warm to room temperature. After stirring the solution for 48 h, the completion of the reaction was checked by HPLC (XTerra® RP18 5 μm, 4.6 × 100 mm, eluent: 0.1% TFA in water; acetonitrile increased from 0% to 100% over 30 min, wavelength: 280 nm, flow rate: 1 mL/min, RT: 10.2 min). The solvent and volatiles were removed under reduced pressure and the residue was dissolved in 2 mL of water. The mixture was purified by preparative HPLC (XTerra®prep 10 μm, 10 × 250 mm, eluent: 0.1%TFA in water; acetonitrile increased from 0% to 100% over 30 min, wavelength: 280 nm, flow rate: 5 mL/min, RT: 13.9 min). **17** was obtained as a white solid after lyophilization (36 mg, 86%). (^{1}H NMR, 300 MHz, 0.5 M DCl in D_2O): δ = 7.68 (d, *J* = 9 Hz, 1H), 7.53 (d, *J* = 9 Hz, 1H), 7.41 (t, *J* = 9 Hz, 1H), 7.26 (t, *J* = 9 Hz, 1H), 4.33 (t, *J* = 9 Hz, 1H), 3.55-3.36 (m, 2H); (^{13}C NMR, 300 MHz, 0.5 M DCl in D_2O): δ = 171.52, 136.36, 127.05, 125.78, 121.66, 120.11, 113.39,

109.58, 54.08, 25.54. ESI-MS *m/z* calculated for $C_{12}H_{12}F_3N_2O_2^+$ $[M+H]^+$ 273.08; found 273.28. HRMS (ESI) for $C_{12}H_{12}F_3N_2O_2^+$ $[M+H]^+$ requires 273.0845; found 273.0846.

2.2.2 General Procedure for [^{18}F]trifluoromethylation for optimization of the labeling conditions

Irradiated [^{18}F]fluoride in ^{18}O-enriched water was unloaded from the target by He flow and captured using an ion-exchange resin (QMA light Sep-Pak cartridge, Waters) that was pre-activated using 5 mL of 0.5 M $KHCO_3$ and 10 mL of distilled water. The captured [^{18}F]fluoride was released using 0.7 mL of a K_{222}/K_2CO_3 solution (prepared from Kryptofix 222 (181 mg, 0.48 mmol) and K_2CO_3 (29 mg) in 8.5 mL of MeCN and 1.5 mL of water) or 0.075 M tetrabutylammonium bicarbonate solution into the vial. The eluted solution was dried at 100 °C, and azeotropic drying was performed twice with anhydrous acetonitrile (1 mL).

To the dried [^{18}F]fluoride, a solution of precursor **3, 8,** or **15**, copper iodide (CuI), methyl chlorodifluoroacetate (MCDFA), and tetramethylethylenediamine (TMEDA) in DMF was added, and the reaction mixture was vigorously mixed. The reaction vial was sealed with Teflon and heated at 150 °C for 15 min. After completion of the reaction, the vial was cooled to room temperature. The [^{18}F]trifluoromethylation

labeling efficiency was measured with ITLC-SG using 95% acetonitrile in water as the eluent.

2.2.3 Radiosynthesis

To increase the product radioactivity and to reduce the radiation exposure, the radiosynthesis of [^{18}F]CF_3- L-Trp was performed in a TRACERLab F_X-F_N module (GE Medical Systems, Germany).

[^{18}F]Fluoride from the cyclotron was eluted into a reaction vial using 0.7 mL of a K_{222}/K_2CO_3 solution, and the solvent was evaporated by N_2 purging. To the reaction vial, a solution of **15** (5.3 mg, 0.009 mmol), CuI (5.1 mg, 0.027 mmol), MCDFA (6 μL, 0.054 mmol), and TMEDA (8 μL, 0.054 mmol) in 180 μL of DMF was added. The reaction was mixed and heated at 150 °C for 15 min. To remove the protecting groups, 2.4 mL of 1 N HCl was added at room temperature, and the reaction mixture was heated at 110 °C for 10 min. Purifications were performed using preparative HPLC (XTerra®prep 10 μm, 10 × 250 mm, eluent: 0.3% AcOH in water; EtOH increased 0% to 20% from 0 to 20 min, from 20% to 100% from 20 to 25 min, and remained at 100% from 25 to 30 min, wavelength: 280 nm, flow rate: 6 mL/min, retention time: 13.9 min). The purified product was neutralized with 200 μL of $NaHCO_3$, normal saline was added to adjust its isotonicity, and it was filtered through a sterile Millex®-FG filter (Merck Millipore, U.S.A.) for injection. Its radiochemical purity and molar activity were measured using analytical HPLC (XTerra® RP18 5

μm, 4.6 × 100 mm, 17% acetonitrile in 0.1% TFA in water, isocratic from 0 to 10 min, wavelength: 280 nm, flow rate: 1 mL/min, retention time: 4.9 min).

2.2.4 Stability test

To measure the serum stability of [^{18}F]CF_3-L-Trp, a solution with the same composition used for injection (7% EtOH in normal saline) was prepared. The prepared solution (185 kBq, 10 μL) was mixed with human or mouse serum (100 μL), and the mixtures were incubated in a shaking incubator at 37 °C. The stability of [^{18}F]CF_3-L-Trp in human or mouse serum was determined using ITLC-SG (eluent: 80% EtOH, R_f of [^{18}F]CF_3-L-Trp = 0.8–1 and R_f of free [^{18}F]fluoride = 0–0.2) at 0, 30, and 60 min and 2, 4, and 6 h.

2.2.5 Serum protein binding assay

The degree of serum protein binding of [^{18}F]CF_3-L-Trp was measured using gel filtration as previously reported.[36,37] To prevent non-specific binding, the PD-10 columns were treated with 1% bovine serum albumin (BSA) in 0.1 M DTPA (1 mL) and washed with deionized water (50 mL) and phosphate buffered saline (PBS) (30 mL). Labeled [^{18}F]CF_3-L-Trp (185 kBq, 10 μL) was mixed with human or mouse serum (100 μL), and the mixtures were then incubated in a shaking incubator at 37 °C

for 10 and 60 min. At 10 and 60 min, each mixture was loaded onto the preconditioned PD-10 columns (n = 3). The PD-10 columns were eluted with PBS (1 mL), and thirty fractions were collected in test tubes. The radioactivity of each collected fraction was measured using a γ-scintillation counter (^{18}F, 400-1200 keV), and the presence of protein in each fraction was confirmed using Coomassie blue staining. The percentage of serum protein binding of [^{18}F]CF_3-L-Trp was calculated from the radioactivity of the fractions.

2.2.6 Biodistribution study

0.1 mL of [^{18}F]CF_3-L-Trp or [^{18}F]CF_3-D-Trp (185 kBq) was intravenously injected into male BALB/c mice (4-5 weeks old, n = 4 in each group, 18±1 g) without anesthesia. For blind testing, each group of mice was randomly selected after injection and sacrificed at 10, 60, or 120 min. Blood was obtained from the carotid artery, and the other organs were separated immediately. After the blood and other organs were weighed, the radioactivity of each organ was determined using a ɤ-scintillation counter. The results are expressed as the percentage of injected dose per gram of tissue (%ID/g); the values are expressed as the mean ± SD.

2.2.7 [^{18}F]CF_3-L-Trp PET acquisition in rats (n=3 at each time point)

Male Sprague-Dawley (SD) rats (8 weeks), weighing between 250 and 315 g, were anesthetized with 2% (v/v) isoflurane at 1 L/min oxygen flow and were intravenously injected with prepared [^{18}F]CF_3-*L*-Trp (199±10 MBq). At 5, 10, 20, 40 and 80 mins after [^{18}F]CF_3- L-Trp injection, the rats were sacrificed by CO_2 gas and the brain was extracted and washed with normal saline. Extracted brain was positioned in the imaging chamber. PET and T2-weighted images were taken by simultaneous PET/MRI scanner. Static data were acquired at energy window 400-700 KeV for 20 min. PET images were reconstructed automatically using Sophia software and analyzed using amide program. T2-weighted MR images were acquired for brain anatomy and were reconstructed to DICOM using aspect imaging program.

2.2.8 Autoradiography in rats

Male Sprague-Dawley rats (8 weeks) weighing between 250 g and 330 g were used in the experiments. The radiochemical purity and chiral purity of the [^{18}F]CF_3-L-Trp used for injection was over 99%. Purified [^{18}F]CF_3-L-Trp (330 MBq, 120 μg) was injected into the rats through the tail vein without anesthesia. The rats were sacrificed 10 min after the injection of [^{18}F]CF_3-L-Trp. The brain was dissected and kept in a pre-cooled container with dry ice. Coronal brain sections 30 μm in thickness were obtained using a cryostat microtome (Leica CM 1800, Leica Inc., Germany) and

thaw-mounted on glass slides. The slides were exposed to a BAS-IP MS 2040E imaging plate, and the rat brain autoradiograms were obtained using a Bio-imaging Analyzer System (FLA-2000, FUJIFILM Inc., Japan).

Preparation of standards for quantification

Standards were prepared for each experiment to quantify the specific areas of ingestion in the brain. Gelatin (2 g) (Sigma-Aldrich, U.S.A.) was dissolved in distilled water (10 mL) and the solution was incubated overnight at 60 °C in water bath the night before. Purified [^{18}F]CF_3-L-Trp (37 MBq/mL) was serially diluted with distilled water to prepare standard solutions with different concentrations. Each standard solution (200 μL) was added to the gelatin solution (800 μL) and mixed carefully to avoid the formation of air bubbles. The gelatin standard solutions were taken up in 1 mL syringes, and the syringes were placed in a freezer for 15 min. The cured standard solutions in the syringes were removed from the syringe, cut to a suitable size, fixed with frozen section compound (FSC 22® Clear, Leica Inc., Germany), and sliced to a 30 μm thickness. The sliced standards were thaw-mounted on glass slides, and the slides were exposed to the imaging plate simultaneously with the brain slides.

2.2.9 Metabolites study

Non-radioactive CF_3-L-Trp (5 mg, 0.2 mL of water) was administered by intravenous injection without anesthesia, and male BALB/c mice (5 weeks, 23±1 g) were sacrificed by decapitation at 10 or 60 min. After sacrificing the mice, the whole

brain, blood, and urine were removed and stored on ice. The whole brain was homogenized (Polytron PT3000, Kinematica, Westbury, Canada) in 10 volumes (w/v) of 0.1 M perchloric acid ($HClO_4$) containing 10 mg/mL sodium bisulfite and 1 mM EDTA. The homogenate was centrifuged at 3300 rpm for 10 min at 4 ℃, and the resulting supernatant was filtered through a 0.2 μm polyvinylidene fluoride (PVDF) filter (Whatman™, U.K.). The blood sample was centrifuged at 3300 rpm for 10 min at 4 ℃ to separate the plasma, and a protein-free sample was obtained from the plasma by adding 5 M $HClO_4$ (30 μL). The mixture was then mixed for 15 s, centrifuged at 3300 rpm for 10 min, and filtered as described above. The urine sample (0.2 mL) was diluted with 0.1% TFA in water (0.5 mL) and filtered as described above. The synthesized major metabolites, 5-hydroxy-CF_3-L-tryptophan (CF_3-HTP) and CF_3-serotonin, were prepared by electrophilic substitution using Togni's reagent and were used as references (RT of CF_3-HTP : 20.0 min, RT of CF_3-serotonin : 15.3 min).

The metabolites from the brain, blood, and urine were analyzed using HPLC (XTerra® RP18 5 μm, 4.6 × 100 mm, eluent: 0.1% TFA in water; acetonitrile increased from 0% to 30% from 0 to 50 min; from 30% to 100% from 50 to 51 min; and isocratic at 100% from 51 to 60 min, wavelength: 280 nm, flow rate: 1 mL/min) and LC-MS (LTQ velos spectrometer, Thermo Fisher Scientific, U.S.A.). The mass spectra (*m/z*) of the major metabolites were analyzed using the LTQ velos mass spectrometer.

2.3 [^{18}F]Trifluoromethyl-L-α-methyltryptophan ([^{18}F]CF_3-L-AMT)

2.3.1 Chemistry

2.3.1.1 Synthesis of iodo D- or L-AMT derivatives as precursor

2.3.1.1.1 2-(tert-butoxycarbonylamino)-3-(1*H*-indol-3-yl)-2-methylpropanoic acid (19)

To a solution of α-methyl-DL-tryptophan (2 g, 9.2 mmol) in MeOH (31 mL) at room temperature under argon atmosphere, di-tert-butyl dicarbonate (3.2 mL, 13.7 mmol) and Et_3N (2.6 mL, 18.3) was added slowly. The reaction mixture was stirred overnight and concentrated *in vacuo*. The crude product **19** was obtained as a yellow waxy solid and used for next step without any purification. (^{1}H NMR, 300 MHz, Acetone-d): δ = 10.06 (s, 1H), 7.56 (d, J=9 Hz, 1H), 7.30 (d, J=9 Hz, 1H), 7.10 (s, 1H), 7.00 (t, J=9 Hz, 1H), 6.91 (t, J=9 Hz, 1H), 5.77 (s, 1H), 3.41 (s, 2H), 1.52 (s, 3H), 1.39 (s, 9H); (^{13}C NMR, 75 MHz, Acetone-d): δ = 206.15, 176.20, 155.31, 137.19, 129.63, 125.14, 121.86, 119.80, 119.46, 111.97, 60.61, 28.62

2.3.1.1.2 tert-Butyl 2-(tert-butoxycarbonylamino)-3-(1*H*-indol-3-yl)-2-methylpropanoate (20)

To a mixture of crude **19** (929 mg, 2.9 mmol), benzyltriethylammonium chloride (665 mg, 2.9 mmol) and dried potassium carbonate (2.02 g, 14.6 mmol) in N,N-

dimethylacetamide (3 mL), t-Butyl bromide (3.3 mL, 29.2 mmol) was added slowly with vigorous stirring at room temperature under argon atmosphere. The reaction mixture was heated at 55^{o}C for 2.5 hr and quenched by 350 mL of cold water which was cooled down in refrigerator before 30 mins. Precipitates were extracted with EtOAc and the organic layer was washed with water and brine. The reaction mixture was dried over anhydrous sodium sulfate, filtered and concentrated *in vacuo*. The crude product was purified by flash column chromatography on silica gel (EtOAc/Hex = 1:4) afford **20** (536 mg, 49% yield in 2 steps) as a colorless waxy solid. (^{1}H NMR, 300 MHz, Acetone-d): δ = 7.56 (d, *J*= 9 Hz, 1H), 7.33 (d, *J*=9 Hz, 1H), 7.1 (s, 1H), 7.05 (t, *J*=9 Hz, 1H), 6.95 (t, *J*=9 Hz, 1H), 5.81 (s, 1H), 3.22-3.47 (dd, J_1=15 Hz, J_2=45 Hz), 1.42 (s, 9H), 1.40 (s, 12H); (^{13}C NMR, 75 MHz, Acetone-d): δ = 206.21, 174.24, 155.26, 137.12, 129.74, 125.09, 121.83, 119.86, 119.38, 111.93, 81.04, 60.78, 28.67, 28.03. ESI-MS m/z calculated for $C_{21}H_{31}N_2O_4^+$ [M+H]+ 375.48 found 375.36

2.3.1.1.3 tert-Butyl 3-(3-*tert*-butoxy-2-(tert-butoxycarbonylamino)-2-methyl-3-oxopropyl)-1*H*-indol-1-carboxylate (21)

To a solution of **20** (306 mg, 0.82 mmol) in acetonitrile (1.6 mL), di-tert-butyl dicarbonate (0.47 mL, 2 mmol) and 4-dimethylaminopyridine (20 mg, 0.16 mmol) was added at room temperature under N_2. The reaction mixture was stirred for 15 mins and completion of the reaction was checked by the TLC. The solvent was removed under reduced pressure and the residue was dissolved with EtOAc. The

organic layer was washed with 1 N HCl and water two times respectively, dried over anhydrous sodium sulfate, filtered and concentrated under reduced pressure. The crude product was purified by flash column chromatography on silica gel (EtOAc/Hex = 1:7) to afford **21** (390 mg, 99% yield) as a colorless waxy solid. (^{1}H NMR, 300 MHz, Acetone-d): δ = 8.10 (d, J=9 Hz, 1H), 7.59 (d, J=9 Hz, 1H), 7.40 (s, 1H), 7.24(t, J=9 Hz, 1H), 7.15 (t, J=9 Hz, 1H), 5.91 (s, 1H), 3.25-3.45 (dd, J_1=15 Hz, J_2=30 Hz, 2H), 1.63 (s, 9H), 1.44 (s, 12H), 1.43 (s, 9H); (^{13}C NMR, 75 MHz, Acetone-d): δ = 205.96, 173.83, 155.19, 150.11, 135.88, 132,58, 125.55, 124.80, 123.09, 120.47, 116.81, 115.61, 84.02, 81.49, 60.43, 28.23, 28.04, 27.88 ESI-MS m/z calculated for $C_{26}H_{39}N_2O_6^+$ [M+H]+ 475.60 found 475.

2.3.1.1.4 (S)-tert-Butyl 3-(3-tert-butoxycarbonylamino)-2-methyl-3-oxopropyl)-2-iodo-1*H*-indole-1-carboxylate (22a)

Mercury trifluoroacetate (167 mg, 0.39 mmol) was added at room temperature under Ar to a solution of **21** (143 mg, 0.3 mmol) in DCM (2 mL). The reaction mixture was stirred for 30 mins and washed with sat KI solution. The organic layer was dried over sodium sulfate and filtered. To the reaction mixture, iodine (114 mg, 0.45 mmol) was added and the reaction mixture was stirred another 3 hrs under argon atmosphere. The reaction mixture was quenched by 10% sodium sulfite, washed with water and brine, dried over anhydrous magnesium sulfate and filtered. After concentrated under reduced pressure, the crude product was purified by silica gel column chromatography with eluent. (E.A/Hex = 1:20 ~ 1:10). The chiral mixture

was purified by chiral preparative HPLC (ChiralpakID®prep 5 μm, 10 mm × 250 mm Eluent: 2.5% isopropyl alcohol in n-hexane). **22a** was eluted at 11.3 min and obtained as a colorless waxy solid after concentration *in vacuo*. (74 mg, 41%) (^{1}H NMR, 300 MHz, Acetone-d): δ = 8.01 (d, J=9 Hz, 1H), 7.50 (d, J=9 Hz, 1H), 7.17 (t, J=9 Hz, 1H), 7.09 (t, J=9 Hz, 1H), 6.01 (s, 1H), 3.22-3.67 (dd, J_1=15 Hz, J_2=105 Hz), 1.68 (s, 9H), 1.44 (s, 21H); (^{13}C NMR, 75 MHz, Acetone-d): δ = 206.09, 173.91, 155.73, 149.96, 138.90, 131.92, 127.22, 124.91, 123.16, 120.53, 115.59, 85.71, 80.84, 61.09, 28.30, 28.25, 28.04; HRMS (ESI) for $C_{26}H_{37}IN_2NaO_6^+$ $[M+Na]^+$ requires 623.4755 found 623.1585; $[\alpha]^{D}_{20}$ = -0.4 (c=1.0, CH_3Cl)

2.3.1.1.5 (R)-tert-Butyl 3-(3-tert-butoxycarbonylamino)-2-methyl-3-oxopropyl)-2-iodo-1*H*-indole-1-carboxylate (22b)

Mercury trifluoroacetate (167 mg, 0.39 mmol) was added at room temperature under argon atmosphere to a solution of **21** (143 mg, 0.3 mmol) in DCM (2 mL). The reaction mixture was stirred for 30 mins and washed with saturated potassium iodide solution. The organic layer was dried over sodium sulfate and filtered. To the reaction mixture, iodine (114 mg, 0.45 mmol) was added and the reaction mixture was stirred another 3 hrs under argon atmosphere. The reaction mixture was quenched by 10% sodium sulfite, washed with water and brine, dried over anhydrous magnesium sulfate and filtered. After concentrated under reduced pressure, the crude product was purified by silica gel column chromatography with eluent. (E.A/Hex = 1 : 20 ~ 1 : 10). The chiral mixture was purified by chiral preparative HPLC (ChiralpakID®prep

5 μm, 10 mm × 250 mm Eluent: 2.5% isopropyl alcohol in n-hexane). **22b** was eluted at 9.9 min and obtained as a colorless waxy solid after concentration *in vacuo*. (73 mg, 40.5%) (^{1}H NMR, 300 MHz, Acetone-d): δ = 8.01 (d, J=9 Hz, 1H), 7.50 (d, J=9 Hz, 1H), 7.17 (t, J=9 Hz, 1H), 7.09 (t, J=9 Hz, 1H), 6.01 (s, 1H), 3.22-3.67 (dd, J_1=15 Hz, J_2=105 Hz), 1.68 (s, 9H), 1.44 (s, 21H); (^{13}C NMR, 300 MHz, Acetone-d): δ = 206.09, 173.91, 155.73, 149.96, 138.90, 131.92, 127.22, 124.91, 123.16, 120.53, 115.59, 85.71, 80.84, 61.09, 28.30, 28.25, 28.04; HRMS (ESI) for $C_{26}H_{37}IN_2NaO_6^+$ $[M+Na]^+$ requires 623.4755 found 623.1585; $[\alpha]^D_{20}$ = +0.4 (c=1.0, CH_3Cl)

2.3.1.2 Synthesis of non-radioactive standard

2.3.1.2.1 (R,S)-tert-butyl-2-(tert-butoxycarbonylamino)-2-methyl-3-(2-(trifluoromethyl)-1*H*-indol-3-yl)propanoate (23)

To a solution of **20** (260 mg, 0.69 mmol) in MeOH (3.5 mL), Copper iodide (26 mg, 0.14 mmol) and 40% Togni's reagent (654 mg, 0.83 mmol) was added at room temperature under argon atmosphere. The reaction mixture was heated at 70^{o}C for 2 hrs and diluted with EtOAc (2 mL) followed by the addition of sodium hydrogencarbonate (5 mL). The crude product mixture was extracted using EtOAc and the organic layer was washed with water and brine respectively. The reaction mixture was dried over anhydrous magnesium sulfate and filtered. After the solvent was removed under reduced pressure, the crude product was purified by silica gel column chromatography (E.A/Hex = 1:10). **23** was obtained as a colorless waxy solid after concentration *in vacuo*. (150 mg, 49%) (^{1}H NMR, 300 MHz, Acetone-d): δ =

10.99 (s, 1H), 7.65 (d, J=9 Hz, 1H), 7.40 (d, J=9 Hz, 1H), 7.22 (t, J=9 Hz, 1H), 7.03 (t, J=9 Hz, 1H), 3.35-3.81 (dd, J_1=15 Hz, J_2=96 Hz), 1.45 (s, 9H), 1.43 (s, 9H), 1.24 (s, 3H); ESI-MS m/z calculated for $C_{22}H_{30}F_3N_2O_4^+$ $[M+H]^+$ requires 443.48 found 443.40

2.3.1.2.2 (R,S)-2-carboxy-1-(2-(trifluoromethyl)-1*H*-indol-3-yl)propan-2-aminium 2,2,2-trifluoroacetate (24)

In a 25 mL of round bottom flask, **23** (46 mg, 0.1 mmol) was dissolved with DCM (1 mL) under argon atmosphere. Dimethyl sulfide (1 mL, 14 mmol) and 1,2-ethanedithiol (1 mL, 1.4 mmol) was added and the reaction mixture was cooled down to 0°C using ice-water bath. Trifluoroacetic acid (1 mL, 13.5 mmol) was slowly added and the reaction mixture was allowed to reach room temperature where it was stirred for 48h. After completion of reaction by monitoring with HPLC, the volatiles were removed under reduced pressure and the residue was dissolved with 2 mL of water. The mixture was purified with preparative HPLC (XTerra®prep 10 μm, 10 × 250 mm, Eluent: 0.1%TFA in water; CH_3CN increased for 0% to 100% for 30 min at 5 mL/min). **24** was eluted at 9.3 min and obtained as a white solid after lyophilization (25 mg, 88%). (^{1}H NMR, 300 MHz, 0.5 M DCl in D_2O): δ = 7.40 (d, J=9 Hz, 1H), 7.26 (d, J=9 Hz, 1H), 7.13 (t, J=9 Hz, 1H), 6.98 (t, J=9 Hz, 1H), 3.13-3.45 (dd, J_1=6 Hz, J_2=15 Hz), 1.41 (s, 9H); (^{13}C NMR, 300 MHz, 0.5 M DCl in D_2O): δ = 197.99, 160.11, 151.47, 149.58, 145.47, 144.64, 137.14, 132.23, 85.21, 55.83, 45.81; HRMS (ESI) for $C_{13}H_{14}F_3N_2O_2^+$ $[M+H]^+$ requires 287.1002 found 287.0995;

2.3.2 Radiosynthesis

Proton beam irradiated ^{18}O-enriched water to produce [^{18}F]fluoride by $^{18}O(p,n)^{18}F$ reaction using the 16.5 Mev- cyclotron (PETtrace 10, GE healthcare, Uppsala, Sweden). Irradiated [^{18}F]fluoride in ^{18}O-enriched water was unloaded from target by He flow and captured by ion-exchange resin (QMA light Sep-Pak cartridge, waters) which was pre-activated by 5 mL of 0.5 M K_2CO_3 and 10 mL of distilled water. Captured [^{18}F]fluoride was released by 0.7 mL of K_{222}/K_2CO_3 solution (prepared from kryptofix 222 (181 mg, 0.48 mmol) and K_2CO_3 (29 mg) in 8.5 mL of CH_3CN and 1.5 mL of water) or 0.075 M tetrabutylammonium bicarbonate solution into the vial. The eluted solution was dried at 100℃ and azeotropic drying was performed twice with anhydrous acetonitrile (1 mL).

To the vial, a solution of **22a** or **22b** with copper(I) iodide (Cu(I)I), methyl chlorodifluoroacetate (MCFDA) and tetramethylethylenediamine (TMEDA) in N,N-Dimethylformamide (DMF) was added and vigorously mixed using vortex. The vial was sealed with Teflon and heated at 150ºC for 15 minutes. The vial was removed from heating and cooled in a cold water bath for 5 minutes. For the remove of protection groups, 2.4 mL of 1 N HCl was added via syringe without needle and heated at 110ºC for 10 minutes. [^{18}F]trifluoromethylation labeling efficiencies were monitored by ITLC-SG using 95% CH_3CN in water as eluents.

All the radiosynthesis of [^{18}F]CF_3-L-AMT or [^{18}F]CF_3-D-AMT for the autoradiography was performed in a TRACERLab FX-FN module (GE medical

Systems, Germany). 10.8 mg of precursors with 11 mg of Cu(I)I, 9 μL of MCFDA and 13.5 μL of TMEDA in 0.3 mL of DMF were used. All the other conditions were same as in the manual. Purifications were performed using a preparative HPLC (XTerra®prep 10 μm, 10 × 250 mm, Eluent : 0.3% AcOH in water; CH_3CN increased for 0% to 20% from 0 to 20 min 20% to 100% from 20 to 25 min 100% for 5 min at 7 mL/min). The purified solution of radiolabeled compound was neutralized by $NaHCO_3$, diluted with normal saline and filtered through a sterile Millex®-FG filter (Merck Millipore, USA) for injection.

2.3.3 Stability test

To measure the in vitro stabilities of [^{18}F]CF_3-L-AMT, we prepared the same compositions of [^{18}F]CF_3-L-AMT with the solutions for injection. The solutions were stored at room temperature for 6 h and analyzed by ITLC-SG (eluents: 80% EtOH). For the serum stability test, 25 μL of the prepared solutions were mixed with 325 μL of human serum or mouse serum and incubated at 37°C for 6 h. When the radioactivity was measured, ethanol was added to serum mixture and centrifuged (3,000 rpm) for 5 min to precipitate the serum proteins. The supernatant of the mixture was analyzed in the same way as previously.

2.3.4 Biodistribution (in mice)

0.1 mL of [^{18}F]CF_3-L-AMT or [^{18}F]CF_3-D-AMT (50 kBq/mL) was intravenously injected into male BALB/c mice (4-5 weeks old, n = 4 in each group, 18±1 g) without anesthesia. For blind testing, each group of mice were randomly selected after injection and sacrificed at 10, 60, or 120 min. Blood was obtained from the carotid artery and other organs were separated immediately. After blood and other organs were weighed, the radioactivity of each organs were counted using a ɤ-scintillation counter. Results are expressed as the percentage of injected dose per gram of tissue (%ID/g). Values are expressed as the mean±SD.

2.3.5 Autoradiography (in rat)

Male Sprague-Dawley rats (8-10 weeks), weighing between 250 g and 330 g, were used in the experiments. They were kept in our animal facility (22-24 ^{o}C, 8 a.m. to 8 p.m. day and night cycle) and provided food and water ad libitum. The food was prohibited at least 16 hour before the experiment but water was provided ad libitum. All the rats were injected between 4 to 6 p.m. to avoid the effect of circadian rhythm. All the experimental procedures were approved by Institutional Animal Care and Use Committee at Seoul National University Hospital.

Radiochemical purity and chiral purity of [^{18}F]CF_3-L-AMT or [^{18}F]CF_3-D-AMT for injection were over 99%. Purified [^{18}F]CF_3-L-AMT or [^{18}F]CF_3-D-AMT (175-395

MBq, 40-140 μg) were injected into rats through tail vein without anesthesia. The rats were killed at 5, 10, 20 40 80 min post-injection of [^{18}F]CF_3-L-AMT and at 10, 20, 40, 80 min post injection of [^{18}F]CF_3-D-AMT. The brain were dissected and kept in the pre-cooled container with dry ice. 30 μm thickness of coronal brain sections were obtained using cryostat microtome (Leica CM 1800, Leica Inc., Germany) and thaw-mounted on glass slides. The slides were exposed to BAS-IP MS 2040E imaging plates and rat brain autoradiograms were obtained by Bio-imaging Analyzer System (BAS-2500)

Standard Preparation. To quantify the brain-specific region of ingestion, we prepared the ^{18}F standard in all single experiments. 2 g of jelatin (Sigma-Aldrich) was dissolved in distilled water and the solution was incubated at 60^{o}C in water bath for overnight in a previous day of experiment. Purified [^{18}F]CF_3-L-AMT or [^{18}F]CF_3-D-AMT (Range: 5-12 MBq/mL) was diluted with distilled water to make 1 mL solution and the solution was serially diluted in duplicate. Serial diluted solution was added to 800 μL of jelatin solution and the standard solutions were carefully mixed not to make air bubbles. After placed in a freezer for 15 min, hardened standard solutions were sliced 30 μm thickness and thaw-mounted on glass slides. The standard solution slides were exposed to the imaging plated at the same time as the brain slides.

Lithium treatment model. Lithium treated rat model was devised to evaluate the difference brain distribution of [^{18}F]CF_3-L-AMT between normal and serotonin metabolism enhanced SD rats. Lithium chloride (LiCl) was dissolved in water and the solution was administered 2 times at 10AM and 5 PM per day for 5 days (85

mg/kg, i.p.). Li-treated rats deprived of food 16 h before experiment and water was provided ad libitium. The following experimental procedures were the same as before.

3 RESULTS AND DISCUSSION

3.1 [^{18}F]Trifluoromethyl- L-tryptophan ([^{18}F]CF_3- L-Trp)

3.1.1 Chemistry

We synthesized a protected L-Trp **3** and its 2-bromo **8** and 2- iodo derivatives **15** as precursors for the [^{18}F]trifluoromethylation of the 2-position of Trp. **3** was synthesized via a three-step synthetic process in which the amines and carboxylic acid were protected by Boc and tert-butyl ester, respectively (Scheme 1).

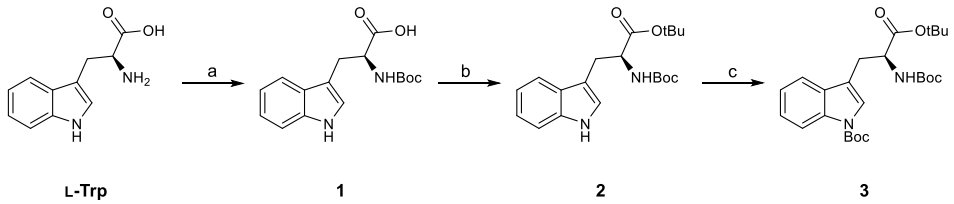

SCHEME 1 Synthesis of protected L-Trp (**3**). Reagents and conditions: a) $(Boc)_2O$, Et_3N, MeOH, RT, overnight, 100%; b) $(CH_3)_3C$-Br, K_2CO_3, BTEAC, DMAC, 55°C, 2.5 h, 49%; c) $(Boc)_2O$, DMAP, DCM, RT, 15 min, 99%.

The bromo precursor **8** was synthesized via the introduction of bromine at the 2-position by electrophilic substitution using N-bromosuccinamide (NBS) according to a previously reported procedure (Scheme 2).[26] **4** was synthesized from commercially available L-Trp methyl ester under acidic conditions; no other regioisomers were detected. As in the synthesis of precursor **3**, both the primary and indole amine were

protected by Boc to give **6** in quantitative yield. The methyl ester was replaced with the tert-butyl ester to be removed in one-step acid hydrolysis in the final step of ^{18}F-labeling.

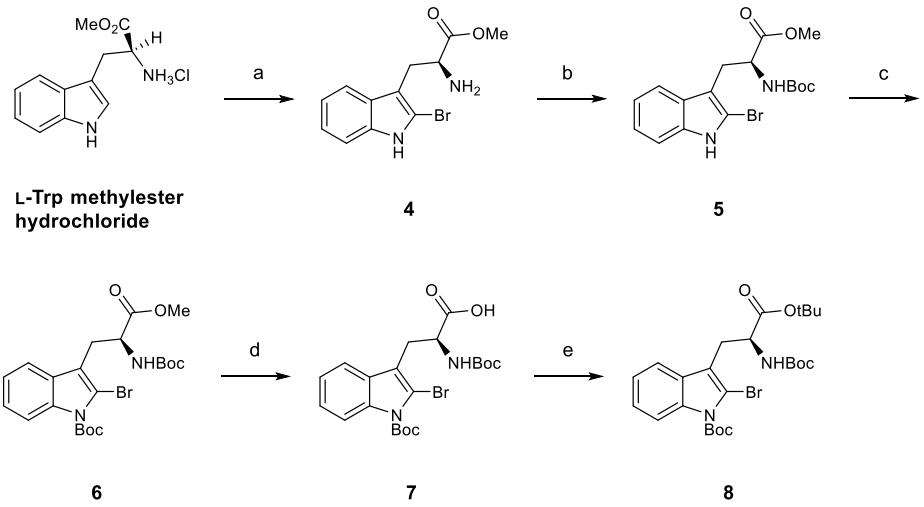

SCHEME 2 Synthesis of bromo precursor (**8**). Reagents and conditions: a) *N*-bromosuccinimide (NBS), AcOH/HCO_2H (4 : 1, v/v), RT, 20 min; b) $(Boc)_2O$, Et_3N, MeOH, RT, overnight, 46% (2 steps); c) $(Boc)_2O$, DMAP, DCM, RT, 10 min, 92%; d) LiOH monohydrate, THF/MeOH/H_2O (1 : 1 : 1, v/v), 0°C to RT, 20 min, 89%; e) $(CH_3)_3C$-Br, K_2CO_3, BTEAC, DMAC, 55°C, 2.5 h, 43%.

The iodo precursor **15** was synthesized by regioselective 2-iodination via Pd-cyclometalation, iodine insertion, and ligand exchange (Scheme 3). Iodo L-Trp methyl ester **11** was purified by simple filtration. The yield of the iodination after Boc protection and purification of intermediate **12** through a four-step process was calculated and found to be quite high (66%). **15** was then synthesized using a method

similar to that depicted in Scheme 2. The D-enantiomer of **15** was also synthesized from the commercially available D-Trp methyl ester. The chiral purity of **15** and its isomer were evaluated using HPLC with a chiral column, and no racemization was detected (Figure 5).

Non-radioactive CF_3-Trp **17** was prepared as a reference material of [^{18}F]CF_3-L-Trp (Scheme 4). The high electron density at the 2-positon of the indole ring enabled the introduction of the trifluoromethyl group by electrophilic substitution.[38] The protecting groups were removed by TFA and the radical scavenger dimethyl sulfide and 1,2-ethanedithiol, and purification of **17** was performed using HPLC. The yield was 89% based on the isolated product after lyophilization.

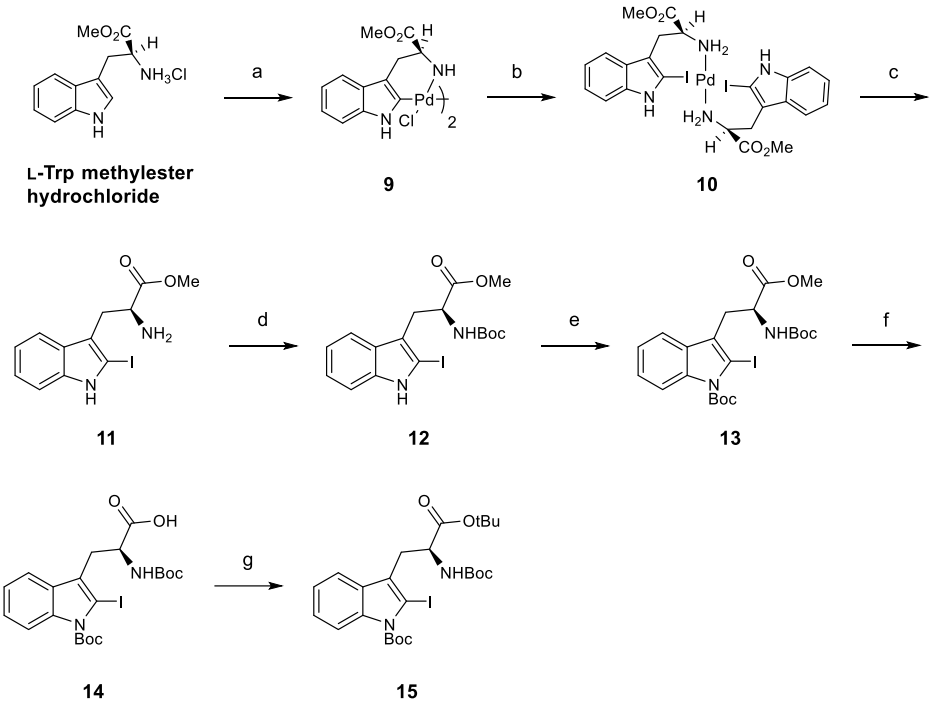

L-Trp methylester hydrochloride

9

10

11

12

13

14

15

SCHEME 3 Synthesis of bromo precursor (**15**). Reagents and conditions: a) $Pd(OAc)_2$, MeCN, RT, 48 h; b) I_2, MeOH, RT, 2.5 h; c) 1,10-phenanthroline monohydrate, DCM, RT, 4 h; d) $(Boc)_2O$, Et_3N, MeOH, RT, overnight, 66% (4 steps); e) $(Boc)_2O$, DMAP, DCM, RT, 10 min, 97%; f) LiOH monohydrate, THF/MeOH/H_2O (1 : 1 : 1, v/v), 0°C to RT, 20 min, 99%; g) $(CH_3)_3C$-Br, K_2CO_3, BTEAC, DMAC, 55°C, 2.5 h, 58%.

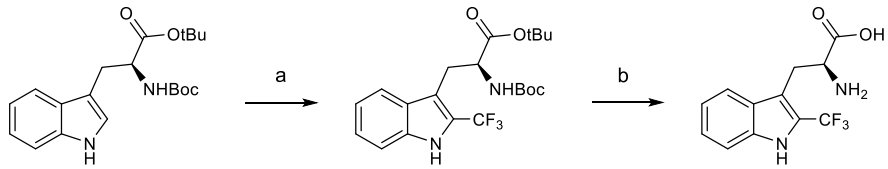

SCHEME 4 Synthesis of non-radioactive standard (**17**). Reagents and conditions: a) Cu(I)I, Togni's reagent (contains 60% diatomaceous earth), MeOH, 70°C, 2 h, 50%; b) TFA, $HSCH_2CH_2SH$, $(CH_3)_2S$, 0°C to RT, 48 h, 86%.

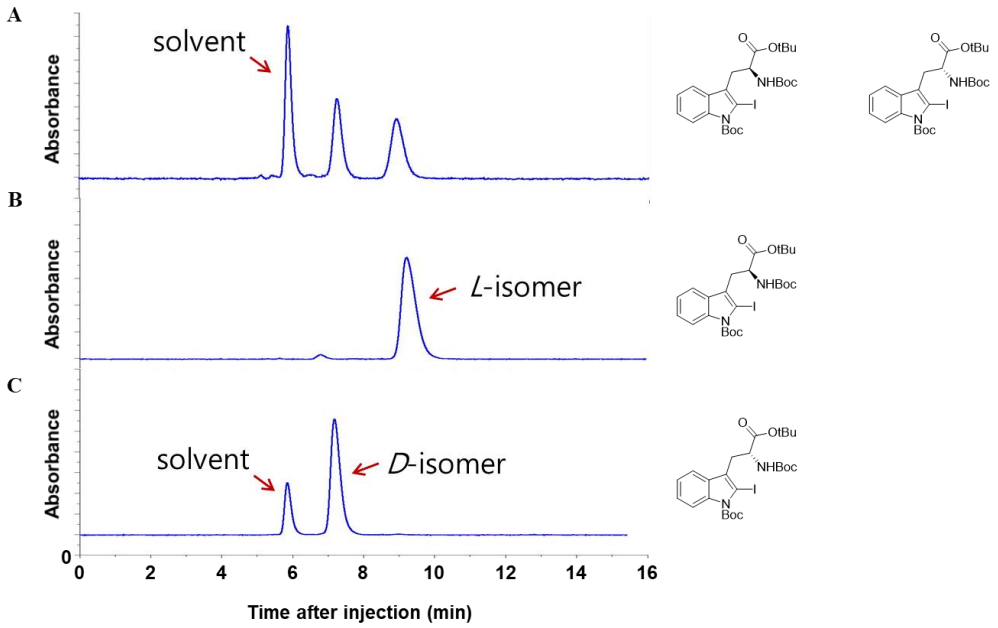

FIGURE 5. HPLC chromatograms of racemic mixture of protected iodo precursor (15) (A), L-form of protected iodo precursor (15a) (B) and D-form of protected iodo precursor (15b) (C). Blue: UV (280 nm). Chromatograms were obtained on a Diacel Chiral pak ID column. Mobile phase was 2.5% Isopropyl alcohol in *n*-Hexane and flow rate was 5 ml/min.

3.1.2 Optimization of the [^{18}F]trifluoromethylation conditions

In this study, we synthesized enantiopure [^{18}F]CF_3-L-Trp with the same chiral center as natural tryptophan. Protected tryptophan with different functional groups at 2-position (**3**, **8**, and **15)** were investigated for Cu(I)-mediated [^{18}F]trifluoromethylation. Essentially, the [^{18}F]trifluoromethylation reaction requires an aromatic compound activated by a halogen residue as a precursor.[30,31] However, the halogen-free **3** could also be used as a precursor via direct C-H functionalization due to the high electron density of indole at the 2-position. Thus, we tested the labeling efficiency of the [^{18}F]trifluoromethylation reaction using these three precursors.

We first optimized the conditions for [^{18}F]trifluoromethylation on the 2-position of the indole ring

(Table 1). When the amine of the indole was not protected, the radiochemical yield (RCY) was very low (4%), demonstrating the importance of the amine protecting group (entry 1). The RCY increased when a protected precursor was used (10%) (entry 2). The synthesized precursors **3, 8,** and **15** were subjected to [^{18}F]trifluoromethylation on the 2-position of the indole ring to determine the most appropriate leaving group. The iodo precursor **15** showed the highest RCY for [^{18}F]trifluoromethylation (56%) (entry 4), the bromo precursor **8** the second highest (22%) (entry 3), and the protonated precursor **3** the lowest (10%). The RCY of **15** was 5.5 times and 2.5 times higher than that of **3** and **8**, respectively. Then, we further

tested the use of different amounts of substrate **15** (entry 4-6). When 5 μmol (2.7 mg) of **15** was used, the RCY was higher than when 2.5 μmol (1.4 mg) was used (34%). However, the RCY did not increase further when 9 μmol (5.3 mg) of **15** was used (54%). When the amount of the reagents MCDFA or TMEDA was increased, a sludge was formed (entry 7). Decreased amounts of MCDFA and TMEDA resulted in decreased RCY (30%) (entry 8). Since the labeling synthesis took place at 150 °C, a solvent with a higher boiling point, DMSO, was tried. However, in DMSO, the reaction did not proceed at all (0%) (entry 9). When the phase transfer catalyst was changed from K_{222}/K_2CO_3 to tetrabutylammonium bicarbonate (TBAB), no significant difference was observed (50%, entry 10).

TABLE 1. [^{18}F]trifluoromethylation reaction using various precursors.

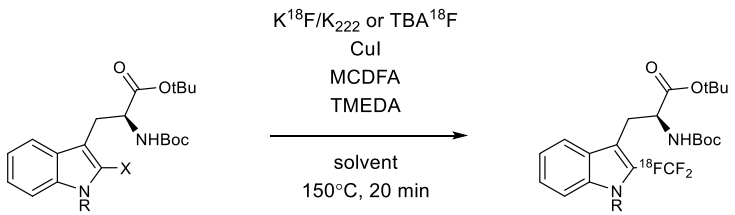

Entry	R	X	Substrate (μmol)	Reagents			Solvent	RCC[a] (%)
				CuI	MCDFA	TMEDA		
1	H	H	5	5.1 mg	6 μL	8 μL	DMF	4
2	Boc	H	5	5.1 mg	6 μL	8 μL	DMF	10
3	Boc	Br	5	5.1 mg	6 μL	8 μL	DMF	22
4	Boc	I	5	5.1 mg	6 μL	8 μL	DMF	56
5	Boc	I	9	5.1 mg	6 μL	8 μL	DMF	54
6	Boc	I	2.5	5.1 mg	6 μL	8 μL	DMF	34
7	Boc	I	5	5.1 mg	12 μL	16 μL	DMF	-[b]
8	Boc	I	5	5.1 mg	3 μL	4 μL	DMF	30
9	Boc	I	5	5.1 mg	3 μL	4 μL	DMSO	0
10[c]	Boc	I	5	5.1 mg	3 μL	4 μL	DMF	50

a) RCY (%) was measured by radio-TLC;
b) Reaction mixture became sludge;
c) [^{18}F]TBAF was used as a phase transfer catalyst

3.1.3 Automatic radiosynthesis

The automatic radiosynthesis of [^{18}F]CF_3-L-Trp for subsequent *in vitro* characterization and for further animal experiments was using an F_X-F_N automation module (Scheme 5). Compared to manual synthesis, the amounts of the iodo precursor **15**, the other reagents, and solvent were doubled for the automatic synthesis, since the reaction vessel was larger. For the removal of the protection groups, aqueous 1 N HCl was used instead of TFA. The residue after synthesis could be removed cleanly using water and acetone not to damage the automation module. The synthesized [^{18}F]CF_3-L-Trp was purified using prep-HPLC. The total synthesis time was 70 min including purification, and the RCY of [^{18}F]CF_3-L-Trp was 6±1.5% based on the isolated product (Figure 6).

The purified [^{18}F]CF_3-L-Trp was analyzed using analytical HPLC, and the retention time of [^{18}F]CF_3-L-Trp in the chromatogram was consistent with that of non-radioactive CF_3-L-Trp. The radiochemical purity of [^{18}F]CF_3-L-Trp was greater than 99%, and no other peaks were detected.

We could achieve enough high molar activity (0.44-0.76 GBq/μmol) for metabolic imaging of [^{18}F]CF_3-L-Trp. The enantiomeric purity was also determined using analytical HPLC with a chiral column, which confirmed no racemization occurred (Figure 7).

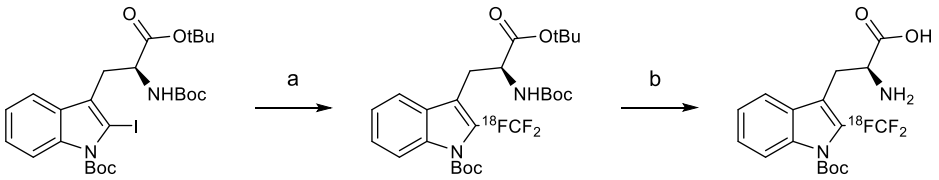

17 $[^{18}F]CF_3$-L-Trp

SCHEME 5. Radiosynthesis of $[^{18}F]CF_3$-L-Trp. Reagents and conditions: a) K_{222}/K_2CO_3 or TBAB, CuI, MCDFA, TMEDA, DMF, 150°C, 15 min; b) aq 1N HCl, 110°C, 10 min.

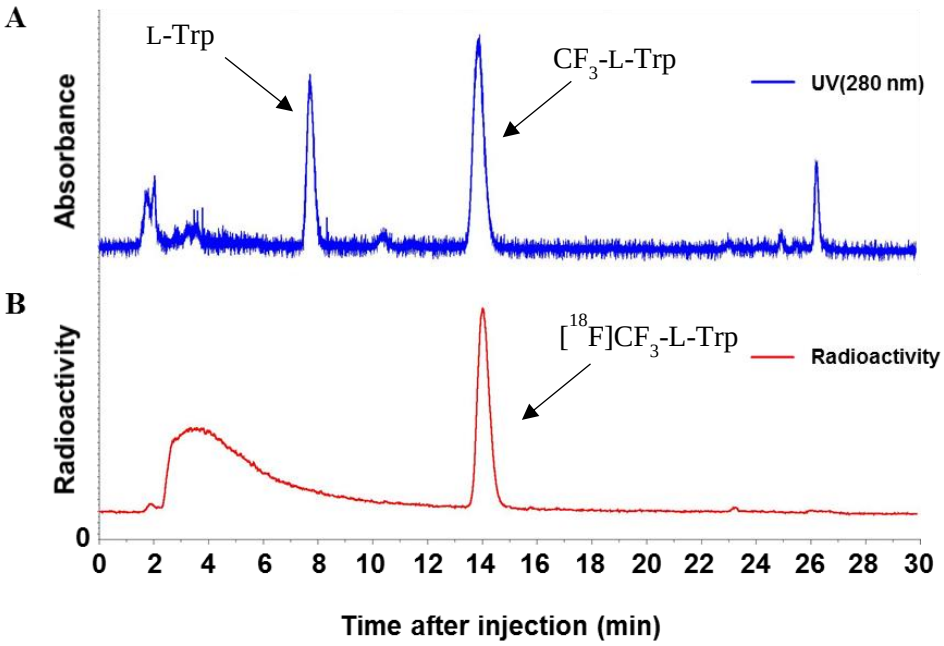

FIGURE 6. HPLC chromatograms of reaction mixrue of $[^{18}F]CF_3$-L-Trp for purification. Chromatograms were obtained by (A) UV (280 nm) (B) radioactivity detection.

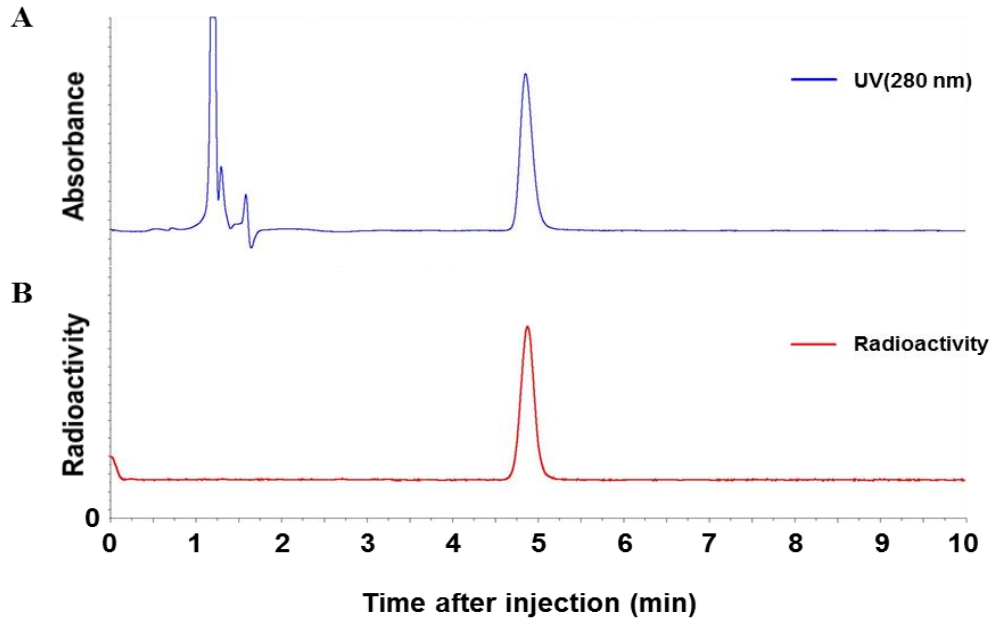

FIGURE 7. Analytical HPLC chromatograms of non-radioactive CF_3-Trp (A) and radioactive [^{18}F]CF_3-L-Trp (B) after purification. Chromatograms were obtained by (A) UV (280 nm) (B) radioactivity detection.

3.1.4 Stability test

Prior to *in vivo* application, we performed *in vitro* characterization of [^{18}F]CF_3-L-Trp. Decomposition of [^{18}F]CF_3-L-Trp increases non-specific accumulation and has an undesirable effect on brain PET imaging. Stability studies of [^{18}F]CF_3-L-Trp were performed in the prepared medium (7% ethanol) at room temperature for 6 h, and in mouse or human serum at 37 °C for 6 h. [^{18}F]CF_3-L-Trp did not degrade at all in the 7% ethanol solution, which indicated that it can be stored at room temperature at least

for 6 h. In mouse or human serum, less than 3% of the decomposed product was detected over the entire time period investigated (Figure 8).

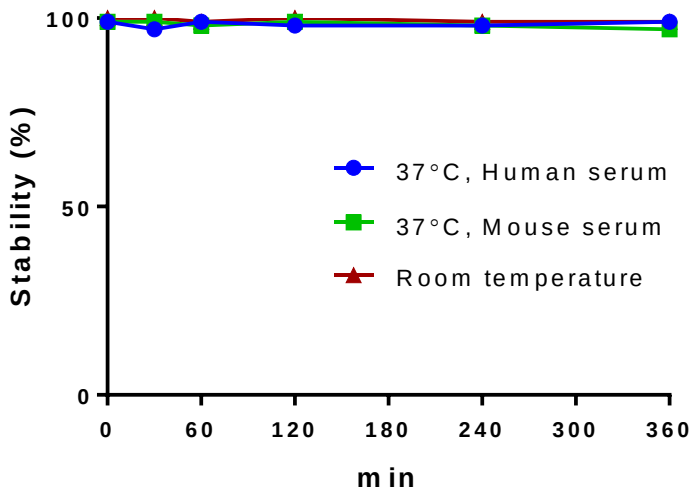

FIGURE 8. Stability test results of [^{18}F]CF_3-L-Trp. [^{18}F]CF_3-L-Trp was incubated with human and mouse sera at 37 °C and with 7% EtOH at room temperature.

3.1.5 Serum protein binding assay

Serum protein binding was measured by incubating [^{18}F]CF_3-L-Trp in mouse or human serum at 37 °C for 10 and 60 min and subsequently separating the free and bound fractions by gel filtration. The separated fractions were analyzed using a gamma counter, and the protein-bound percentages were calculated using the measured radioactivity values. [^{18}F]CF_3-L-Trp showed low binding to human and mouse serum protein: 0.12% and 0.26% to human serum protein at 10 and 60 min,

respectively, and 0.1% and 0.34% to mouse serum protein at 10 and 60 min, respectively (Table 2). Thus, the majority of [^{18}F]CF_3-L-Trp would be present as the free form in blood, which could favor its transport into the brain via amino acid transporters.

TABLE 2. Protein bound fractions (%) of [^{18}F]CF_3-L-Trp in human and mouse sera at 37°C.

	Protein bound (%)	
	Human serum	Mouse serum
10 min	0.12 ± 0.01	0.10 ± 0.00
60 min	0.26 ± 0.03	0.34 ± 0.02

3.1.6 Biodistribution study

The systemic distribution of [^{18}F]CF_3-L-Trp was investigated in BALB/c mice at 10 and 60 min after intravenous injection through the tail vein (Table 3). The enantiomer [^{18}F]CF_3-D-Trp was also studied simultaneously for comparison rather than using a blocking agent such as 2-amino-2-norbornanecarboxylic acid (BCH).

The uptake of [^{18}F]CF_3-L-Trp (2.06 ± 0.22% ID/g) was significantly higher than that of [^{18}F]CF_3-D-Trp (0.48 ± 0.04% ID/g) at 10 min in the mouse brain ($p < 0.01$). This result suggests that [^{18}F]CF_3-L-Trp can penetrate BBB via the L-type amino acid transport system (LAT).

Muscle, heart, and bone also showed significantly higher uptakes of [^{18}F]CF_3-L-Trp than [^{18}F]CF_3-D-Trp ($p < 0.01$) at 10 min. These results also indicate the specific uptake of L-form amino acids in these tissues through the LAT. The higher uptakes of [^{18}F]CF_3-L-Trp in brain, muscle, and bone were persistent until 1 h.

However, in blood, the radioactivity of [^{18}F]CF_3-D-Trp (3.48 ± 0.24% ID/g) was significantly higher than that of [^{18}F]CF_3-L-Trp (2.75 ± 0.09% ID/g) at 10 min. The high blood activity of [^{18}F]CF_3-D-Trp was attributed to its lower uptake in various tissues. [^{18}F]CF_3-D-Trp showed significantly higher uptake in the spleen and lungs at 10 min, which also indicated that the high blood activity contributed to radioactivity in blood-rich organs such as the spleen and lungs.

Both tracers showed the highest uptake level in the kidney at 10 min (10.33 ± 0.93% ID/g for [^{18}F]CF_3-L-Trp and 11.31 ± 1.17% ID/g for [^{18}F]CF_3-D-Trp). The bone uptakes of [^{18}F]CF_3-L-Trp were 6.80 ± 0.74 and 9.34 ± 0.62% ID/g at 10 and 60 min, respectively, and were significantly higher than that of [^{18}F]CF_3-D-Trp ($p < 0.01$) at all the investigated time points. The high radioactivity in bone indicated the possibility of *in vivo* defluorination. The degree of *in vivo* defluorination was considered to be higher for [^{18}F]CF_3-L-Trp than [^{18}F]CF_3-D-Trp.

TABLE 3. Results of the biodistribution study of [^{18}F]CF_3-L-Trp and [^{18}F]CF_3-D-Trp in normal BALB/c mice. Data are % ID/g tissue (mean ± SD, n = 4)

Isomer	**L**		**D**	
Tissue	**10 min**	**60 min**	**10 min**	**60 min**
Blood	2.75 ± 0.09**	0.59 ± 0.10	3.48 ± 0.24	0.55 ± 0.06
Muscle	1.52 ± 0.03**	0.88 ± 0.11**	0.89 ± 0.11	0.42 ± 0.04
Brain	2.06 ± 0.22**	0.43 ± 0.08**	0.48 ± 0.04	0.24 ± 0.01
Heart	3.19 ± 0.20**	0.58 ± 0.10	1.94 ± 0.20	0.72 ± 0.24
Lung	2.59 ± 0.19**	0.67 ± 0.16	3.42 ± 0.21	0.60 ± 0.05
Liver	3.35 ± 0.09	0.68 ± 0.16*	3.82 ± 0.37	0.38 ± 0.05
Spleen	2.88 ± 0.07**	0.47 ± 0.05	3.85 ± 0.28	0.49 ± 0.06
Stomach	2.58 ± 0.32	0.40 ± 0.16	2.80 ± 0.42	0.38 ± 0.09
Intestine	3.02 ± 0.20	1.08 ± 0.15	2.88 ± 0.38	1.00 ± 0.24
Kidney	10.33 ± 0.93	2.05 ± 0.27**	11.31 ± 1.17	0.86 ± 0.15
Bone	6.80 ± 0.74**	9.34 ± 0.62**	3.54 ± 0.57	2.69 ± 0.29

Depicted p values (2-tail t-test) refer to differences between the L- and D-isomers. *p < 0.05; **p < 0.01.

3.1.7 PET/MR study in rats (n=3 at each time point)

Static PET/MR images were obtained at 5, 10, 20, 40 and 80 mins after intravenous administration of [^{18}F]CF_3-L-Trp into Sprague-Dawley rats. Whole brain

activities were plotted with time and The whole-brain radioactivity peaked at 10 min and then decreased (Figure 8A). PET/MR images at 10 min showed wide distribution of [^{18}F]CF_3-L-Trp in the rat brain (Figure 8B) and the distribution pattern was different with other known serotonin synthesis imaging PET agent. In particular, the uptake of raphe nucleus (dorsal and medial), which are known to be present in the cell body of serotonergic neurons was comparatively very low. Instead, pineal gland, thalamus, hypothalamus and midbrain showed particularly high uptake. Pineal gland metabolize serotonin to melatonin to modulate sleep patterns and other regions were known to be present in terminal nerves of serotonergic neurons and serotonin transporter (SERT). However, the distribution pattern in the brain alone could not demonstrate the involvement of [^{18}F]CF_3-L-Trp in serotonin metabolism, the low uptake in raphe nucleus, and the state of [^{18}F]CF_3-L-Trp in the brain.

The specific uptake regions of [^{18}F]CF_3-L-Trp in the rat brain could not be clearly distinguished from adjacent regions due to the low spatial resolution of micro PET system. In addition to brain uptake, high radioactivity was accumulated in bone because of the *in vivo* defluorination of [^{18}F]CF_3-L-Trp. Another PET tracer 7-[^{18}F]fluorotryptophan also showed the highest radioactivity in pineal gland and also high uptake in serotonergic neuron rich regions like dorsal raphe nucleus and hypothalamus.[23] On the other hand, [^{18}F]CF_3-L-Trp showed faster wash out than 7-[^{18}F]fluorotryptophan from those regions, which represents the rapid excretion of it from the neuronal cells or inhibited reuptake of it into the neuronal cells.

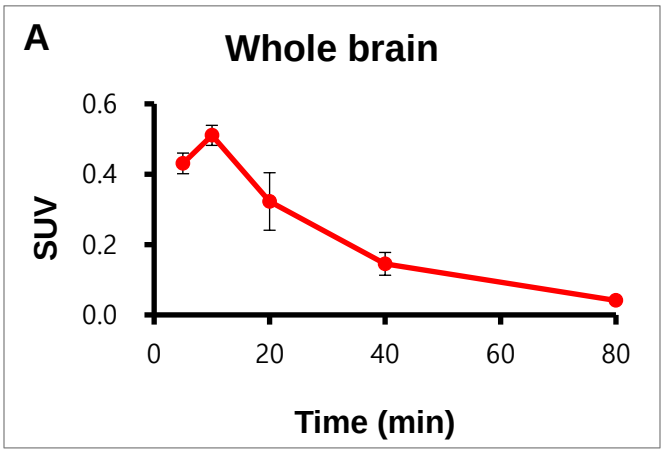

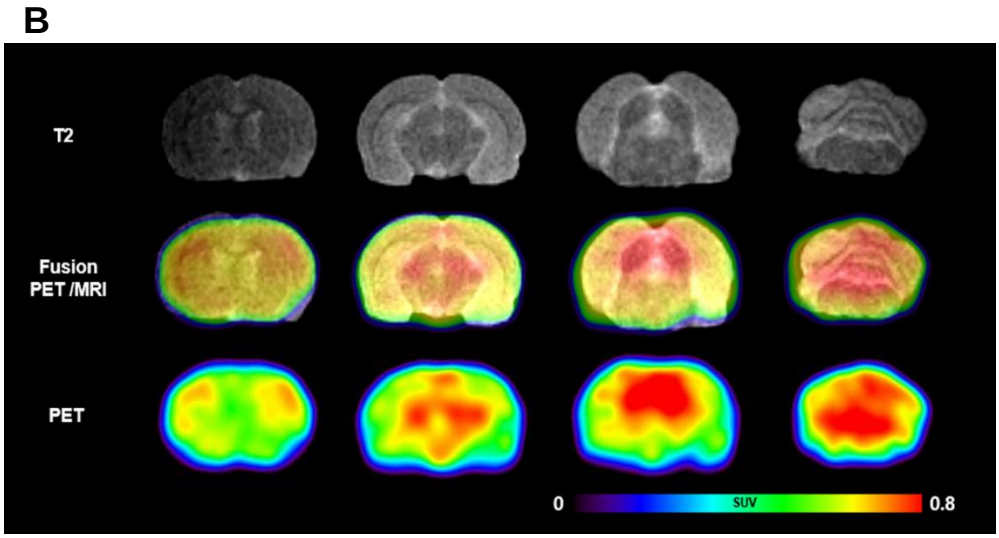

FIGURE 9. PET/MR imaging of [^{18}F]CF_3-L-Trp in SD rats (n=3 at each time point). Static data was acquired at 5, 10, 20, 40 and 80 mins. (A) Whole brain activities were plotted with time after intravenous administration of [^{18}F]CF_3-L-Trp (199±10 MBq). (B) Representative brain images were simultaneously obtained at 10 min after intravenous administration of [^{18}F]CF_3-L-Trp (204 MBq). SUV: Standardized uptake value, defined as activity (MBq/mL) within the volume of interest divided by the injected dose per body weight (MBq/g).

3.1.8 Autoradiography

We then performed autoradiography, which provides higher spatial resolution images than PET, to observe the distribution pattern of [^{18}F]CF_3-L-Trp in the rat brain more clearly (Figure 10). Based on the results of the PET studies, the autoradiography time using [^{18}F]CF_3-L-Trp was set to 10 min after injection, since the uptake of [^{18}F]CF_3-L-Trp in the brain was highest at 10 min.

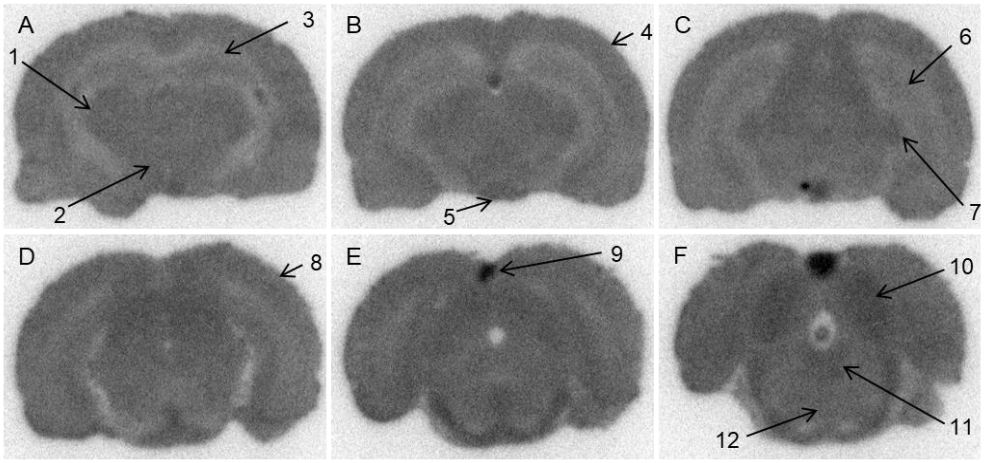

FIGURE 10. Brain autoradiography of [^{18}F]CF_3-L-Trp in a rat brain. The SD rat was sacrificed 10 min after intravenous injection of [^{18}F]CF_3-L-Trp (328 MBq). Frozen sections with a thickness of 30 μm were obtained by cryostat microtome, and autoradiograms were obtained using BAS imaging plates. Some of the structures clearly visualized include the (1) thalamus, (2) hypothalamus, (3) hippocampus (dorsal), (4) parietal cortex, (5) mammillary body, (6) hippocampus (ventral), (7) medial geniculate nucleus (8) occipital cortex (9) pineal body (10) superior colliculus (11) dorsal raphe nucleus, and (12) medial raphe nucleus.

The distribution pattern of [^{18}F]CF_3-L-Trp was related to the serotonergic neurons. The highest accumulation of [^{18}F]CF_3-L-Trp was observed in the pineal gland (5.41%

ID/g). The pineal gland is an endocrine gland that modulates the sleep pattern by producing melatonin from serotonin. Other serotonergic-neuron-rich brain regions such as the parietal cortex, hippocampus (ventral and dorsal), mammillary body, thalamus, hypothalamus, and raphe nucleus (dorsal, medial) also showed high uptakes. Relatively low uptake of [^{18}F]CF_3-L-Trp was observed in the white matter. Another autoradiography study using a serotonergic agent [^{14}C]AMT also reported high accumulation in pineal gland.[39] Similarly with [^{18}F]CF_3-L-Trp, [^{14}C]AMT also accumulated in caudate, parietal cortex, thalamus, hypothalamus, hippocampus, and mamillary body, that was consistent with this study. However, high uptake in dorsal raphe nucleus was not found unlike with [^{14}C]AMT.[39]

3.1.9 Metabolites study

To investigate whether CF_3-L-Trp is metabolized to CF_3-5-HTP or CF_3-serotonin by tryptophan hydroxylase, non-radioactive CF_3-L-Trp was injected into normal BALB/c mice through the tail vein, and the metabolites of CF_3-L-Trp in the brain, blood, and urine were analyzed using HPLC at 10 and 60 min post-injection (Figure 11). In the chromatograms, the CF_3-serotonin peaks had relative areas of 9% and 31% in the brain at 10 and 60 min, respectively, and the CF_3-5-HTP peak was not detected (Figure 11B). Thus, CF_3-L-Trp was metabolized into CF_3-serotonin by serotonin metabolism in serotonergic system. However, as with [^{11}C]AMT, it was limited to provide the absolute serotonin synthesis rate due to the presence of large portion of unmetabolized CF_3-L-Trp in the brain.

A CF_3-tryptamine peak with a slightly shorter retention time than and a similar area to that of the CF_3-serotonin peak was observed at 60 min in the brain. It could be synthesized by decarboxylation of CF_3-L-Trp. The CF_3-serotonin peaks in the blood had relative areas of 7% and 78% at 10 and 60 min, respectively. No CF_3-5-HTP peak was found in the blood (Figure 11C). Only the CF_3-L-Trp peak was observed in the urine (Figure 11D). The mass spectrum (*m/z*) of the CF_3-serotonin metabolite peak was recorded using LTQ mass spectrometry, and the ESI-MS positive ion of CF_3-serotonin was found at *m/z* 245.25 (calculated *m/z* of $C_{11}H_{12}F_3N_2O^+$: 245.23) (Figure 12). A higher level of CF_3-serotonin was detected in the blood than in the brain because the circulating platelets lead to increased serotonin uptake.[40]

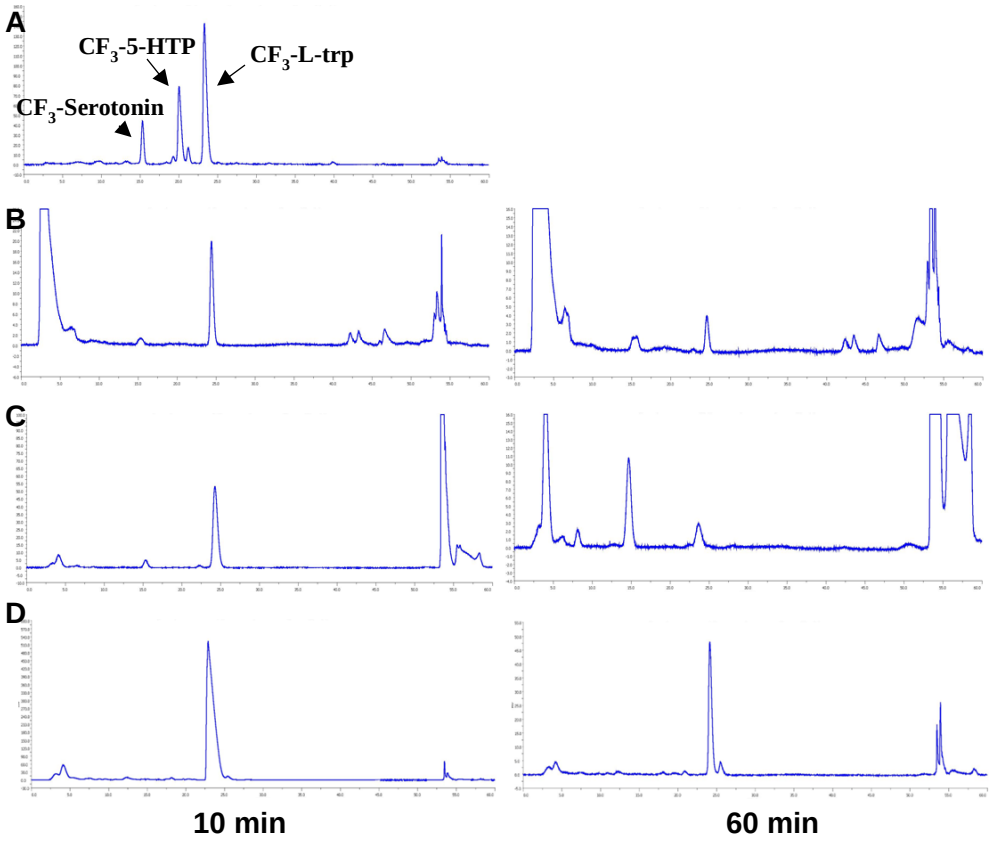

FIGURE 11. HPLC chromatograms of CF_3-L-Trp metabolites in BALB/c mice at 10 and 60 min. The chromatograms show (A) the synthesized standards; and metabolites from (B) the whole-brain homogenate, (C) the plasma, and (D) the urine.

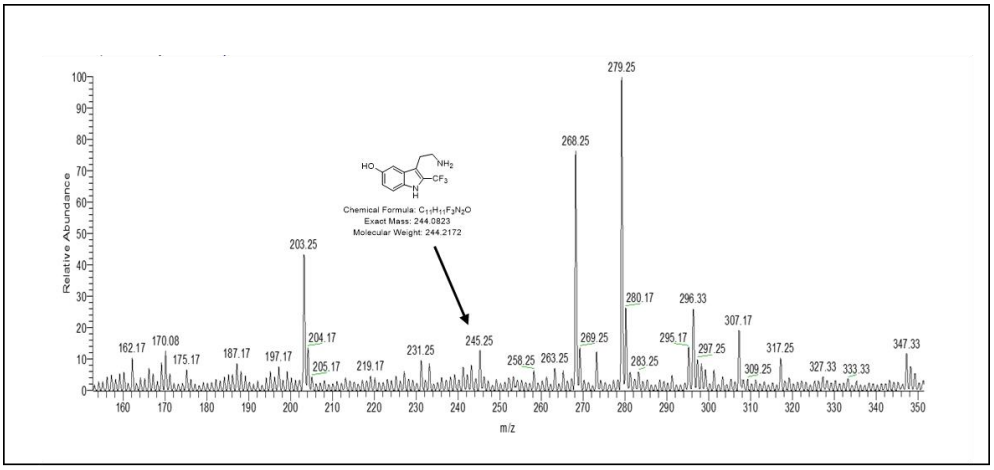

FIGURE 12. Mass spectra of CF_3-serotonin metabolite. The sample was obtained from brain homogenates at 60 min after intravenous administration of CF_3-L-Trp.

3.2 [^{18}F]Trifluoromethyl-L-α-methyltryptophan ([^{18}F]CF_3-L-AMT)

3.2.1 Chemistry

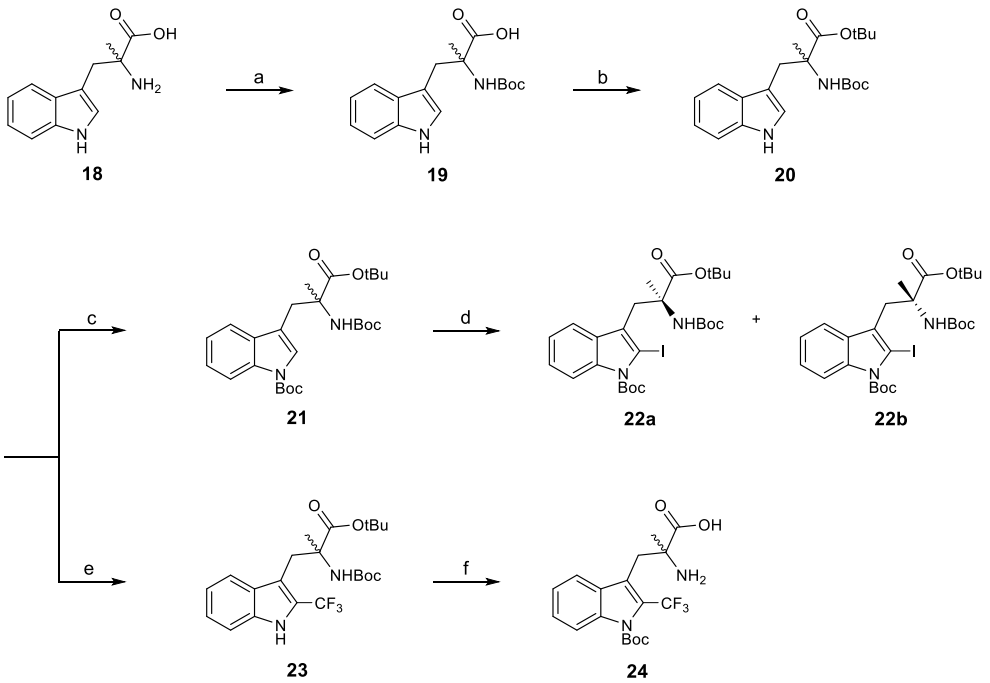

SCHEME 6. Synthesis of precursors (22a and 22b) and non-radioactive standard. Reagents and conditions: a) $(Boc)_2O$, Et_3N, MeOH, RT, overnight, 99%; b) $(CH_3)_3C$-Br, K_2CO_3, BTEAC, DMAC, 55°C, 2.5 h, 49%; c) $(Boc)_2O$, DMAP, DCM, RT, 15 min, 99%; d) $Hg(OTf)_2$, I_2, KI, DCM (1:1), RT, 41%, e) CuI, Togni's reagent (contains 60% diatomaceous earth), MeOH, 70°C, 2 h, 48%; f) TFA, $HSCH_2CH_2SH$, $(CH_3)_2S$, 0°C to RT, 48 h, 88%.

Synthesis of L- or D-iodo AMT (I-AMT) as precursor is shown in **scheme 6**. We used commercially available racemic (R,S)-AMT for starting material. Enantiopure AMT was very expensive and during the reactions, it could be racemized to make the other enantiomer. Since the primary amine or carboxylic acid decreases the radiolabeling efficiency of [^{18}F]trifluoromethylation[30], both groups should be protected not to influence the reactivity for radiolabeling. For simple and fast removal of protection groups under a mild condition after labeling, we protected primary amine at α-position with t-butoxycarbonyl (Boc) group to afford **19** in 99% yield. After removal of solvent, the tert-butyl esterification was performed in a same reaction RBF without purification (**20**, 49%). Because the amine in the indole ring also could affect the labeling efficiency, we protected the secondary amine with Boc group using 4-dimethylaminopyridine (DMAP). After reaction, we could remove DMAP easily in a work-up using aq 1 N HCl to yield **21**. (99%)

To radiolabel [^{18}F]trifluoromethylation, arenes or heteroarenes need to be activated with iodine for the cross-coupling. Even if the carbon on 2 position of indole ring can be labeled without any functionalization, radiolabeling efficiency of [^{18}F]trifluoromethylation was under 10% which was not sufficient to apply for the further experiments. Therefore, the iodination at 2 position of indole ring was necessary to obtain higher radiolabeling efficiency and not to make other regioisomers.

At first we tried palladium(II) mediated iodination to introduce iodine at 2 positon of indole ring without racemization[27]. But this method required multi steps and we

could not use the enantioprue AMT for the starting material. So we tried mercury(II) mediated iodination. This method was only single step and could be applied to the protected AMT **21**. With this method, the intermediates purification steps were not needed except for NMR or Mass spectrometry assay.

Tyrptophan has two enantiomers, the naturally occurring L-tryptophan and the artificially synthesized D-tryptophan, and mainly the natural L-tryptophan isomer penetrate the BBB. We expected that [^{18}F]CF_3-AMT would have similar character. Therefore, the synthesis of L-isomer is required to prevent the undesired radiation exposure. Since the I-AMT is racemic mixtures, we have to separate the mixture into the each enantiomer. Conventional method to prepare the enantiomer is using the chiral auxiliary but it needs extra steps, introduction and removal of the auxiliary. Moreover, the other enantiomer still remains even after purification. To solve the problems and to save the time and cost, we used simple HPLC purification method using chiral column. The mobile condition was 2.5% IPA in n-Hex, so it was easy. And the retention time of **22a** and **22b** were sufficient to be purified to 9.9 min and 11.3 min (Figure 13).

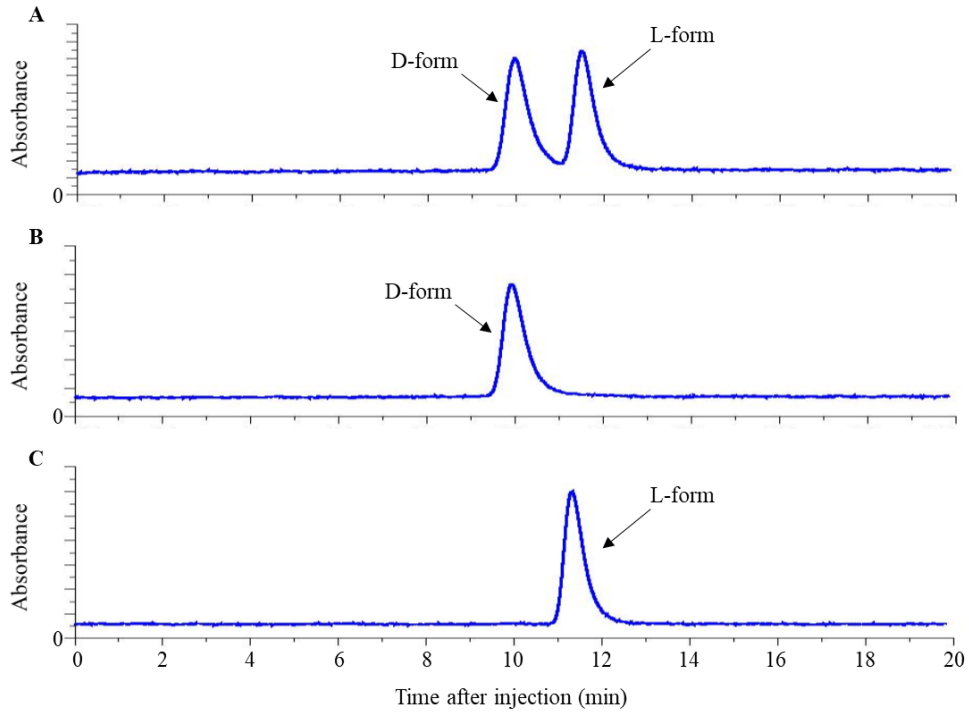

FIGURE 13. HPLC chromatograms of racemic mixture of protected I-AMT (22) (A), L-isomer of protected I-AMT (22a) (B) and D-isomer of protected I-AMT (22b) (C). Blue: UV (280 nm). Chromatograms were obtained on a Diacel Chiralpak ID column. Mobile phase was 2.5% Isopropyl alcohol in *n*-Hexane and flow rate was 5 ml/min.

Non-radioactive CF_3-AMT **7** was synthesized by electrophilic substitution using togni's reagent[38] (Scheme 6). The intermediate was the same as that for synthesizing precursor and trifluoromethyl group was easily displaced to the 2 position of indole ring (**23**, 48%). Previous experience with removing the protection groups of 2-fluorotryptophan has led to a careful attempt to deprotect Boc and t-butyl ester. We tried TFA/radical scavengers combination to afford standard compound[41]. We used

dimethyl sulfide and 1,2-ethanedithiol as scavengers, and unlike 2-fluorotryptophan, no significant degradation was detected in preparative HPLC chromatography. After lyophilization, we obtained white solid of **24** in yield of 88%.

3.2.2 Radiosynthesis

It was difficult to introduce [^{18}F]fluorine itself at 2 position of indole ring due to the high electron density and stability. To increase the availability of [^{18}F]labeled tryptophan, we tried copper(I) mediated [^{18}F]trifluoromethylation by cross coupling. We want to apply the [^{18}F]trifluoromethylation for the late stage, but it was reported that free amine and carboxylic acid decrease the radiolabeling efficiency in the previous research. So, using protected 2-iodo AMT, we optimized the condition for [^{18}F]trifluoro methylation at 2 position of indole ring (Table 4). The drawback of this method is to use large amount of precursor and yield the low specific activity of [^{18}F]trifluoromethylated compound. Even if the molar activity of tracer for metabolism imaging is not crucial comparing to the receptor imaging, **24** could block the transport of [^{18}F]CF_3-AMT into the brain. To increase the molar activity, we tried the different condition of labeling reaction to find out the minimal amount of precursor and 2.7 mg of precursor was sufficient to yield [^{18}F]**25a** or [^{18}F]**25b** in manual (Entry **2**). After labeling, we tried deprotection of Boc groups in a one-pot reaction using acid such as 4 N HCl in 1,4-dioxnae, trifluoroacetic acid (TFA) or aq 1 N HCl. When we use 4 N HCl in 1,4-dioxane under room temperature, we found out the indole was easily broken. On the other hand, TFA or aq 1 N HCl could remove

the protection groups not making significant degradation of indole ring. TFA was not proper to use in the Fx-Fn automation module due to the corrosive vapor.

For the preclinical studies in practical, we set up the condition for labeling in the Fx-Fn automation module (Scheme 7). We increased the amount of **22a** or **22b** (10.8 mg, 18 μmol), MCFDA (9 μL), TMEDA (13.5 μL) and DMF (300 μL) in the module and obtained the protected [^{18}F]**25a** or [^{18}F]**25b** in over 50% yield by ITLC. The reaction temperature would be good at 150°C. When the temperature was increased, DMF was dried soon and when the temperature was decreased, the labeling efficiency was decreased. For the last, the reaction time over 15 min could not help to increase the labeling efficiency. As in manual, aq 1 N HCl worked successfully in one-pot reaction. On the other hand, HCl in organic solvent, such as methanol, made it difficult to purify [^{18}F]CF_3-L-AMT or [^{18}F]CF_3-D-AMT by the all compounds coming together on the preparative HPLC system. We used 0.3% acetic acid buffer and ethanol and the purified solution of [^{18}F]CF_3-L-AMT or [^{18}F]CF_3-D-AMT involved in 17~18% ethanol. To neutralize the pH and decrease the portion of ethanol for injection, we added 8.4% $NaHCO_3$ into the solution and it was diluted with normal saline. We checked pH of the solution was ~7 by pH paper and controlled ethanol content was under 10%. Gas chromatography confirmed that the amount of organic solvent such as acetonitrile, DMF was negligible in the final product solution.

TABLE 4. Optimization of the amount of substrate and reagents or reaction solvent for [^{18}F]trifluoromethylation.

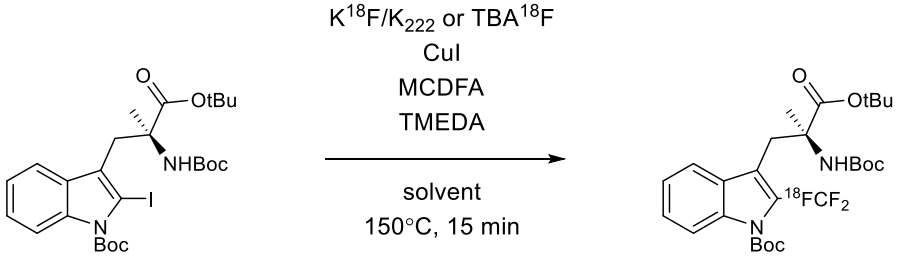

22a **25a**

Entry	Substrate (mg)	Reagents			Solvent[a]	RCC(%)[b]
		CuI	MCDFA	TMEDA		
1	1.4	11 mg	6 μL	9 μL	DMF	35.4
2	2.7	11 mg	6 μL	9 μL	DMF	72.1
3	5.4	11 mg	6 μL	9 μL	DMF	65.7
4	2.7	11 mg	12 μL	16 μL	DMF	-[c]
6	2.7	11 mg	6 μL	9 μL	DMSO	0

Solvent volume was 200 μL; b) RCC(%) was measured based on the ITLC (95% CH_3CN);Reaction solution became slugge; MCDFA : Methyl chlorodifluoroacetate, TMEDA : N,N,N,N-Tetramethylethylenediamine.

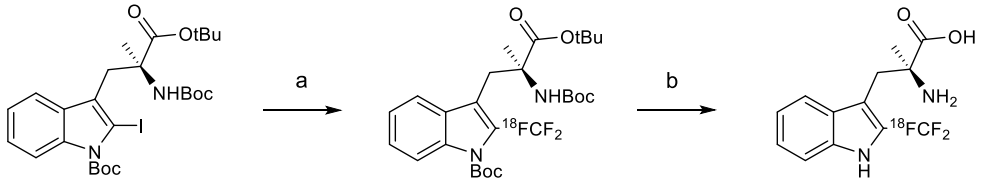

22a **25a** **[^{18}F]CF$_3$-L-AMT**

SCHEME 7. Radiosynthesis of [^{18}F]CF$_3$-L-AMT. Reagents and conditions: a) K_{222}/K_2CO_3 or TBAB, CuI, MCDFA, TMEDA, DMF, 150°C, 15 min; b) aq 1N HCl, 110°C, 12 min.

We took the analytical HPLC chromatogram of [^{18}F]CF$_3$-L-AMT after purification and the retention time was 7.2 min, which was similar to the non-radioactive standard **24** (Figure 14a). According to the Figure 14b, the radiochemical purity was over 99% and no other radioactive or non-radioactive compounds were detected. To measure the molar activity of [^{18}F]CF$_3$-L-AMT, we draw standard curve with 5 different concentrations of **24**. The molar activity was 1188±248 MBq/μmol (n=9) after purification and 880±270 MBq/μmol (n=12) for injection which was higher than the molar activity of [^{11}C]AMT (55mCi/mmol)[42]. As the time passed by, the molar activity was decreased, we did all animal studies as fast as possible. It is also important to confirm the enantiomeric purity of prepared product. Because L-form mainly penetrate the BBB[43] to image the serotonergic system, D-form may give the additional radiation exposure. We tried several kinds of chiral columns but only chiralpak®WH column which was packed with amino acid derivative and copper(II) complex could separate the each enantiomer completely. We checked the enantiomeric purity of [^{18}F]CF$_3$-L-AMT or [^{18}F]CF$_3$-D-AMT after purification and

the retention time was 13.8 and 43.5 min respectively (Figure 15). No racemization was detected to yield over 99% enantiomeric pure product.

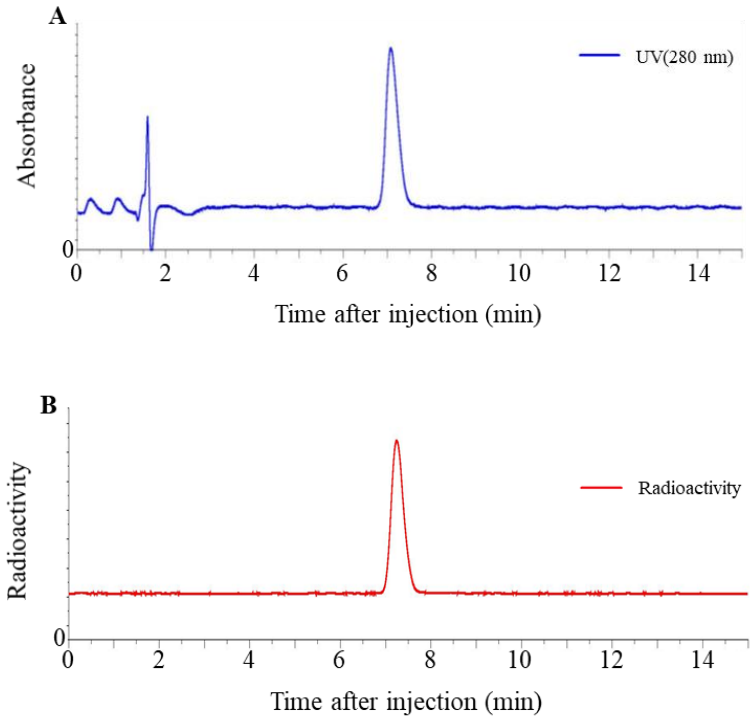

FIGURE 14. Analytical HPLC chromatograms of the non-radioactive standard 24 (A) and [^{18}F]CF_3-L-AMT (B) after purification. Chromatograms were obtained by UV (280 nm) (A) and radioactivity (B).

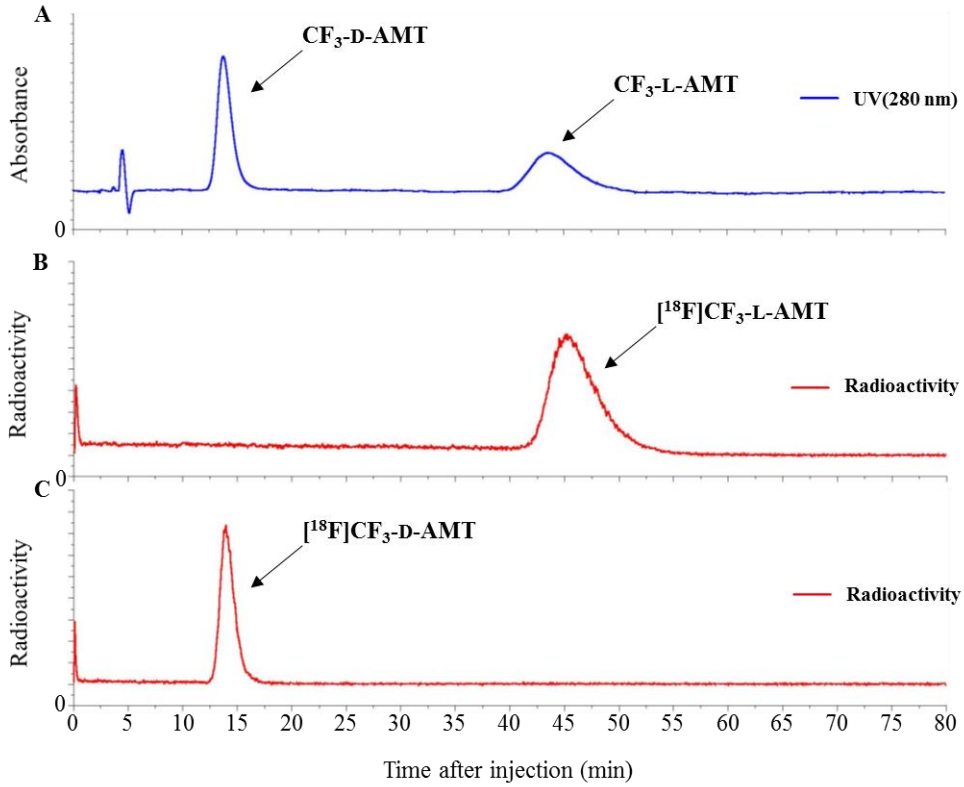

FIGURE 15. HPLC chromatograms of racemic mixture of the non-radioactive standard (24) (A), radioactive [^{18}F]CF$_3$-L-AMT (B), and [^{18}F]CF$_3$-D-AMT (C). Blue: UV (280 nm), Red: Radioactivity. Chromatograms were obtained on a Diacel Chiral pak WH column. Mobile phase was 10 mM $CuSO_4$ and MeOH (9:1) and flow rate was 1.5 ml/min. Column temperature was 50^{o}C.

3.2.3 Stability test

Before applying [^{18}F]CF_3-L-AMT into the *in vivo* system, in vitro stability tests in human and mouse serum at 37°C and in prepared medium at room temperature were performed. We checked the stability at 0, 0.5, 1, 2, 4, 6 h and during the period no significant degradation form was detected in all conditions. It indicates that the [^{18}F]CF_3-L-AMT could be stored at room temperature for 6 h prior to injection and would not make any radioactive degraded compounds which influence the brain uptake of [^{18}F]CF_3-L-AMT in serotonergic system.

3.2.4 Biodistribution (in mice)

We investigated the biodistribution using [^{18}F]CF_3-L-AMT or [^{18}F]CF_3-D-AMT in brain, blood, and 9 organs at 10, 60, and 120 min after injection in normal BALB/c mice (Table 5). It was helpful to evaluate the distribution in the whole body as well as the brain for understanding the characteristics and radiation exposure in each organs. The main excretory pathway of both tracers was found to be through the kidney (25.49±1.86% ID/g for [^{18}F]CF_3-L-AMT and 36.89±5.54% ID/g for [^{18}F]CF_3-D-AMT at 10 min). Similar to the results of autoradiography, biodistribution study showed that the initial uptake of [^{18}F]CF_3-L-AMT in brain (2.27±0.14% ID/g) was much higher than that of [^{18}F]CF_3-D-AMT (0.34±0.03% ID/g). These results confirmed that L-isomer can be applied to serotonin metabolism through the BBB by LAT and that the penetration of the BBB of D-isomer is limited by the transporter.

Significant amount of radioactivity was found in bone using [^{18}F]CF_3-L-AMT (4.70±0.27% ID/g at 10 min and 4.12±0.35% ID/g at 120 min) compare [^{18}F]CF_3-D-AMT (2.92±0.31% ID/g at 10 min and 1.47±0.14% ID/g at 120 min). Similar to [^{18}F]CF_3-Trp, *in vivo* defluorination of L-isomer was significantly higher than D-isomer. This means that [^{18}F]fluoride was released mainly by the enzymatic metabolism in [^{18}F]CF_3-L-AMT.

TABLE 5. Results of the biodistribution study of [^{18}F]CF_3-L-AMT and [^{18}F]CF_3-D-AMT in normal BALB/c mice. Data are expressed by %ID/g tissue (mean ± SD, n = 4).

Tissue	Isomer	10 min	60 min	120 min
Blood	L	3.02±0.16**	0.70±0.08	0.22±0.03
	D	7.35±0.70	0.78±0.07	0.24±0.02
Muscle	L	1.44±0.07	0.92±0.10**	0.56±0.08*
	D	1.76±0.28	1.16±0.04	0.72±0.05
Brain	L	2.27±0.14**	0.73±0.09**	0.13±0.02**
	D	0.34±0.03	0.11±0.01	0.04±0.00
Heart	L	3.65±0.34	0.95±0.07**	0.29±0.03**
	D	3.37±0.55	1.26±0.08	0.54±0.04
Lung	L	3.34±0.22**	0.86±0.26	0.36±0.02*
	D	6.62±0.42	0.91±0.14	0.29±0.04

Liver	L	5.95±0.29**	1.11±0.17**	0.32±0.05*
	D	18.60±1.41	1.65±0.19	0.42±0.06
Spleen	L	4.01±0.26**	0.72±0.12**	0.35±0.13
	D	5.37±0.64	1.26±0.08	0.45±0.04
Stomach	L	4.28±1.31	0.80±0.08	0.30±0.15
	D	3.37±0.30	0.85±0.15	0.30±0.05
Intestine	L	4.53±0.37**	1.40±0.09**	0.86±0.14
	D	3.63±0.23	1.64±0.06	0.91±0.07
Kidney	L	25.49±1.86**	4.14±0.51	1.32±0.38
	D	36.89±5.54	3.41±0.49	0.94±0.07
Bone	L	4.70±0.27**	4.42±1.70**	4.12±0.35**
	D	2.92±0.31	1.93±0.21	1.47±0.14

3.2.5 Autoradiography (in rat)

Autoradiography using [^{18}F]CF_3-L-AMT or [^{18}F]CF_3-D-AMT was performed to figure out the specific brain distribution pattern in rat brain. Compared with PET, autoradiography could give much higher resolution images. (PET: 1 mm, autoradiography: 100 μm)

We intravenously injected [^{18}F]CF_3-L-AMT or [^{18}F]CF_3-D-AMT without anesthesia due to that it could affect serotonin metabolism and the uptake of tracer in

rat brain. The time for injection was between 4 and 6 P.M to avoid the effect of circadian rhythm. The rats were fasted the night before the experiment because labeled AMT could be competitively inhibited by the amino acid containing in food. Water was provided ad libitum not to exert influence on the mood. The uptake in rat brain was quantified by using the standard solution[44]. To obtain the reliable results, we made the standard curve on the every single autoradiography and all the standard curves had over $R^2 = 0.99$.

The autoradiograms were obtained 5, 10, 20, 40 and 80 min post injection and Figure 16 showed the representative autoradiogram at 20 min. As expected, the whole brain uptake of L-isomer in rat (1.13±0.19 %ID/mm^2) was 9 times higher than D-isomer (0.13 %ID/mm^2) at 20 min post injection. We also performed 10, 40, 80 min as well but the only specific uptake of [^{18}F]CF_3-D-AMT in rat brain was shown in the cerebral blood and pineal gland (Figure 16b). Unlike other brain regions, pineal gland is not isolated from the body by the BBB system. Although we did not perform the competition assay using [^{18}F]CF_3-AMT and LAT inhibitor, 2-amino-2-norbornanecarboxylic acid (BCH), we could directly compare the uptake of enantiopure L-isomer and D-isomer in rat brain. On the basis of these results, we carefully expect that L-isomer could penetrate BBB by L-type amino acid transport system (LAT) which is the major route for neutral aromatic amino acids.

Compared to D-isomer, L-isomer was distributed widely thorough the whole brain (Figure 16a). The highest uptake of [^{18}F]CF_3-L-AMT (4.56±0.20% ID/mm^2) was shown in pineal gland which metabolize serotonin to melatonin to modulate sleep

patterns in circadian rhythm[45,46]. As it is known that the rate of serotonin synthesis in pineal gland is much higher than in other brain regions[14,47], we found dense radioactivity in pineal gland. Mammillary bodies had some uptake (1.27±0.45% ID/mm^2) which are often categorized as part of the hypothalamus and important for recollective memory[48]. Thalamus (1.46±0.08% ID/mm^2) and hypothalamus (1.86±0.04% ID/mm^2) of diencephalon also had distinct distribution of the tracer but at 80 min post injection, it was difficult to figure out those regions. Cortex, such as frontal or parietal cortex (1.24±0.07% ID/mm^2), had mild uptake as well because of their cognitive functions which are related with serotonergic system. Hippocampus (ventral and dorsal) had similar radioactivity at 20 min (1.24±0.07% ID/mm^2 for ventral and 1.18±0.16% ID/mm^2 for dorsal) but at 40 or 80 min post injection, the radioactivity in hippocampus (ventral and dorsal) were relatively increased to distinguish with adjacent regions. Hippocampus is related with memory store and several subtypes of serotonin receptors are located in the region. Amygdala which is limbic areas with hippocampus and related with emotion expression also had the similar distribution pattern with hippocampus. Raphe nucleus (dorsal and medial) had lower uptake of the tracer than as expected. It is because the cell bodies of serotonergic neurons are laid in brainstem raphe nuclei and these neurons are projected to many brain regions like cortex, basal ganglia, thalamus, hypothalamus, limbic areas like hippocampus and amygdala, etc[49].

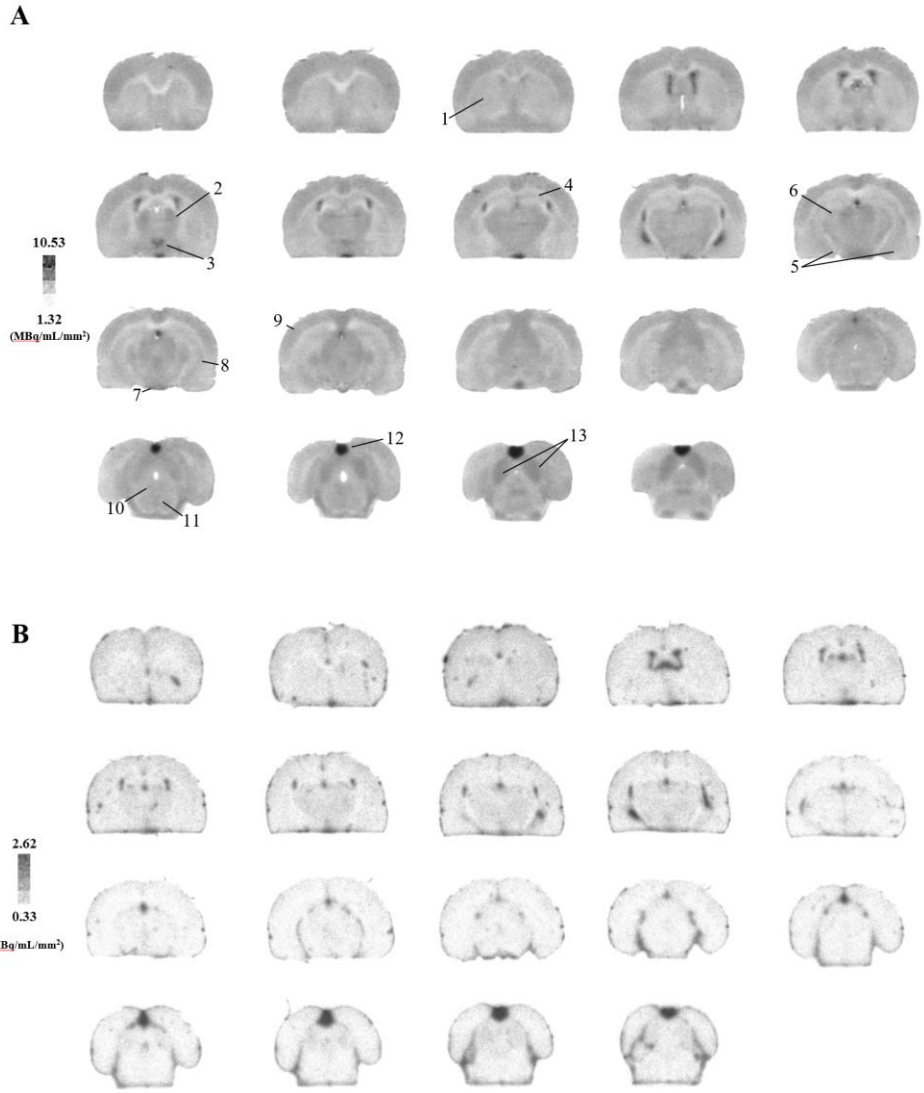

FIGURE 16. Representative autoradiograms in normal SD rat using [^{18}F]CF_3-L-AMT (A) and [^{18}F]CF_3-D-AMT (B). Some of the structures clearly visualized are (1) caudate-putamen, (2) thalamus, (3) hypothalamus, (4) hippocampus (ventral), (5) amygdala, (6) medial geniculate nucleus, (7) mammillary body, (8) parietal cortex (9) hippocampus (dorsal) (10) raphe nucleus (dorsal), (11) raphe nucleus (ventral), (12) pineal gland, (13) superior colliculus. Uptake value (MBq/mL/mm^2) was defined as radioactivity (MBq/mL) within the area of interest.

Li-ion is known to stimulate the synthesis of serotonin, which was once used as a remedy for psychosis[50,51]. To evaluate [^{18}F]CF_3-L-AMT in the serotonin metabolism enhanced model, we treated SD rats with LiCl (85 mg/kg i.p.) 2 times per day for 5 days[52] and the autoradiogram was obtained (Figure 17). The distribution of [^{18}F]CF_3-L-AMT in normal and Li-treated rats were very similar, however the uptake rate and clearance from the brain were different. The distribution patterns in normal and Li-treated SD rats were compared directly with the time-activity curves (TACs) in Figure 18. In normal rats, the uptake of brain regions, except pineal gland, was peaked at 20 min and then decreased into the level of background at 80 min. On the other hand, in Li-treated rats, the uptake rates were faster about 10 min in almost all brain regions and the uptake levels of radioactivity at peak time in some specific brain regions, such as mammillary body or hypothalamus were higher than in normal rats. At 80 min after injection, the radioactivity level (% ID/mm^2) in Li treated rats was remained 2 times more than in normal rats. The results indicate that the uptake rate of [^{18}F]CF_3-L-AMT was faster and the clearance from the brain was slower in the enhanced serotonin metabolism SD rat than in normal SD rat.

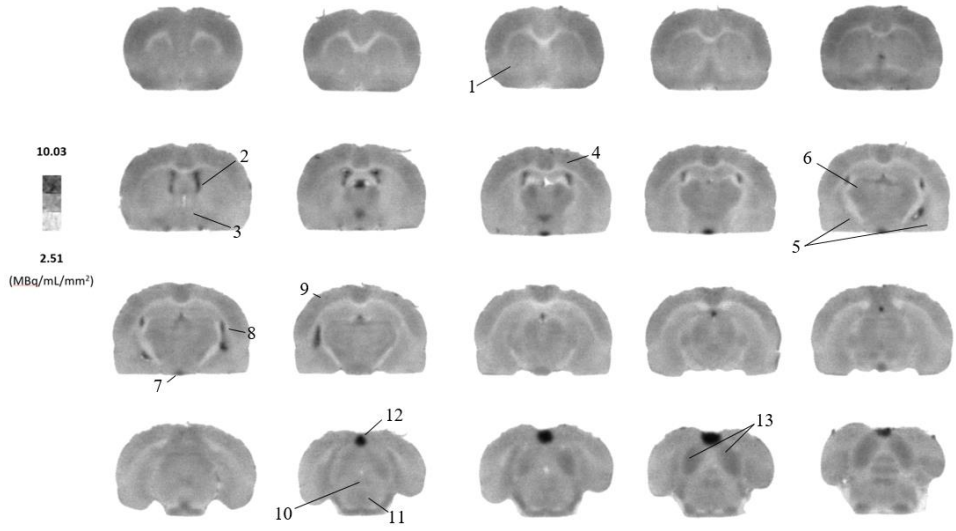

FIGURE 17. Representative autoradiograms in Li-treated SD rat using [^{18}F]CF_3-L-AMT. Some of the structures clearly visualized are (1) caudate-putamen, (2) thalamus, (3) hypothalamus, (4) hippocampus (ventral), (5) amygdala, (6) medial geniculate nucleus, (7) mammillary body, (8) parietal cortex (9) hippocampus (dorsal) (10) raphe nucleus (dorsal), (11) raphe nucleus (ventral), (12) pineal gland, (13) superior colliculus. Uptake value (MBq/mL/mm^2) was defined as radioactivity (MBq/mL) within the area of interest.

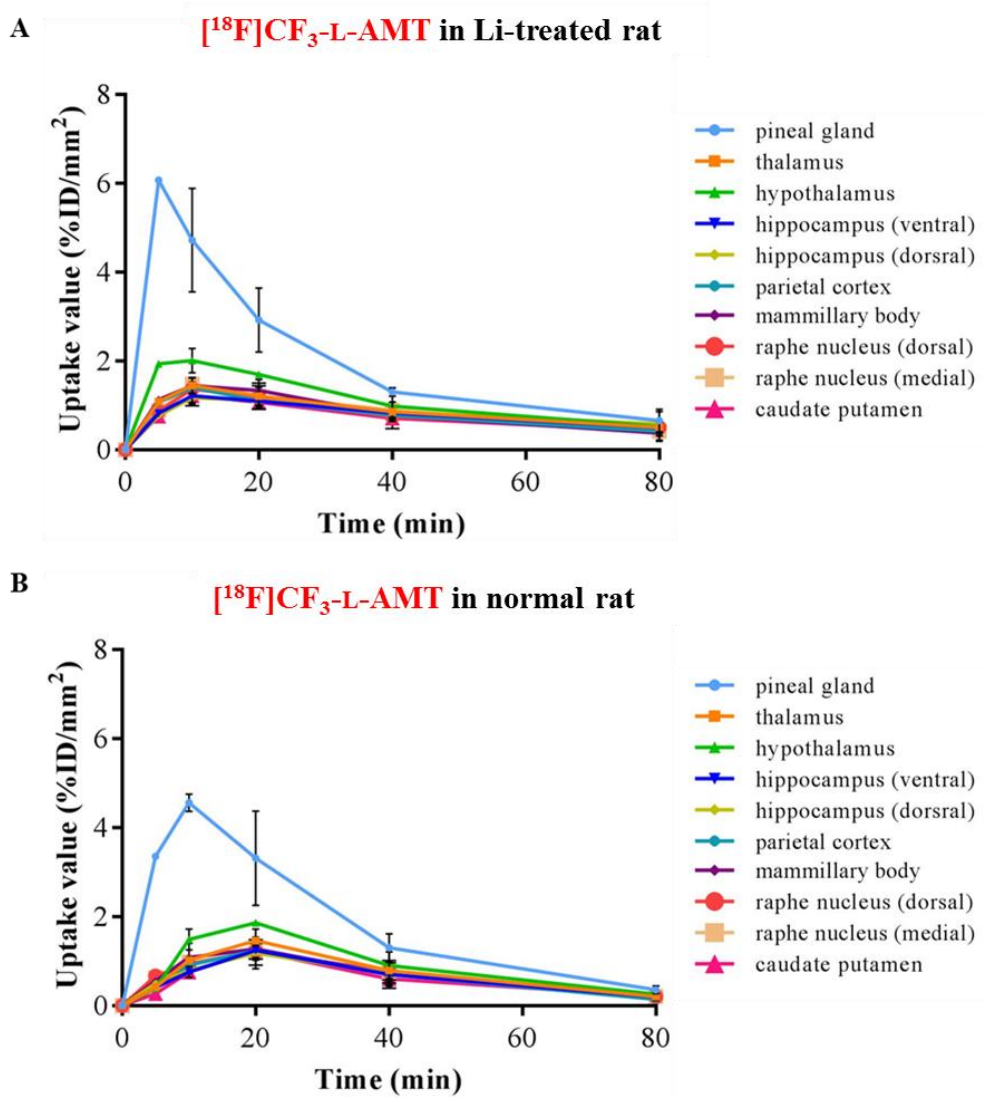

FIGURE 18. Time-activity curves of [^{18}F]CF$_3$-L-AMT in Li-treated SD rat (A) and in normal SD rat (B) at 5, 10, 20, 40, 80 min post-injection (n=2 at each time point). Radioactivity was measured in pineal gland, thalamus, hypothalamus, hippocampus (ventral), hippocampus (dorsal), parietal cortex, mammillary body, raphe nucleus (dorsal), raphe nucleus (medial) and caudate putamen Uptake value was defined as radioactivity (MBq/mL) within the area of interest divided by the injected dose.

TABLE 6. Comparison of the uptake of [^{18}F]CF_3-L-AMT in normal and Li-treated SD rat at 10 and 80 min (n=2 at each time point). Uptake value was defined as radioactivity (MBq/mL) within the area of interest divided by the injected dose.

Structure	10 min			80 min		
	Uptake value (%ID/mm²)			Uptake value (%ID/mm²)		
	Control	Li-treated	Difference (%)	Control	Li-treated	Difference (%)
Pineal body	4.56±0.19	4.72±1.17	2	0.36±0.09	0.66±0.25	29
Thalamus	1.02±0.07	1.45±0.18	17	0.20±0.07	0.51±0.05	43
Hypothalamus	1.49±0.23	2.01±0.28	15	0.25±0.09	0.52±0.04	35
Hippocampus (ventral)	0.75±0.12	1.21±0.19	23	0.20±0.08	0.50±0.14	43
Hippocampus (dorsal)	0.79±0.04	1.17±0.11	20	0.25±0.10	0.58±0.27	40
Parietal cortex	0.91±0.19	1.40±0.21	21	0.14±0.03	0.41±0.20	49
Mammilary body	1.09±0.32	1.45±0.09	14	0.21±0.01	0.38±0.19	29
Raphe nucleus (dorsal)	0.93±0.13	1.37±0.06	19	0.21±0.08	0.51±0.15	42
Raphe nucleus (ventral)	0.98±0.05	1.48±0.05	20	0.21±0.10	0.43±0.16	33
Caudate putamen	0.76±0.13	1.22±0.23	23	0.21±0.10	0.42±0.16	33

3.2.6 Comparison of distribution and metabolism between [^{18}F]CF_3-L-Trp and [^{18}F]CF_3-L-AMT.

To evaluate the effect of α-methylation on tryptophan derivative, the whole body distribution and analysis of metabolites of [^{18}F]CF_3-L-Trp and [^{18}F]CF_3-L-AMT were compared (Figure 19 and Table 7). Since the fast washout in the brain of [^{18}F]CF_3-L-Trp was difficult to obtain PET images and the serotonin synthesis rate, it was needed to develop a labeled tryptophan derivative that could last a long time in the brain as a property of the compound itself, not through the drug. Radiochemical and enantiomeric purity of prepared tracers were over 99%. At 10 min, the brain uptakes of [^{18}F]CF_3-L-AMT and [^{18}F]CF_3-L-Trp were 2.27 ± 0.14 and 2.06 ± 0.22, respectively and the brain uptake of [^{18}F]CF_3-L-AMT (0.73 ± 0.08) at 60 min was

significantly higher than that of [^{18}F]CF_3-L-Trp (0.43 ± 0.08). This result indicated that α-methylation increased the retention in the brain by reducing metabolism by MAO. The bone uptake of [^{18}F]CF_3-L-AMT at 60 min (4.50 ± 0.47) was significantly lower than that of [^{18}F]CF_3-L-Trp (9.34 ± 0.62), suggesting the lower *in vivo* defluorination of [^{18}F]CF_3-L-AMT. Both of the tracers showed high uptakes in the kidney.

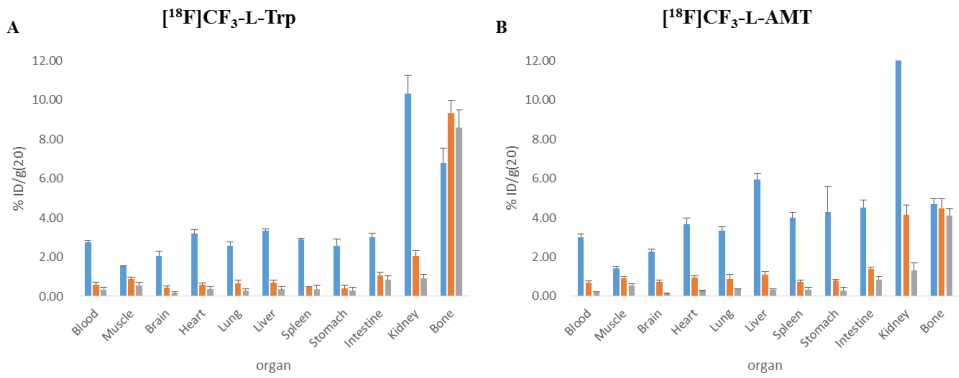

FIGURE 19. Biodistribtuion of [^{18}F]CF_3-L-TRP (A) and [^{18}F]CF_3-L-AMT (B) in normal BALB/c mice at 10, 60, and 120 min post-injection. Values represent mean %ID/g tissue and error bars represent SD (n=4).

TABLE 7. Comparison of brain, blood, and bone distribution of [^{18}F]CF_3-L-Trp and [^{18}F]CF_3-L-AMT in normal BALB/c mice (n=4). Data are % ID/g tissue (mean ± SD, n = 4)

Time (min)	Brain		Blood		Bone	
	[^{18}F]CF_3-L-TRP	[^{18}F]CF_3-L-AMT	[^{18}F]CF_3-L-TRP	[^{18}F]CF_3-L-AMT	[^{18}F]CF_3-L-TRP	[^{18}F]CF_3-L-AMT
10	2.06±0.22	2.27±0.14	2.75±0.09*	3.02±0.16	6.80±0.74*	4.70±0.27
60	0.43±0.08*	0.73±0.09	0.59±0.10	0.70±0.08	9.34±0.62*	4.50±0.47
120	0.17±0.06	0.13±0.02	0.34±0.11	0.22±0.03	8.58±0.91*	4.12±0.35

Depicted p values (2-tail Mann-Whitney test) refer to differences between [^{18}F]CF_3-L-Trp and [^{18}F]CF_3-L-AMT. *$p < 0.05$.

4 CONCLUSION

We successfully synthesized enantiopure [^{18}F]CF_3-L-Trp, which might be resistant to kynurenine pathway enzymes, such as IDO or TDO. Enantiomeric purity could reduce the unnecessary radiation exposure. In PET images and autoradiograms, the distribution of [^{18}F]CF_3-L-Trp in brain showed high uptake in terminal nerves of serotonergic neurons. However, it is not clear that the PET imaging of [^{18}F]CF_3-L-Trp reflect serotonin metabolism due to the low uptake in raphe nucleus. Metabolites study showed that CF_3-L-Trp is metabolized into CF_3-serotonin by serotonin metabolism, but there is a limit to obtain the absolute serotonin synthesis rate because a large unmetabolized form remain in the brain. Another problem CF_3-L-Trp was that rapidly excreted from the brain and did not show any specific brain accumulation. It also took the high *in vivo* defluorination and accumulated in bone.

Based on the these results, [^{18}F]CF_3-L-Trp was not suitable for serotonergic system imaging and need to modify to prolong the residence time in the brain and reduce *in vivo* defluorination. To enhance metabolic character of tryptophan derivative, α-substituted [^{18}F]CF_3-L-AMT was synthesized in the same manner as described for synthesis of [^{18}F]CF_3-L-Trp. Distribution and metabolite study indicated that α-methylation increased the retention of the radiotracer in the brain by reducing metabolism by MAO and decreased *in vivo* defluorination. The low uptake in raphe nucleus and high unmetabolized pool of [^{18}F]CF_3-L-AMT limited the application of this radiotracer for serotonergic system imaging. Nevertheless, experimental data suggest that the distribution patterns of [^{18}F]CF_3-L-AMT in normal and Li-treated SD

rats were related with serotonergic activity and metabolism. Kinetic data may provide information about the disease associated with serotonin synthesis but, it needs some more verifications.

5 REFERENCES

1. Rosa-Neto P, Diksic M, Okazawa h, et al. Measurement of Brain Regional α-[^{11}C]Methyl-L-Tryptophan Trapping as a Measure of Serotonin Synthesis in Medication-FreePatients With Major Depression. *Arch Gen Psychiatry.* 2004;61:556-563.
2. Frick A, Ahs F, Engman J, et al. Serotonin Synthesis and Reuptake in Social Anxiety Disorder: A Positron Emission Tomography Study. *JAMA Psychiatry.* 2015;72(8):794-802.
3. Chugani HT, Kumar A, Kupsky W, Asano E, Sood S, Juhasz C. Clinical and histopathologic correlates of ^{11}C-alpha-methyl-L-tryptophan (AMT) PET abnormalities in children with intractable epilepsy. *Epilepsia.* 2011;52(9):1692-1698.
4. Halmoy A, Johansson S, Winge I, McKinney JA, Knappskog PM, Haavik J. Attention-Deficit/Hyperactivity Disorder Symptoms in Offspring of Mothers With Impaired Serotonin Production. *Arch Gen Psychiatry.* 2010;67(10):1033-1043.
5. Lai MKP, Tsang SWY, Francis PT, et al. Reduced serotonin 5-HT1A receptor binding in the temporal cortex correlates with aggressive behavior in Alzheimer disease. *Brain Research.* 2003;974(1-2):82-87.
6. Orlefors H, Sundin A, Garske U, et al. Whole-body ^{11}C-5-hydroxytryptophan positron emission tomography as a universal imaging technique for neuroendocrine tumors: comparison with somatostatin receptor scintigraphy and computed tomography. *J Clin Endocrinol Metab.* 2005;90(6):3392-3400.
7. Batista CE, Juhasz C, Muzik O, et al. Imaging correlates of differential expression of indoleamine 2,3-dioxygenase in human brain tumors. *Mol Imaging Biol.* 2009;11(6):460-466.
8. Chiotellis A, Mu L, Muller A, et al. Synthesis and biological evaluation of ^{18}F-labeled fluoropropyl tryptophan analogs as potential PET probes for tumor imaging. *Eur J Med Chem.* 2013;70:768-780.

9. Daubert EA, Condron BG. Serotonin: a regulator of neuronal morphology and circuitry. *Trends Neurosci.* 2010;33(9):424-434.
10. Jequier E, Lovenberg W, Sjoerdsma A. Tryptophan Hydroxylase Inhibition: the Mechanism by Which p-Chlorophenylalanine Depletes Rat Brain Serotonin. *Mol Pharmacol.* 1967;3:274-278.
11. Kuhar MJ, Aghajanian GK, Roth RH. Tryptophan hydroxylase activity and synaptosomal uptake of serotonin in discrete brain regions after midbrain raphe lesions: Correlations with serotonin levels and histochemical fluorescence. *Brain Research.* 1972;44(1):165-176.
12. Lovenberg W, Weissbach H, Udenfriend S. aromatic L-amino acid decarboxylase. *J Biol Chem.* 1962;237(1):89-93.
13. King NJ, Thomas SR. Molecules in focus: indoleamine 2,3-dioxygenase. *Int J Biochem Cell Biol.* 2007;39(12):2167-2172.
14. Diksic M, Nagahiro S, Sourkes TL, Yamamoto YL. A New Method to Measure Brain Serotonin Synthesis in vivo. I. Theory and Basic Data for a Biological Model. *J Cereb Blood Flow Metab.* 1990;10:1-12.
15. Chugani DC, Muzik O, Chakraborty P, Mangner T, Chugani HT. Human Brain Serotonin Synthesis CapacityMeasured In Vivo with a-[C-11]Methyl-L-Tryptophan. *Synapse.* 1998;28:33-43.
16. Diksic M, Chaly NT, Sourkes TL, Yamamoto YL, Feindel W. Seorotonin synthesis Rate in Living Dog Brain by Positron Emission Tomography. *Journal of Neurochemistry.* 1991;56:153-162.
17. Missala K, Sourkes TL. Functional cerebral activity of an analogue of serotonin formed *in situ*. *Neurochemistry International.* 1988;12(2).
18. Cohen Z, Tsuiki A, Takada A, Beaudet A, Diksic M, Hamel E. In Vivo-Synthesized Radioactively Labelled α-Methyl Serotonin as a Selective Tracer for Visualization of Brain Serotonin Neurons. *Synapse.* 1995;21:21-28.
19. Chugani DC, Muzik O. α[C-11]Methyl-l-Tryptophan PET Maps Brain Serotonin Synthesis and Kynurenine Pathway Metabolism *J Cereb Blood Flow Metab.* 2000;20(2-9).

20. Lackner A, Heyes MP. Increased Cerebrospinal Fluid Quinolinic Acid, Kynurenic Acid, and L-Kynurenine in Acute Septicemia. *Journal of Neurochemistry.* 1990;55(1):338-341.
21. Saito K, Nowak Jr TS, Syuama K, et al. Kynurenine Pathway Enzymes in Brain: Responses to Ischemic Brain Injury Versus Systemic Immune Activasion. *Journal of Neurochemistry.* 1993;61:2061-2070.
22. Visser AK, Ramakrishnan NK, Willemsen. A T, et al. [^{11}C]5-HTP and microPET are not suitable for pharmacodynamic studies in the rodent brain. *J Cereb Blood Flow Metab.* 2014;34:118-125.
23. Zlatopolskiy BD, Zischler J, Schafer D, et al. Discovery of 7-[^{18}F]Fluorotryptophan as a Novel Positron Emission Tomography (PET) Probe for the Visualization of Tryptophan Metabolism in Vivo. *J Med Chem.* 2018;61(1):189-206.
24. Sono M, Roach MP, Coulter ED, Dawson JH. Heme-Containing Oxygenases. *Chem Rev.* 1996;96(7):2841-2887.
25. Leeds JM, Brown PJ, McGeehan GM, Brown FK, Wiseman JS. Isotope Effects and Alternative Substrate Reactivities for Tryptophan 2,3-Dioxygenase. *J Biol Chem.* 1993;24(25):17781-17786.
26. Miyake FY, Yakushijin K, Horne DA. Preparation and synthetic applications of 2-halotryptophan methyl esters: synthesis of spirotryprostatin B. *Angew Chem Int Ed Engl.* 2004;43(40):5357-5360.
27. Vicente J, Saura-Llamas I, Bautista D. Regiospecific Functionalization of Pharmaceuticals and Other Biologically Active Molecules through Cyclopalladated Compounds. 2-Iodination of Phentermine and l-Tryptophan Methyl Ester. *Organometallics.* 2005;24:6001-6004.
28. Philips RS, Cohen LA. Intramolecular General Acid and General Base Catalyses in the Hydrolysis of 2-Halotryptophans and Their Analogues.pdf. *J Am Chem Soc.* 1986;108(8):2023-2030.
29. Osborne AS, Som P, Metcalf JL, Phillips RS. Regioselective nitration of N(alpha),N(1)-bis(trifluoroacetyl)-L-tryptophan methyl ester: efficient synthesis of 2-nitro and 6-nitro-N-trifluoroacetyl-L-tryptophan methyl

ester. *Bioorg Med Chem Lett.* 2008;18(21):5750-5752.

30. Huiban M, Tredwell M, Mizuta S, et al. A broadly applicable [^{18}F]trifluoromethylation of aryl and heteroaryl iodides for PET imaging. *Nat Chem.* 2013;5(11):941-944.
31. van der Born D, Sewing C, Herscheid JK, Windhorst AD, Orru RV, Vugts DJ. A universal procedure for the [^{18}F]trifluoromethylation of aryl iodides and aryl boronic acids with highly improved specific activity. *Angew Chem Int Ed Engl.* 2014;53(41):11046-11050.
32. Madras BK, Sourkes TL. Metabolism of α-methyltryptophan. *Biochemical Pharmacology.* 1965;14:1499-1506

33. Turk J, Panse GT, Marshall GR. Studies with a-Methyl Amino Acids. Resolution and amino protection. *J Org Chem.* 1975;40(7):953-955.
34. Khosla MC, Stachowiak K, Smeby RR, et al. Synthesis of [a-methyltyrosine-4]angiotensin II: Studies of its conformation, pressor activity, and mode of enzymatic degradation. *Proc Natl Acad Sci USA.* 1981;78(2):757-760.
35. Visser AK, Ramakrishnan NK, Willemsen AT, et al. [(11)C]5-HTP and microPET are not suitable for pharmacodynamic studies in the rodent brain. *J Cereb Blood Flow Metab.* 2014;34(1):118-125.
36. Lee JY, Jeong JM, Kim YJ, et al. Preparation of Ga-68-NOTA as a renal PET agent and feasibility tests in mice. *Nucl Med Biol.* 2014;41(2):210-215.
37. Jeong JM KY, Lee YS, LeeDS, Chung, JK, Lee MC. Radiolabeling of NOTA and DOTA with positron emitting 68Ga and investigation of in vitro properties. . *Nucl Med Mol Imaging.* 2009;43:330-336.
38. Shimizu R, Egami H, Nagi T, Chae J, Hamashima Y, Sodeoka M. Direct C2-trifluoromethylation of indole derivatives catalyzed by copper acetate. *Tetrahedron Letters.* 2010;51(45):5947-5949.
39. Nagahiro S, Takada A, Diksic M, Sourkes TL, Missala K, Yamamoto YL. A New Method to Measure Brain Serotonin Synthesis In Vivo. II. A practical Autoradiographic Method Tested in Normal and Lithium-Treated Rats. *J Cereb Blood Flow Metab.* 1990;10(1):13-21.

40. Yano JM, Yu K, Donaldson GP, et al. Indigenous bacteria from the gut microbiota regulate host serotonin biosynthesis. *Cell.* 2015;161(2):264-276.
41. Chiotellis A, Muller Herde A, Rossler SL, et al. Synthesis, Radiolabeling, and Biological Evaluation of 5-Hydroxy-2-[(18)F]fluoroalkyl-tryptophan Analogues as Potential PET Radiotracers for Tumor Imaging. *J Med Chem.* 2016;59(11):5324-5340.
42. Nagahiro S, Diksic TM, Sourkes TL, Missala K, Yamamoto YL. A New Method to Measure Brain Serotonin Synthesis In Vivo. II. A Practical Autoradiographic Method Tested in Normal and Lithium-Treated Rats. *J Cereb Blood Flow Metab.* 1990;10:13-21.
43. Smith QR. Transport of glutamate and Other Amino Acids at the Blood-Brain Barrier. *J Nutr.* 2000;130:1016S-1022S.
44. Mies G, Niebuhr I, Hossmann KA. Simultaneous Measurement of Blood Flow and Glucose Metabolism By Autoradiographic Techniques. *Stroke.* 1981;12(5):581-588.
45. Macchi MM, Bruce JN. Human pineal physiology and functional significance of melatonin. *Front Neuroendocrinol.* 2004;25(3-4):177-195.
46. Arendt J, Skene DJ. Melatonin as a chronobiotic. *Sleep Med Rev.* 2005;9(1):25-39.
47. Lovenberg W, Jequier E, Sfoerdsma A. Tryptophan Hydroxylation Measurement in Pineal Gland, Brainstem, and Carcinoid Tumor. *Science.* 1967;155(13):217-219.
48. Vann SD. Re-evaluating the role of the mammillary bodies in memory. *Neuropsychologia.* 2010;48(8):2316-2327.
49. Visser AK, van Waarde A, Willemsen AT, et al. Measuring serotonin synthesis: from conventional methods to PET tracers and their (pre)clinical implications. *Eur J Nucl Med Mol Imaging.* 2011;38(3):576-591.
50. Sheard MH, Aghajanian GK. Neuronally activated metabolism of brain serotonin effect of lithium. *Life Sciences.* 1970;9:285-290.
51. Perez-Cruet J, Tagliamonte A, Tagliamonte P, Gessa GL. Stimulation of serotonin synthesis by lithium. *The Journal of Pharmacology and*

Experimental Therapeutics. 1971;178(2):325-330.

52. Nagahiro S, Takada A, Diksic M, Sourkes TL, Missala K, Yamamoto YL. A New Method to Measure Brain Serotonin Synthesis In Vivo. II. A Practical Autoradiographic Method Tested in Normal and Lithium-Treated Rats. *J Cereb Blood Flow Metab.* 1990;10:13-21.

SPECTRAL ANALYSIS RESULTS

^{1}H NMR Spectra

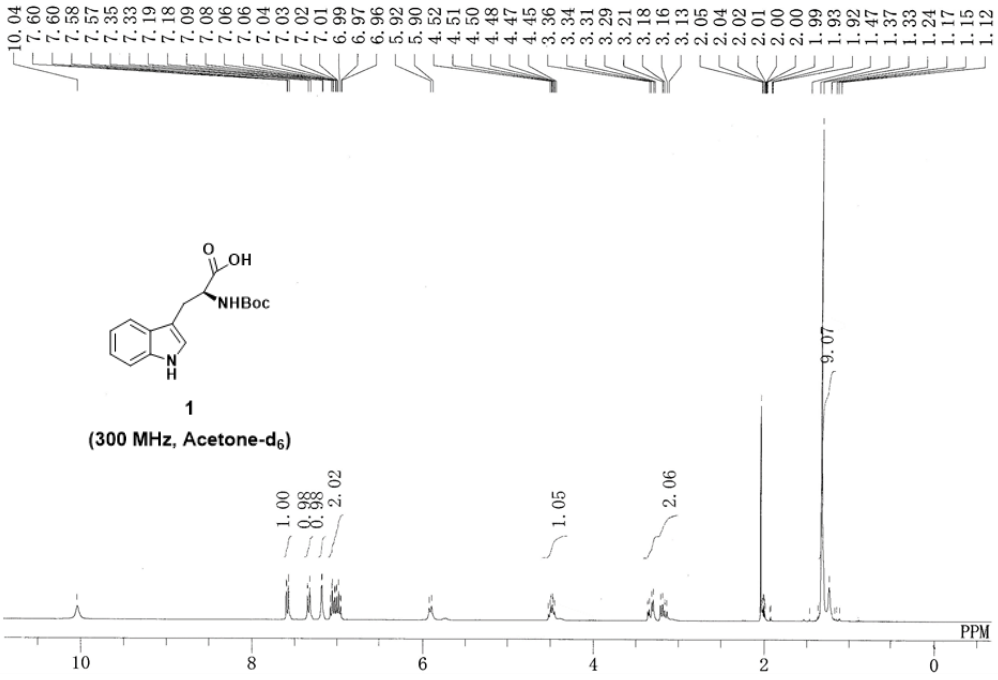
10.04
7.60
7.60
7.58
7.57
7.35
7.33
7.19
7.18
7.09
7.08
7.06
7.06
7.04
7.03
7.02
7.01
6.99
6.97
6.96
5.92
5.90
4.52
4.51
4.50
4.48
4.47
4.45
3.36
3.34
3.31
3.29
3.21
3.18
3.16
3.13
2.05
2.04
2.02
2.01
2.00
2.00
1.99
1.93
1.92
1.47
1.37
1.33
1.24
1.17
1.15
1.12
O
OH
NHBoc
N
H
1
(300 MHz, Acetone-d6)
1.00
0.98
0.98
2.02
1.05
2.06
9.07
PPM
10
8
6
4
2
0

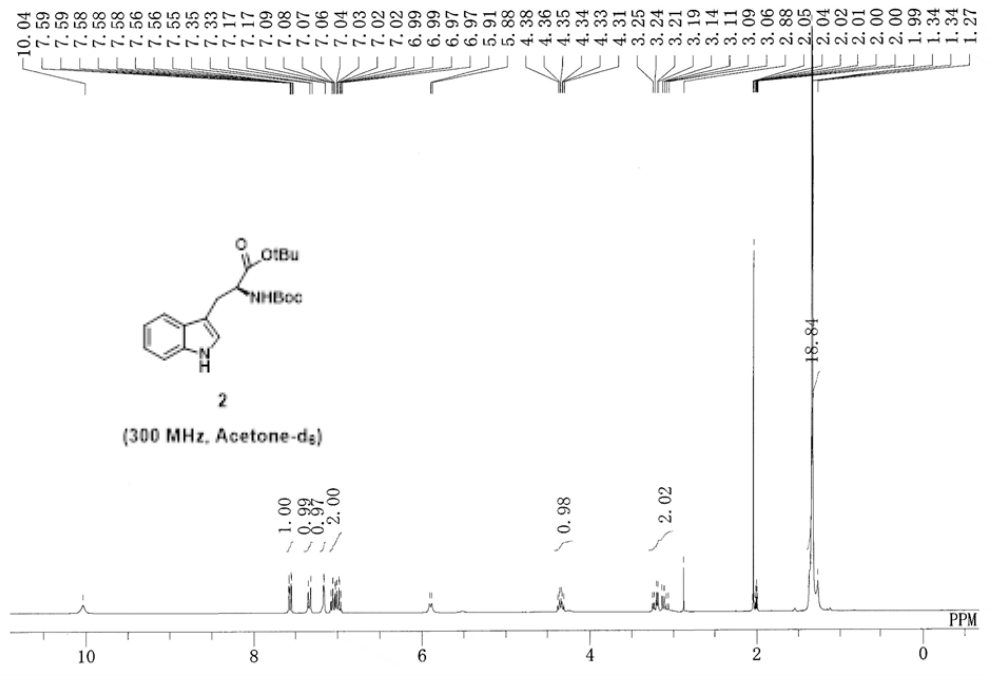
10.04
7.59
7.59
7.58
7.58
7.58
7.56
7.56
7.55
7.35
7.33
7.17
7.17
7.09
7.08
7.07
7.06
7.04
7.03
7.02
7.02
6.99
6.97
6.97
5.91
5.88
4.38
4.36
4.35
4.34
4.33
4.31
3.25
3.24
3.21
3.19
3.14
3.11
3.09
3.06
2.88
2.05
2.04
2.02
2.01
2.00
2.00
1.99
1.34
1.34
1.27
O
OtBu
NHBoc
N
H
2
(300 MHz, Acetone-d6)
1.00
0.99
0.97
2.00
0.98
2.02
18.84
PPM
10
8
6
4
2
0

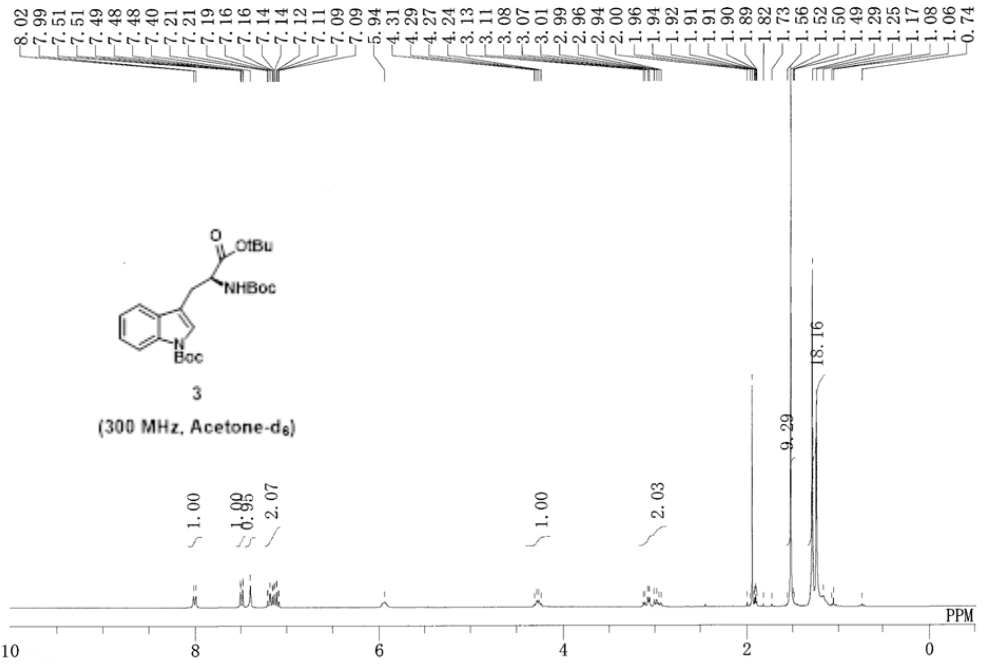
8.02 7.99 7.51 7.51 7.49 7.48 7.48 7.40 7.21 7.21 7.19 7.16 7.16 7.14 7.14 7.12 7.11 7.09 7.09 5.94 4.31 4.29 4.27 4.24 3.13 3.11 3.08 3.07 3.01 2.99 2.96 2.94 2.00 1.96 1.94 1.92 1.91 1.91 1.90 1.89 1.82 1.73 1.56 1.52 1.50 1.49 1.29 1.25 1.17 1.08 1.06 0.74
O
OtBu
NHBoc
N
Boc
3
(300 MHz, Acetone-d6)
1.00
1.00
0.95
2.07
1.00
2.03
9.29
18.16
PPM
10
8
6
4
2
0

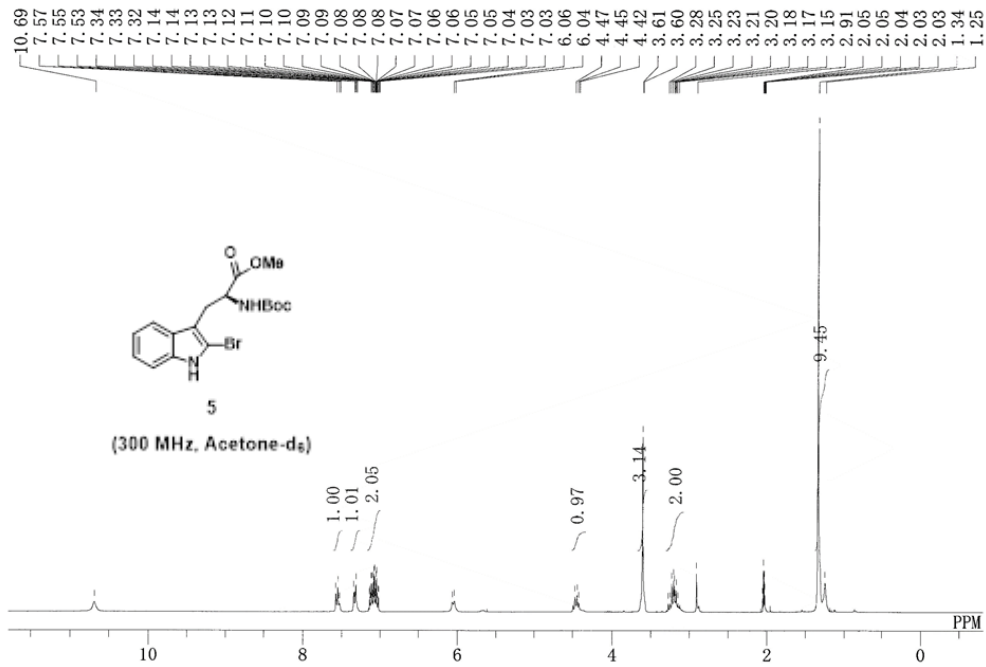
10.69 7.57 7.55 7.53 7.34 7.33 7.32 7.14 7.14 7.13 7.13 7.12 7.11 7.10 7.10 7.09 7.09 7.08 7.08 7.08 7.07 7.07 7.06 7.06 7.05 7.05 7.04 7.03 7.03 6.06 6.04 4.47 4.45 4.42 3.61 3.60 3.28 3.25 3.23 3.21 3.20 3.18 3.17 3.15 2.91 2.05 2.05 2.04 2.03 2.03 1.34 1.25
O
OMe
NHBoc
Br
H
5
(300 MHz, Acetone-d6)
1.00
1.01
2.05
0.97
3.14
2.00
9.45
PPM
10
8
6
4
2
0

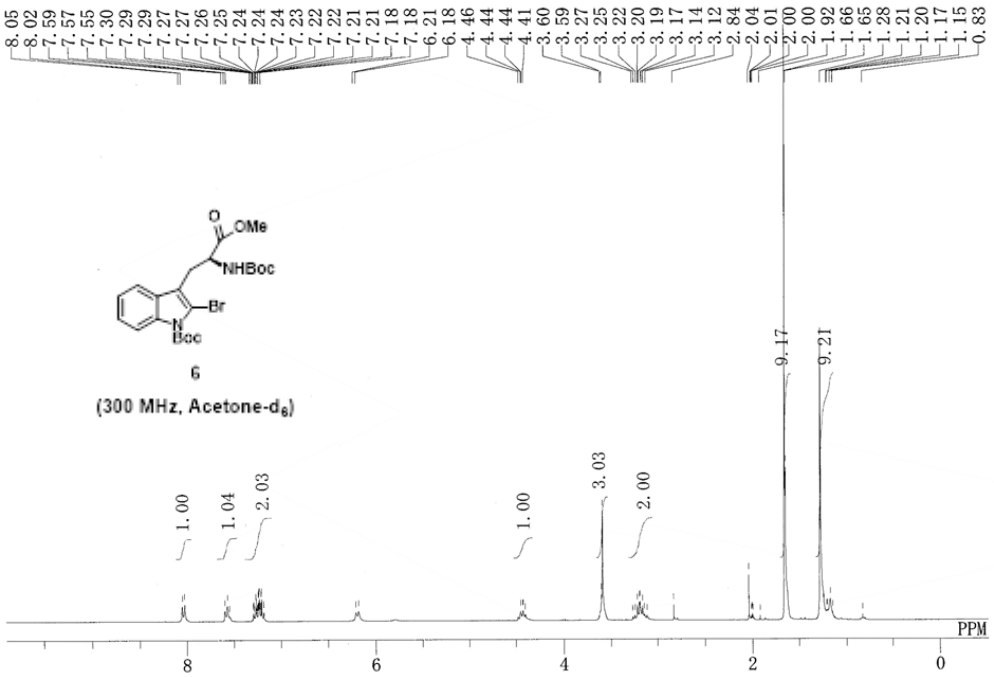
8.05 8.02 7.59 7.57 7.55 7.30 7.29 7.29 7.27 7.27 7.26 7.25 7.24 7.24 7.24 7.23 7.22 7.22 7.21 7.21 7.18 7.18 6.21 6.18 4.46 4.44 4.44 4.41 3.60 3.59 3.27 3.25 3.22 3.20 3.19 3.17 3.14 3.12 2.84 2.04 2.01 2.00 2.00 1.92 1.66 1.65 1.28 1.21 1.20 1.17 1.15 0.83
O
OMe
NHBoc
Br
N
Boc
6
(300 MHz, Acetone-d6)
1.00 1.04 2.03 1.00 3.03 2.00 9.17 9.21
PPM
8 6 4 2 0

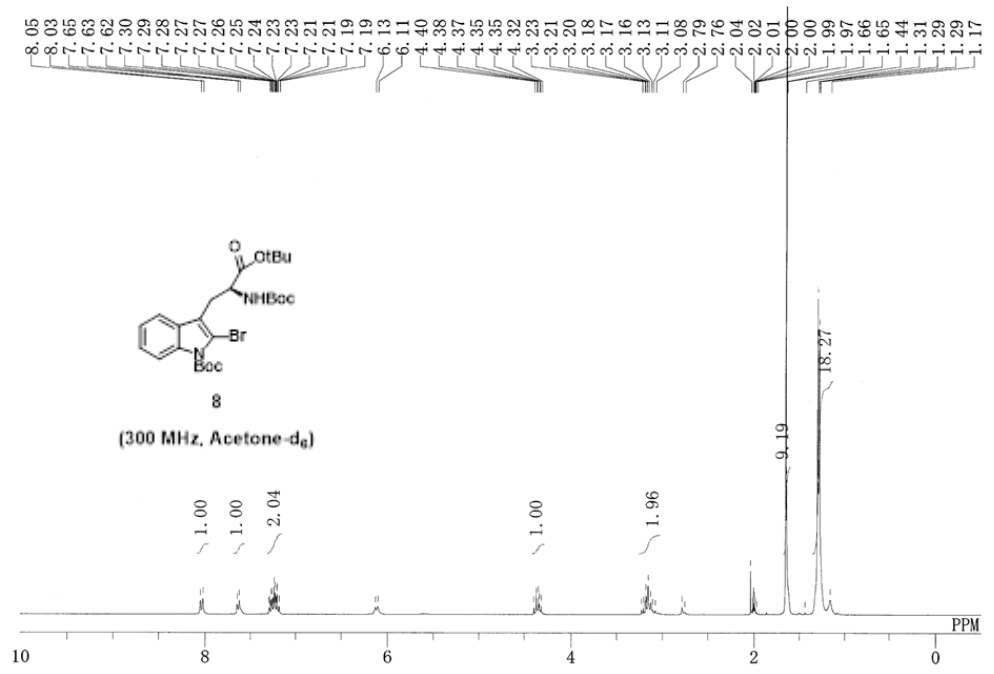
8.05 8.03 7.65 7.63 7.62 7.30 7.29 7.28 7.27 7.27 7.26 7.25 7.24 7.23 7.23 7.21 7.21 7.19 7.19 6.13 6.11 4.40 4.38 4.37 4.35 4.35 4.32 3.23 3.21 3.20 3.18 3.17 3.16 3.13 3.11 3.08 2.79 2.76 2.04 2.02 2.01 2.00 2.00 1.99 1.97 1.66 1.65 1.44 1.31 1.29 1.29 1.17
O
OtBu
NHBoc
Br
N
Boc
8
(300 MHz, Acetone-d6)
1.00 1.00 2.04 1.00 1.96 9.19 18.27
PPM
10 8 6 4 2 0

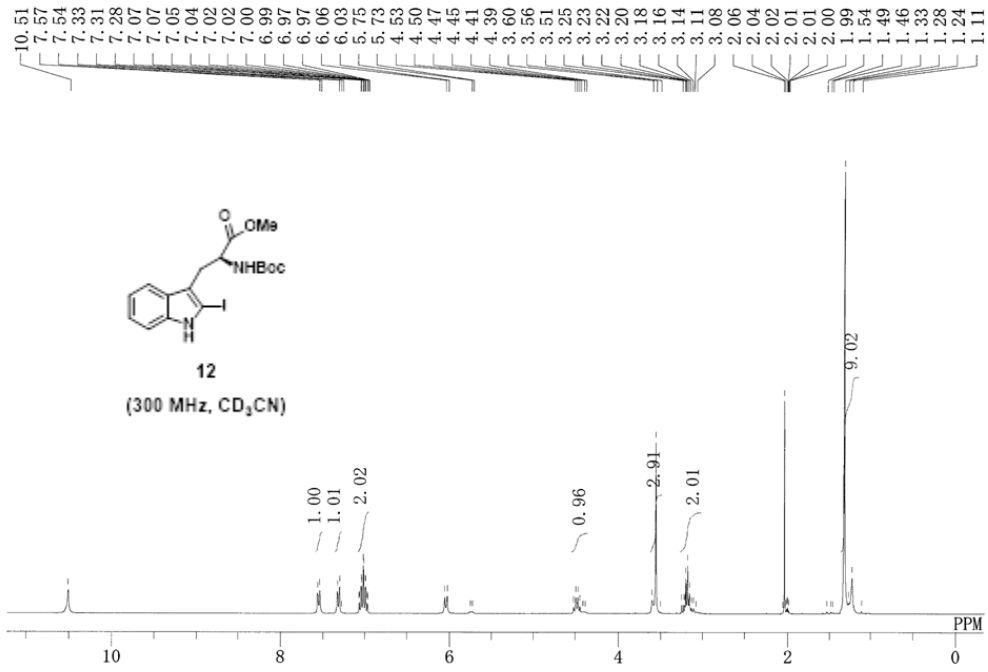
10.51
7.57
7.54
7.33
7.31
7.28
7.07
7.07
7.05
7.04
7.02
7.02
7.00
6.99
6.97
6.97
6.06
6.03
5.75
5.73
4.53
4.50
4.47
4.45
4.41
4.39
3.60
3.56
3.51
3.25
3.23
3.22
3.20
3.18
3.16
3.14
3.11
3.08
2.06
2.04
2.02
2.01
2.01
2.00
1.99
1.54
1.49
1.46
1.33
1.28
1.24
1.11
OMe
NHBoc
I
H
12
(300 MHz, CD3CN)
1.00
1.01
2.02
0.96
2.91
2.01
9.02
PPM
10
8
6
4
2
0

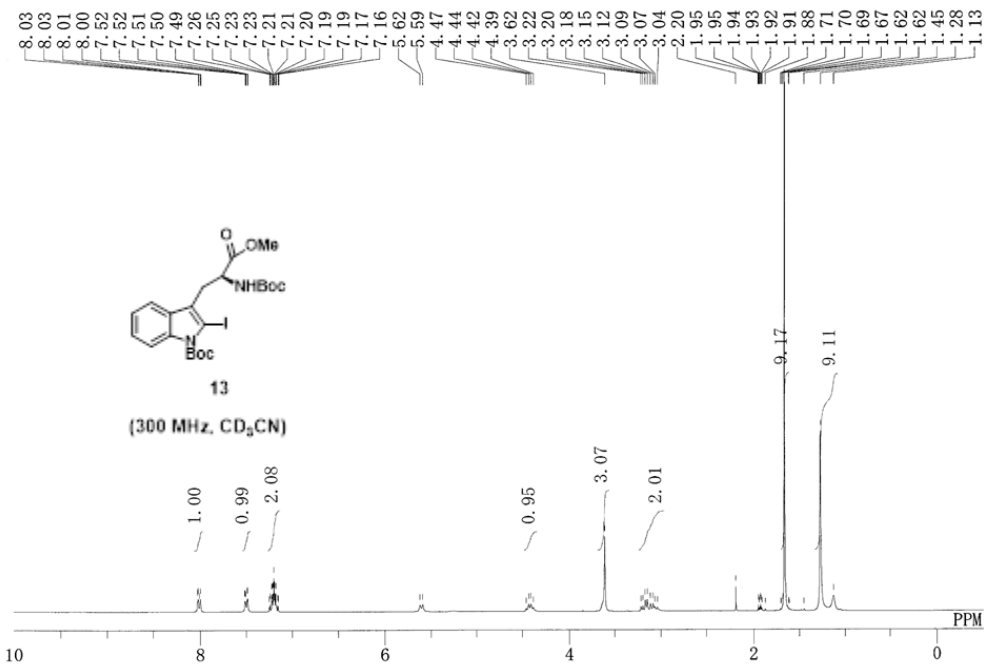
8.03
8.03
8.01
8.00
7.52
7.52
7.51
7.50
7.49
7.26
7.25
7.23
7.23
7.21
7.21
7.20
7.19
7.19
7.17
7.16
5.62
5.59
4.47
4.44
4.42
4.39
3.62
3.22
3.20
3.18
3.15
3.12
3.09
3.07
3.04
2.20
1.95
1.95
1.94
1.93
1.92
1.91
1.88
1.71
1.70
1.69
1.67
1.62
1.62
1.45
1.28
1.13
OMe
NHBoc
I
N
Boc
13
(300 MHz, CD3CN)
1.00
0.99
2.08
0.95
3.07
2.01
9.17
9.11
PPM
10
8
6
4
2
0

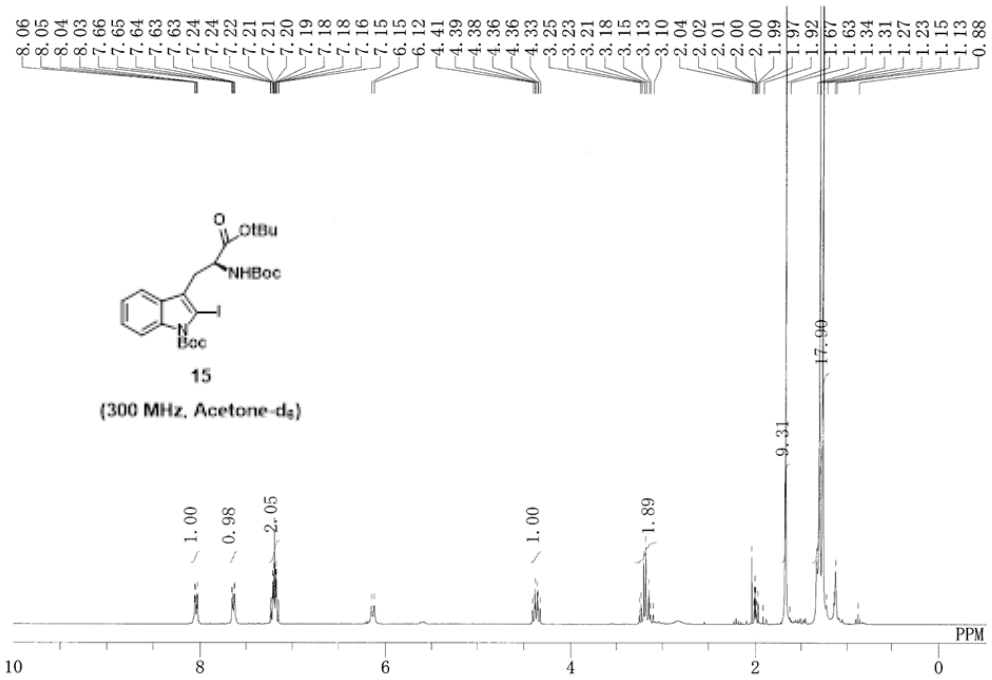
8.06 8.05 8.04 8.03 7.66 7.65 7.64 7.63 7.63 7.24 7.24 7.22 7.21 7.21 7.20 7.19 7.18 7.18 7.16 7.15 6.12 4.41 4.39 4.38 4.36 4.36 4.33 3.25 3.23 3.21 3.18 3.15 3.13 3.10 2.04 2.02 2.01 2.00 2.00 1.99 1.97 1.92 1.67 1.63 1.34 1.31 1.27 1.23 1.15 1.13 0.88
OtBu
NHBoc
I
Boc
15
(300 MHz, Acetone-d6)
1.00 0.98 2.05 1.00 1.89 9.31 17.90
PPM
10 8 6 4 2 0

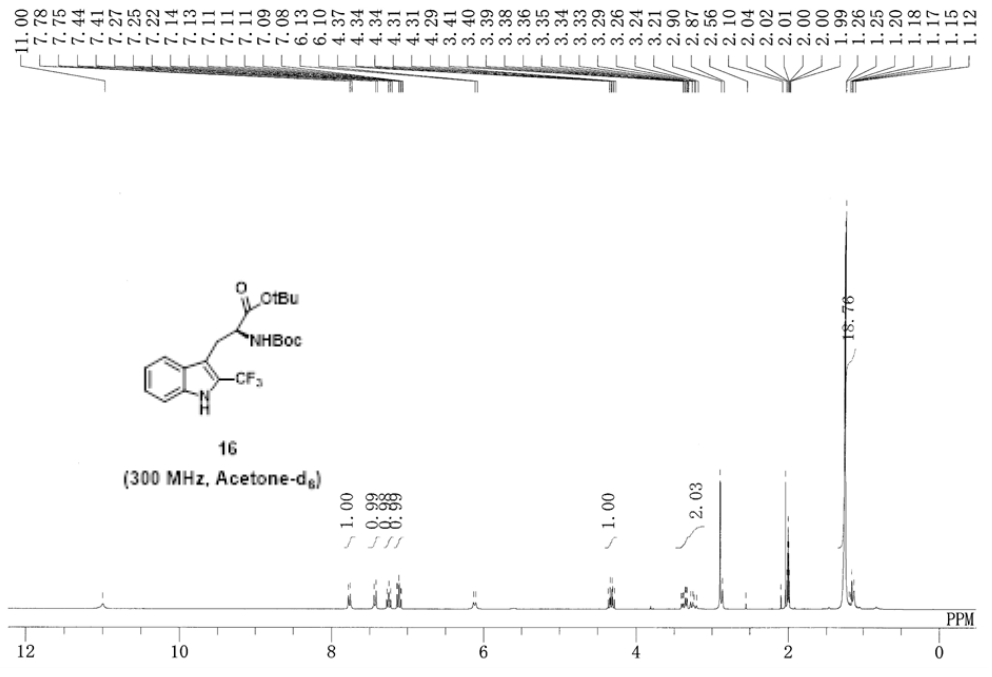
11.00 7.78 7.75 7.44 7.41 7.27 7.25 7.22 7.14 7.13 7.11 7.11 7.09 7.08 6.13 6.10 4.37 4.34 4.34 4.31 4.31 4.29 3.41 3.40 3.39 3.38 3.36 3.35 3.34 3.33 3.29 3.26 3.24 3.21 2.90 2.87 2.56 2.10 2.04 2.02 2.01 2.00 2.00 1.99 1.26 1.25 1.20 1.18 1.17 1.15 1.12
OtBu
NHBoc
CF3
H
16
(300 MHz, Acetone-d6)
1.00 0.99 0.98 0.98 0.97 1.00 2.03 18.76
PPM
12 10 8 6 4 2 0

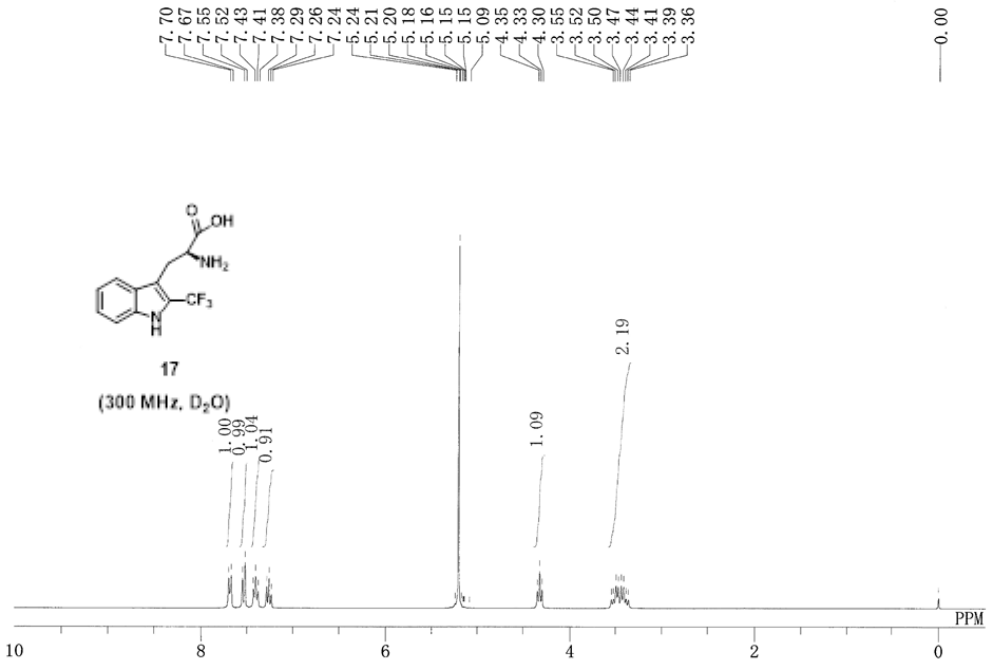
7.70
7.67
7.55
7.52
7.43
7.41
7.38
7.29
7.26
7.24
5.24
5.21
5.20
5.18
5.16
5.15
5.15
5.09
4.35
4.33
4.30
3.55
3.52
3.50
3.47
3.44
3.41
3.39
3.36
0.00
O
OH
NH2
CF3
H
17
(300 MHz, D2O)
1.00
0.99
1.04
0.91
1.09
2.19
PPM
10
8
6
4
2
0

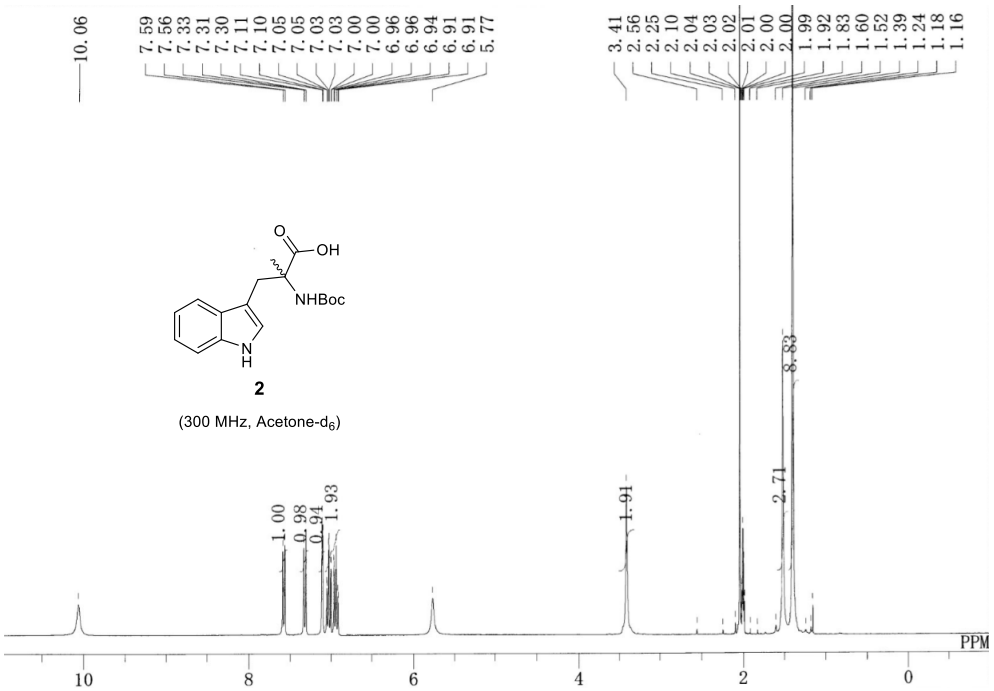
10.06
7.59
7.56
7.33
7.31
7.30
7.11
7.10
7.05
7.05
7.03
7.03
7.00
7.00
6.96
6.96
6.94
6.91
6.91
5.77
3.41
2.56
2.25
2.10
2.04
2.03
2.02
2.01
2.00
2.00
1.99
1.92
1.83
1.60
1.52
1.39
1.24
1.18
1.16
O
OH
NHBoc
N
H
2
(300 MHz, Acetone-d6)
1.00
0.98
0.94
1.93
1.91
2.71
8.83
PPM
10
8
6
4
2
0

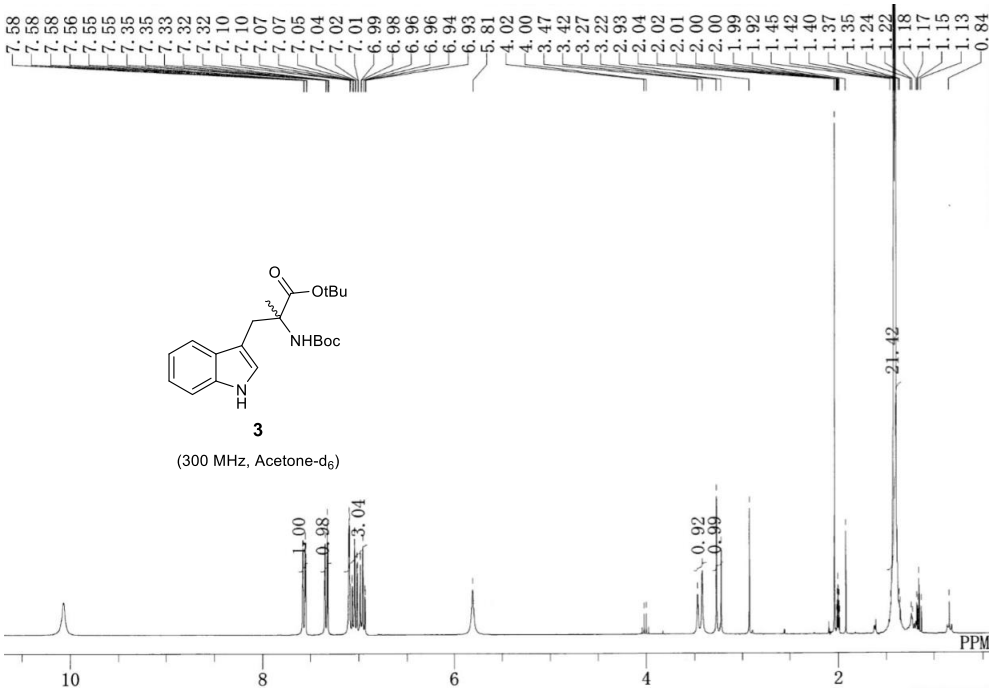
7.58
7.58
7.58
7.56
7.55
7.55
7.35
7.33
7.32
7.32
7.10
7.10
7.07
7.05
7.04
7.02
7.01
6.99
6.98
6.96
6.96
6.94
6.93
5.81
4.02
4.00
3.47
3.42
3.27
3.22
2.93
2.04
2.02
2.01
2.00
2.00
1.99
1.92
1.45
1.42
1.40
1.37
1.35
1.24
1.22
1.18
1.17
1.15
1.13
0.84
O
OtBu
NHBoc
N
H
3
(300 MHz, Acetone-d6)
1.00
0.98
3.04
0.92
0.99
21.42
PPM
10
8
6
4
2

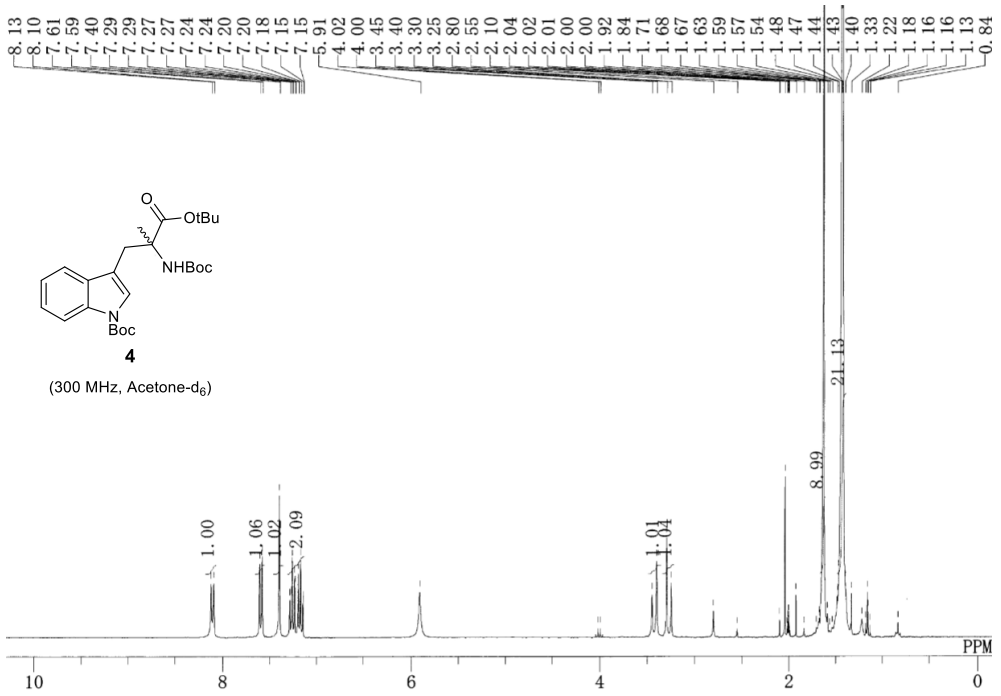

4

(300 MHz, Acetone-d_6)

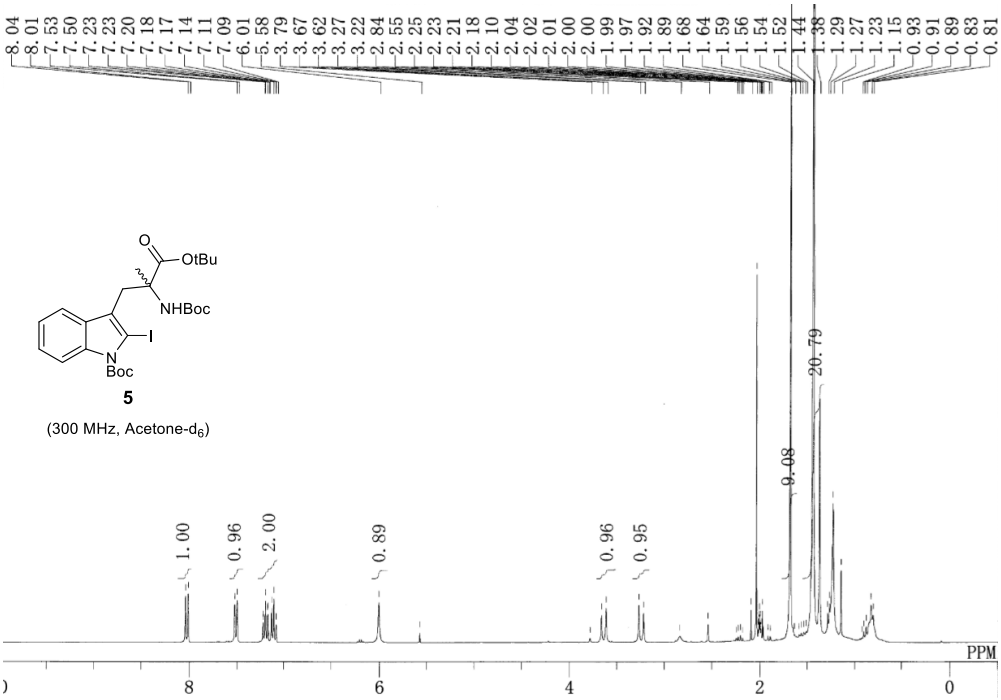

5

(300 MHz, Acetone-d_6)

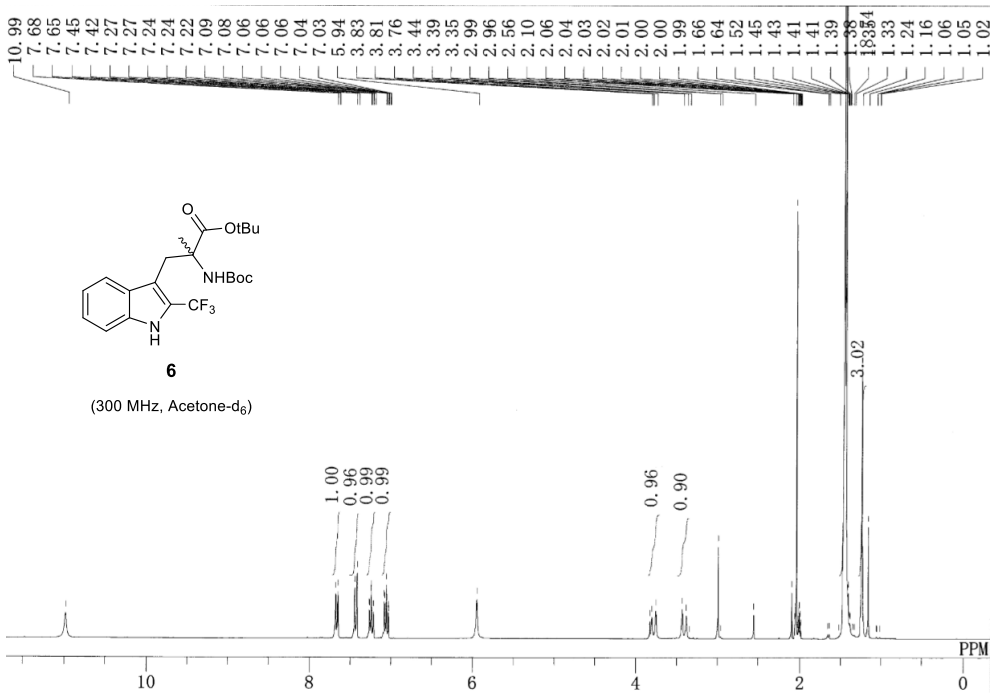
10.99
7.68
7.65
7.45
7.42
7.27
7.27
7.24
7.24
7.22
7.09
7.08
7.06
7.06
7.06
7.04
7.03
5.94
3.83
3.81
3.76
3.44
3.39
3.35
2.99
2.96
2.56
2.10
2.06
2.04
2.03
2.02
2.01
2.00
2.00
1.99
1.66
1.64
1.52
1.45
1.43
1.41
1.41
1.39
1.38
1.33
1.24
1.16
1.06
1.05
1.02
O
OtBu
NHBoc
CF3
N
H
6
(300 MHz, Acetone-d6)
3.02
1.00
0.96
0.99
0.99
0.96
0.90
PPM
10
8
6
4
2
0

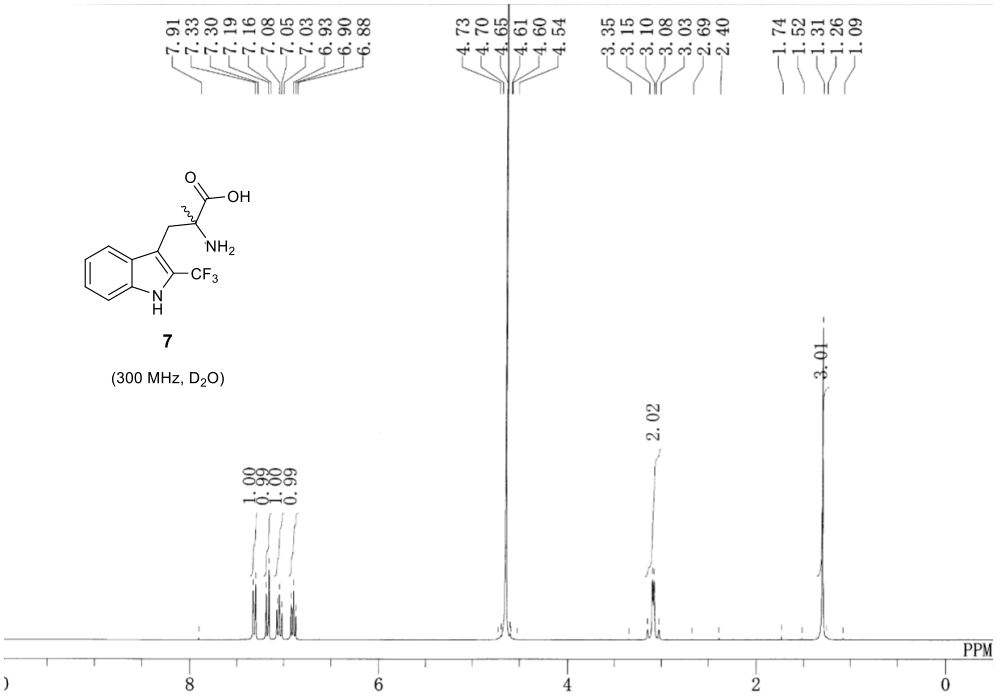
7.91
7.33
7.30
7.19
7.16
7.08
7.05
7.03
6.93
6.90
6.88
4.73
4.70
4.65
4.61
4.60
4.54
3.35
3.15
3.10
3.08
3.03
2.69
2.40
1.74
1.52
1.31
1.26
1.09
O
OH
NH2
CF3
N
H
7
(300 MHz, D2O)
3.01
2.02
1.00
0.99
1.00
0.99
PPM
8
6
4
2
0

SPECTRAL ANALYSIS RESULTS

^{13}C NMR Spectra

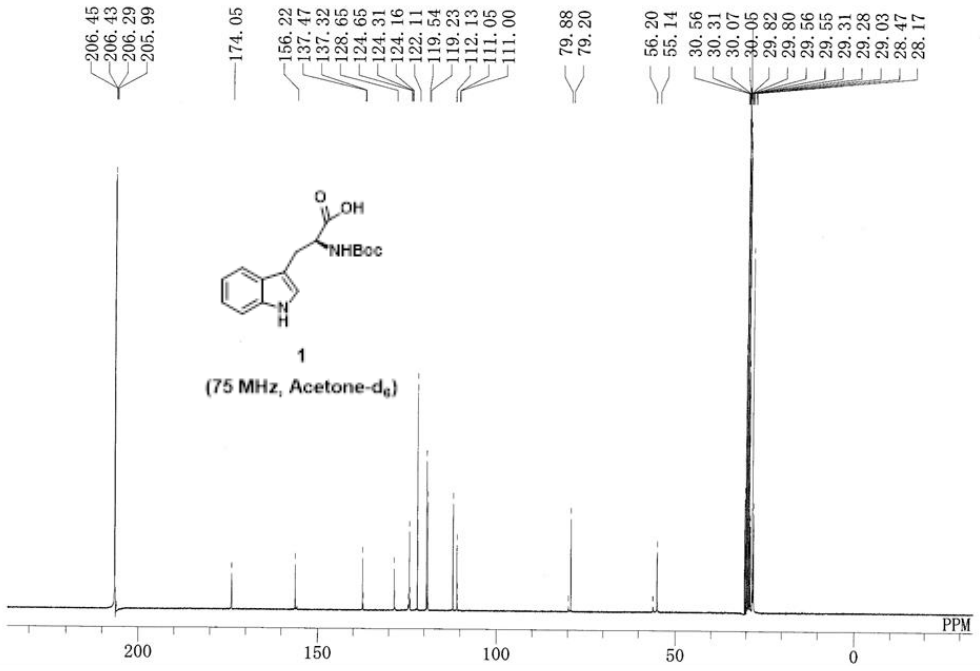
206.45
206.43
206.29
205.99
174.05
156.22
137.47
137.32
128.65
124.65
124.31
124.16
122.11
119.54
119.23
112.13
111.05
111.00
79.88
79.20
56.20
55.14
30.56
30.31
30.07
30.05
29.82
29.80
29.56
29.55
29.31
29.28
29.03
28.47
28.17
O
OH
NHBoc
N
H
1
(75 MHz, Acetone-d6)
PPM
200
150
100
50
0

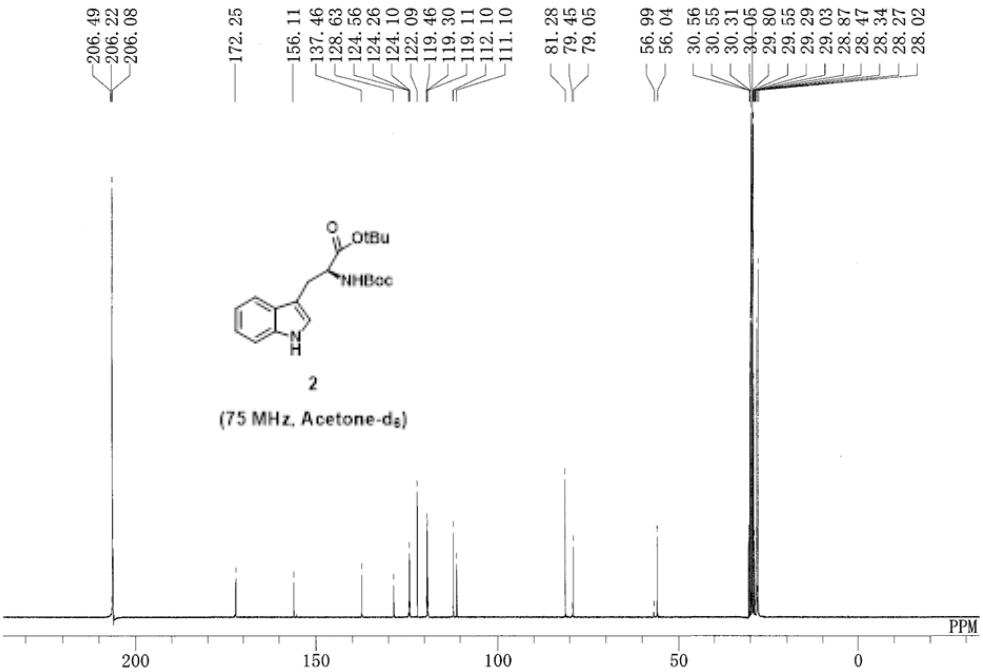
206.49
206.22
206.08
172.25
156.11
137.46
128.63
124.56
124.26
124.10
122.09
119.46
119.30
119.11
112.10
111.10
81.28
79.45
79.05
56.99
56.04
30.56
30.55
30.31
30.05
29.80
29.55
29.29
29.03
28.87
28.47
28.34
28.27
28.02
O
OtBu
NHBoc
N
H
2
(75 MHz, Acetone-d6)
PPM
200
150
100
50
0

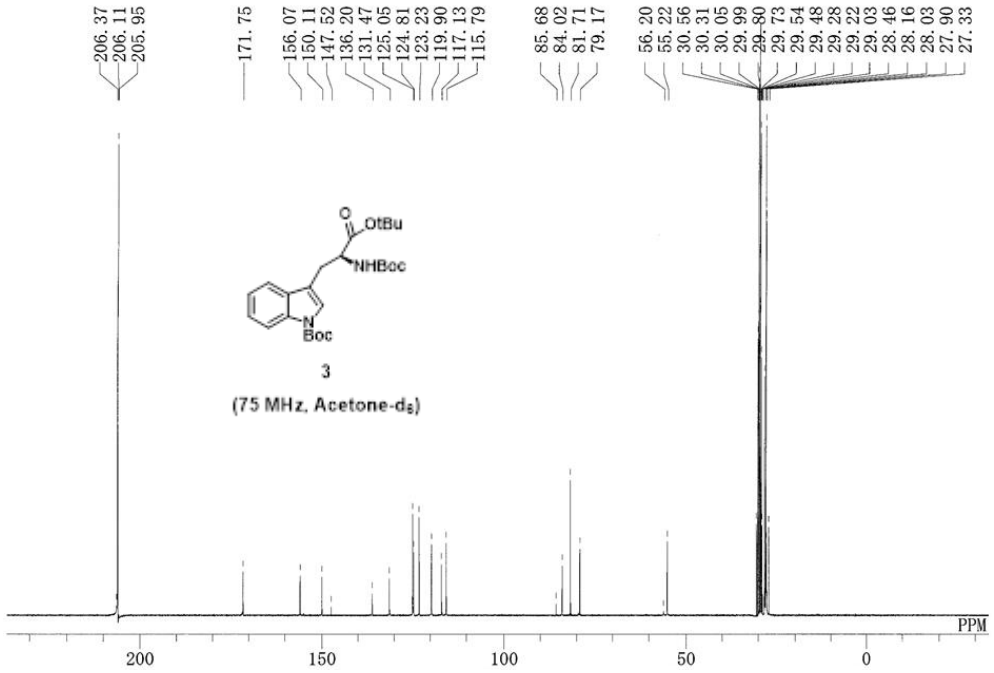
206.37
206.11
205.95
171.75
156.07
150.11
147.52
136.20
131.47
125.05
124.81
123.23
119.90
117.13
115.79
85.68
84.02
81.71
79.17
56.20
55.22
30.56
30.31
30.05
29.99
29.80
29.73
29.54
29.48
29.28
29.22
29.03
28.46
28.16
28.03
27.90
27.33
OtBu
NHBoc
N
Boc
3
(75 MHz, Acetone-d6)
PPM
200
150
100
50
0

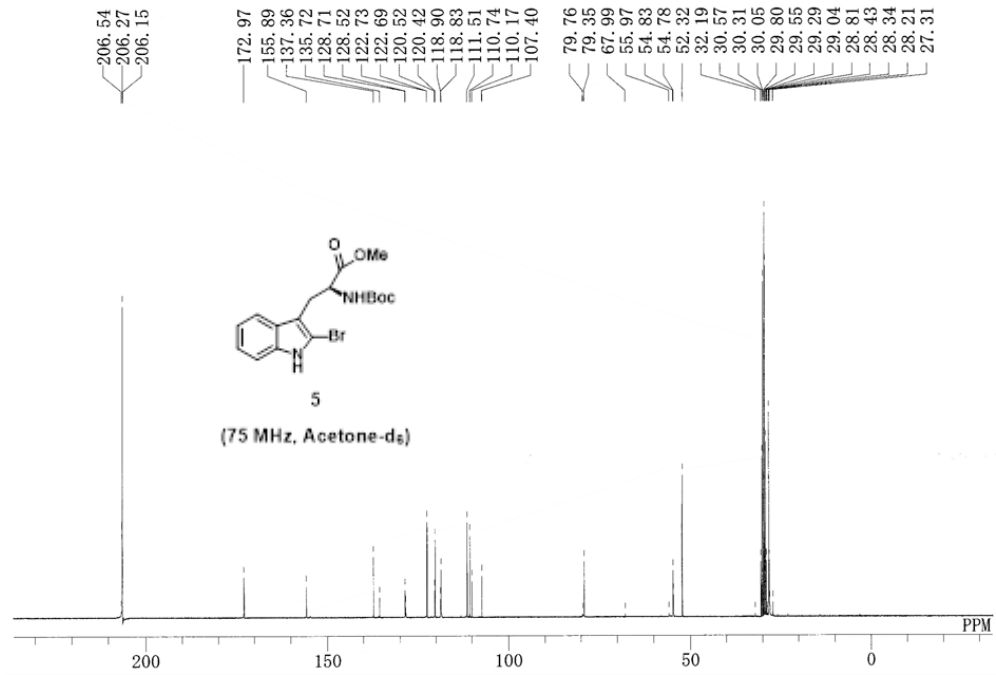
206.54
206.27
206.15
172.97
155.89
137.36
135.72
128.71
128.52
122.73
122.69
120.52
120.42
118.90
118.83
111.51
110.74
110.17
107.40
79.76
79.35
67.99
55.97
54.83
54.78
52.32
32.19
30.57
30.31
30.05
29.80
29.55
29.29
29.04
28.81
28.43
28.34
28.21
27.31
OMe
NHBoc
Br
N
H
5
(75 MHz, Acetone-d6)
PPM
200
150
100
50
0

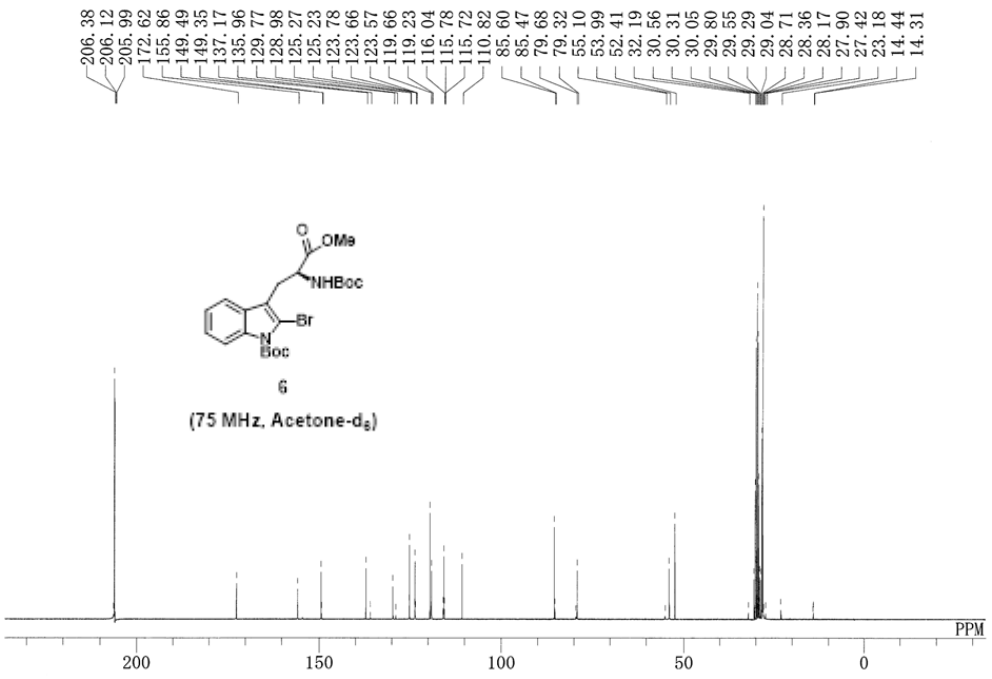
206.38
206.12
205.99
172.62
155.86
149.49
149.35
137.17
135.96
129.77
128.98
125.27
125.23
123.78
123.66
123.57
119.66
119.23
116.04
115.78
115.72
110.82
85.60
85.47
79.68
79.32
55.10
53.99
52.41
32.19
30.56
30.31
30.05
29.80
29.55
29.29
29.04
28.71
28.36
28.17
27.90
27.42
23.18
14.44
14.31
O
OMe
NHBoc
Br
N
Boc
6
(75 MHz, Acetone-d6)
PPM
200
150
100
50
0

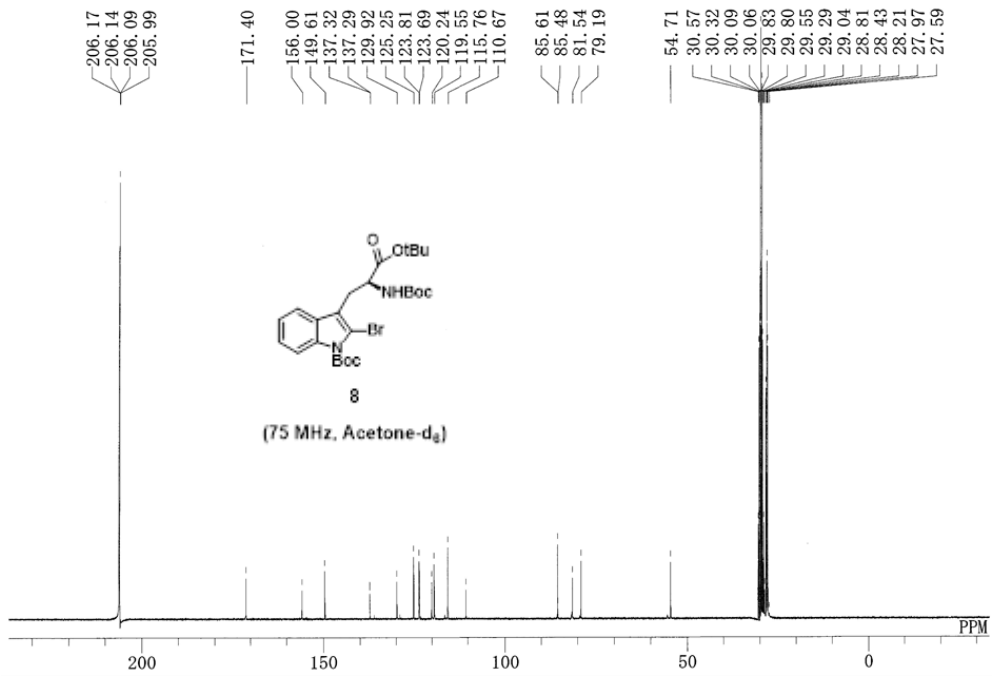
206.17
206.14
206.09
205.99
171.40
156.00
149.61
137.32
137.29
129.92
125.25
123.81
123.69
120.24
119.55
115.76
110.67
85.61
85.48
81.54
79.19
54.71
30.57
30.32
30.09
30.06
29.83
29.80
29.55
29.29
29.04
28.81
28.43
28.21
27.97
27.59
O
OtBu
NHBoc
Br
N
Boc
8
(75 MHz, Acetone-d6)
PPM
200
150
100
50
0

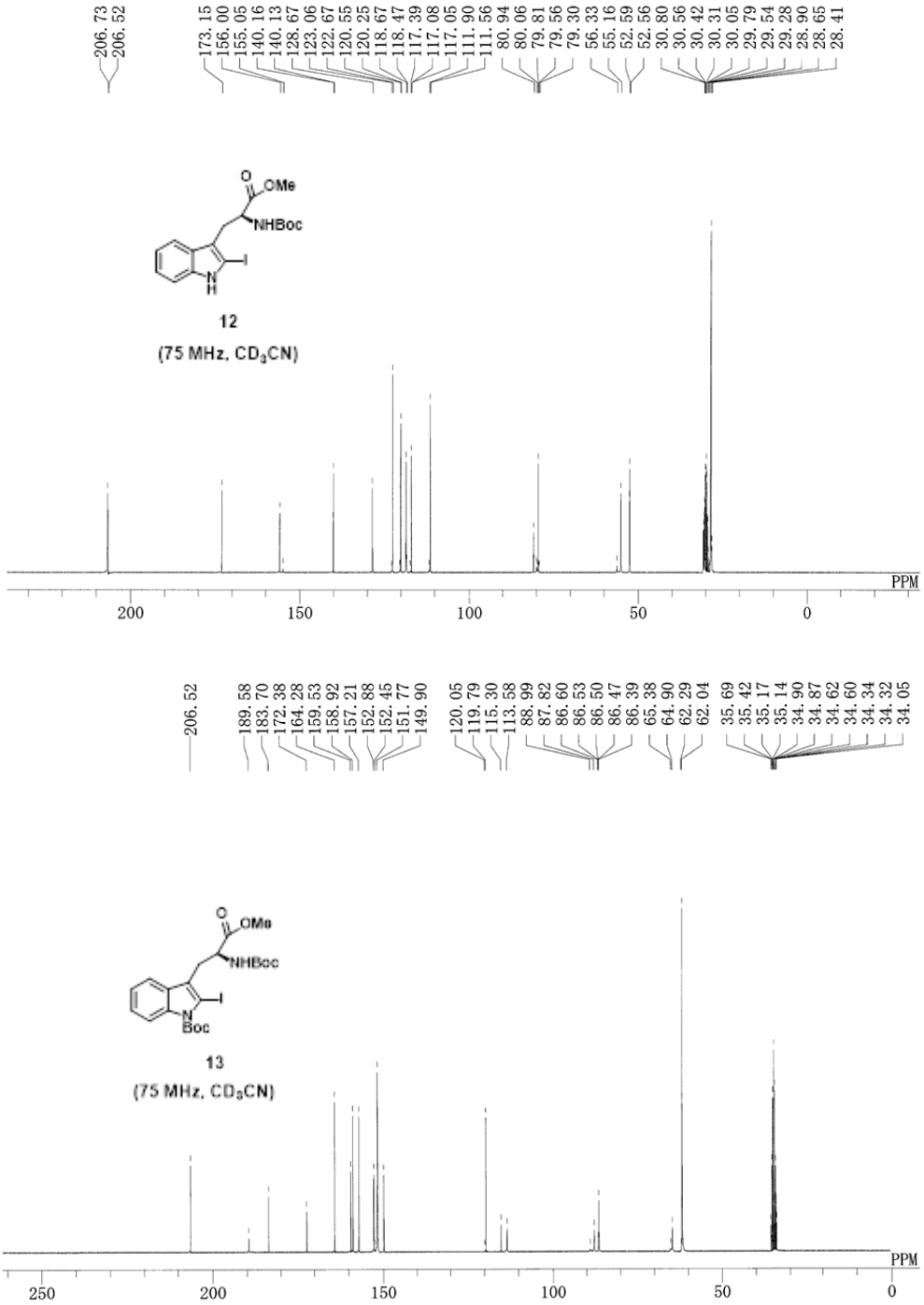
206.73
206.52
173.15
156.00
155.05
140.16
140.13
128.67
123.06
122.67
120.55
120.25
118.67
118.47
117.39
117.08
117.05
111.90
111.56
80.94
80.06
79.81
79.56
79.30
56.33
55.16
52.59
52.56
30.80
30.56
30.42
30.31
30.05
29.79
29.54
29.28
28.90
28.65
28.41
OMe
NHBoc
I
H
12
(75 MHz, CD3CN)
PPM
200
150
100
50
0
206.52
189.58
183.70
172.38
164.28
159.53
158.92
157.21
152.88
152.45
151.77
149.90
120.05
119.79
115.30
113.58
88.99
87.82
86.60
86.53
86.50
86.47
86.39
65.38
64.90
62.29
62.04
35.69
35.42
35.17
35.14
34.90
34.87
34.62
34.60
34.34
34.32
34.05
OMe
NHBoc
I
N
Boc
13
(75 MHz, CD3CN)
PPM
250
200
150
100
50
0

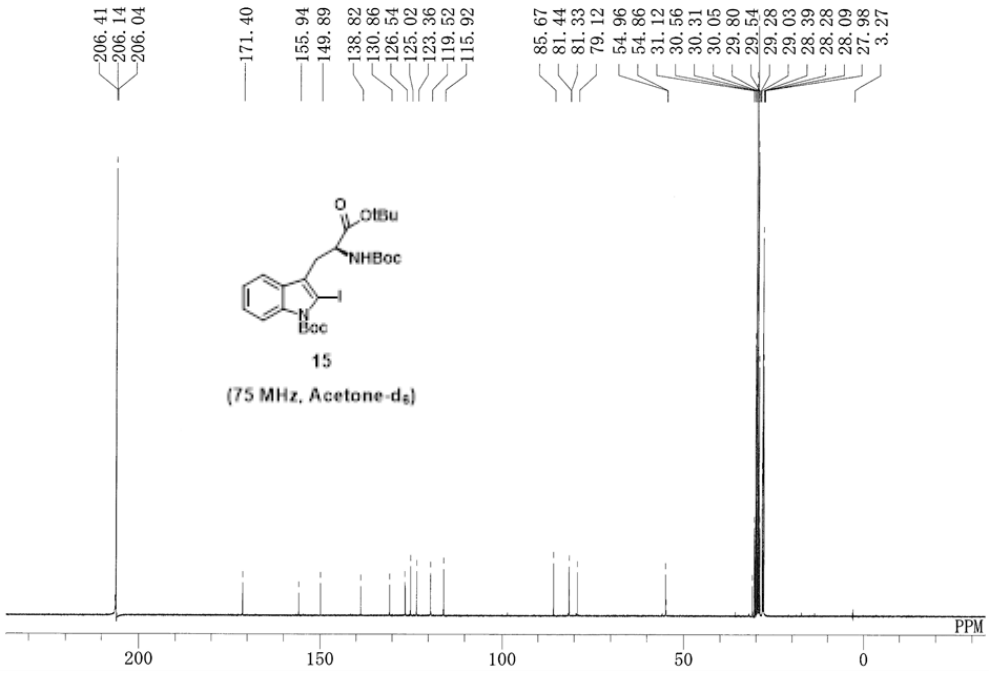

15

(75 MHz, Acetone-d_6)

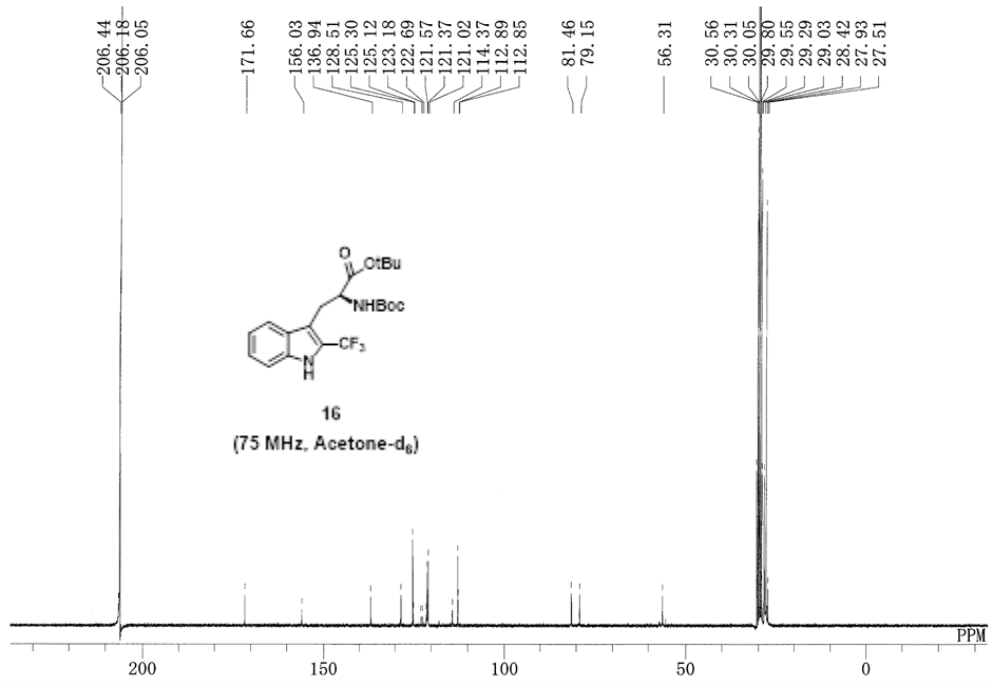

16

(75 MHz, Acetone-d_6)

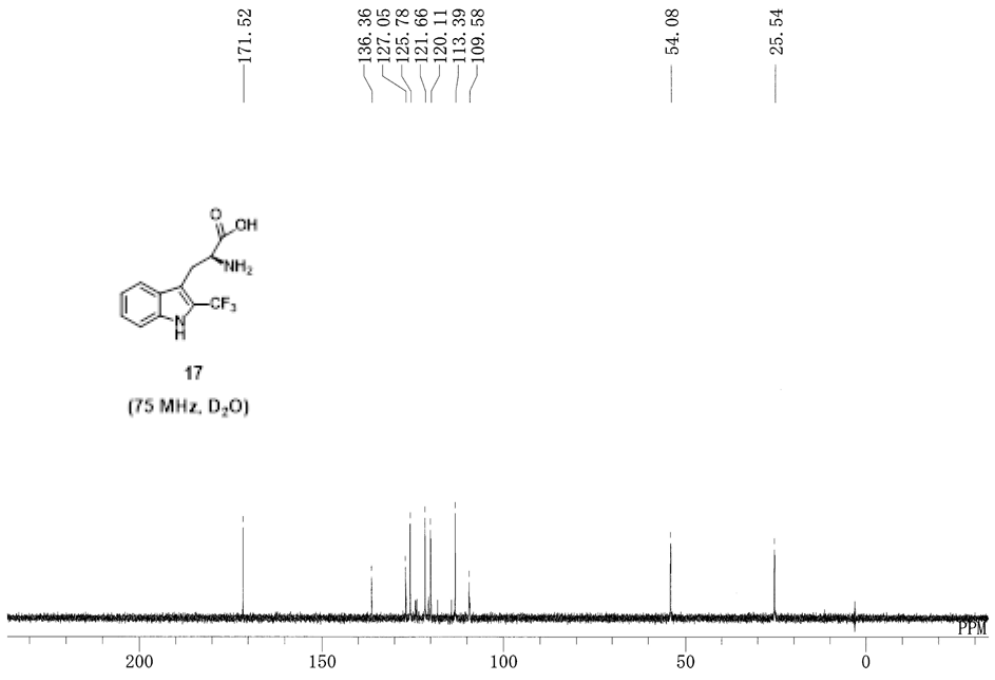
171.52
136.36
127.05
125.78
121.66
120.11
113.39
109.58
54.08
25.54
OH
NH2
CF3
H
17
(75 MHz, D2O)
PPM
200
150
100
50
0

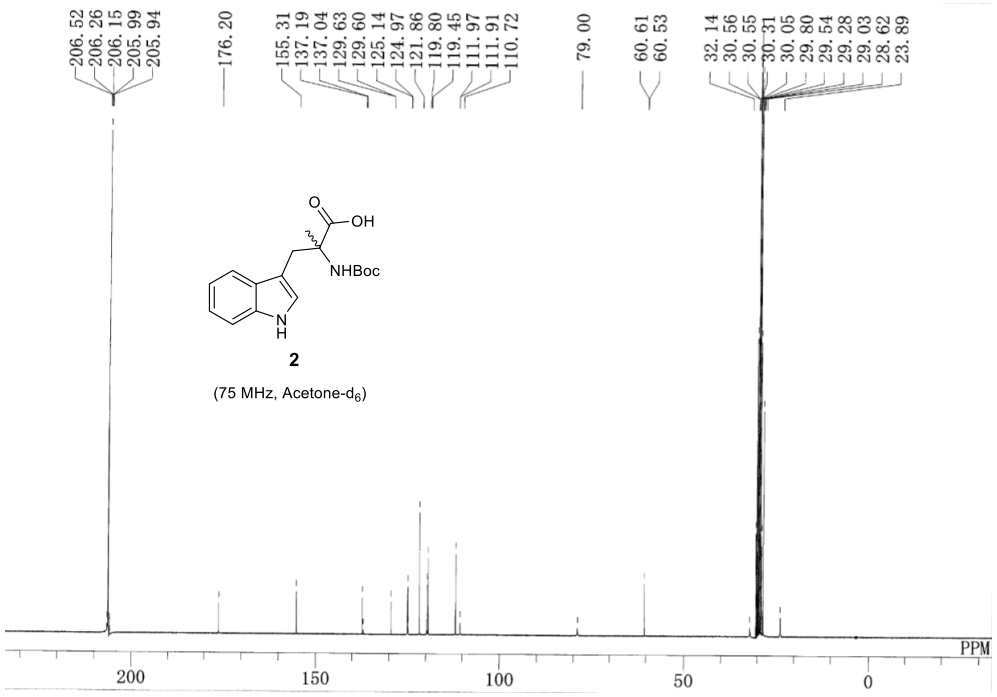

2

(75 MHz, Acetone-d_6)

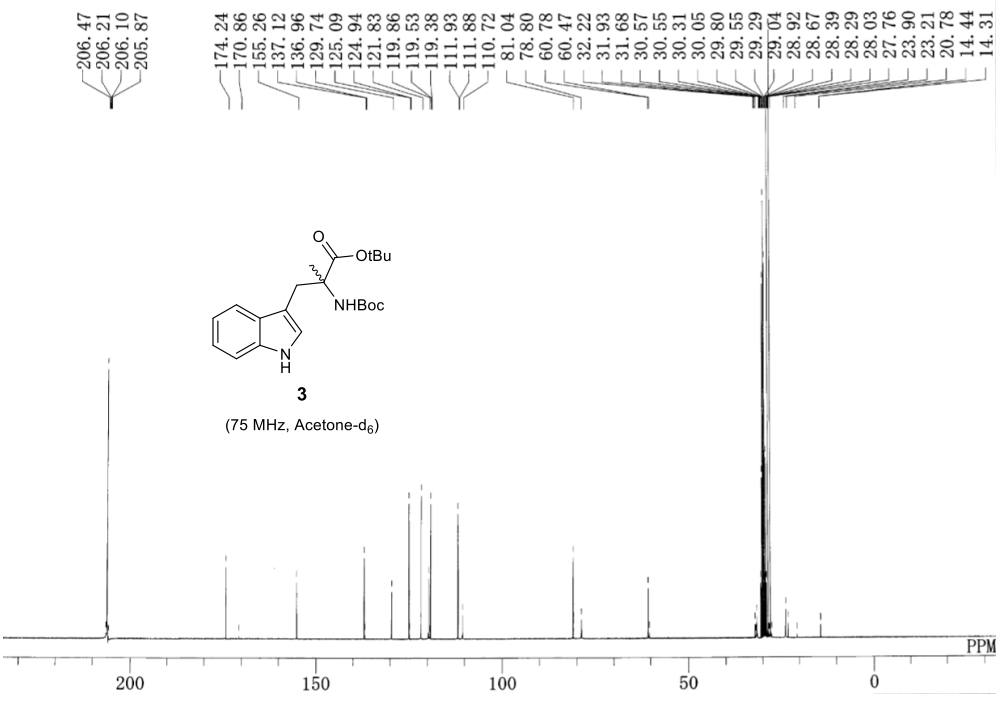

3

(75 MHz, Acetone-d_6)

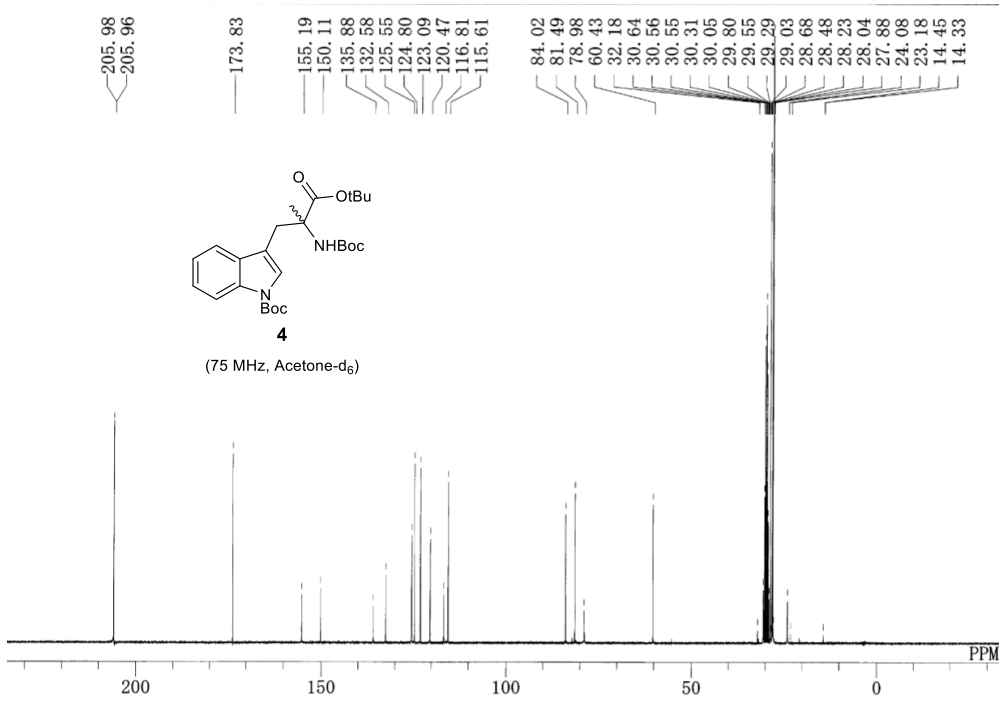

4

(75 MHz, Acetone-d_6)

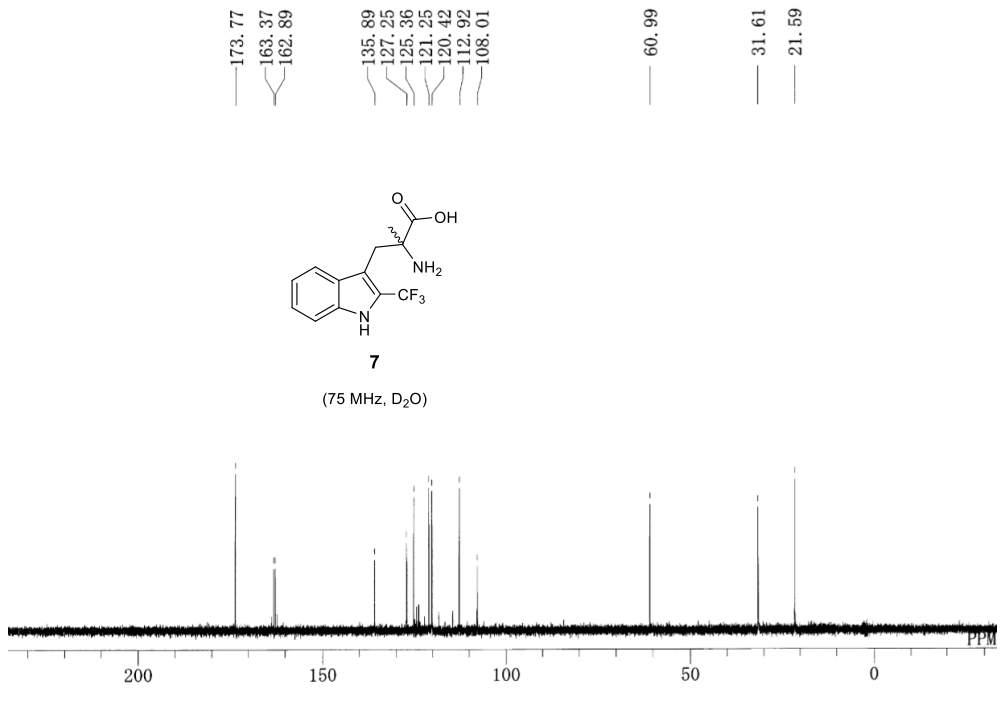

7

(75 MHz, D_2O)

SPECTRAL ANALYSIS RESULTS

^{19}F NMR Spectra

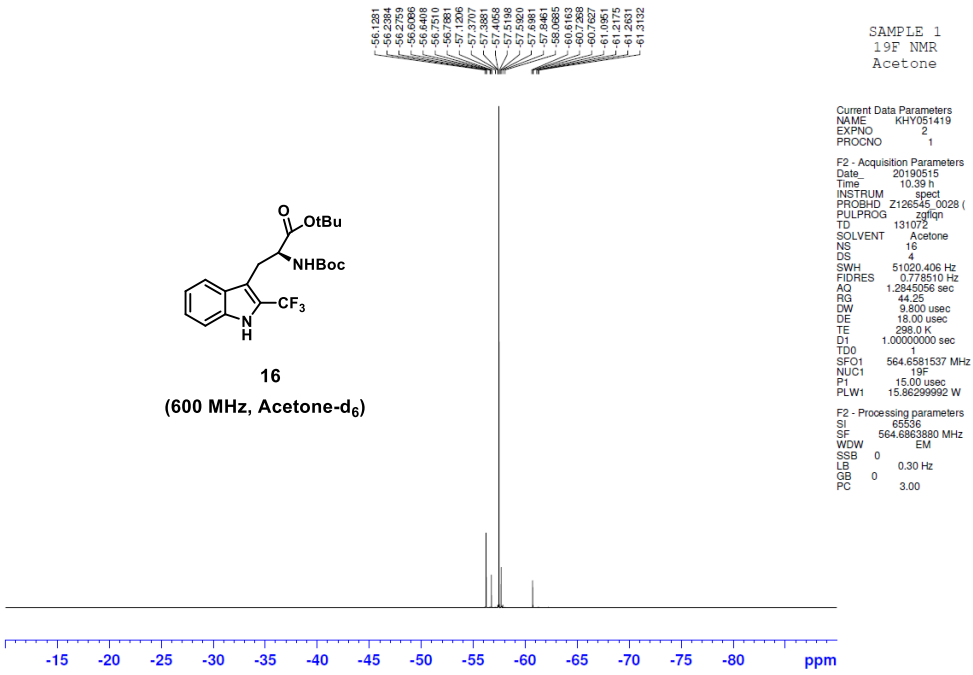

16

(600 MHz, Acetone-d_6)

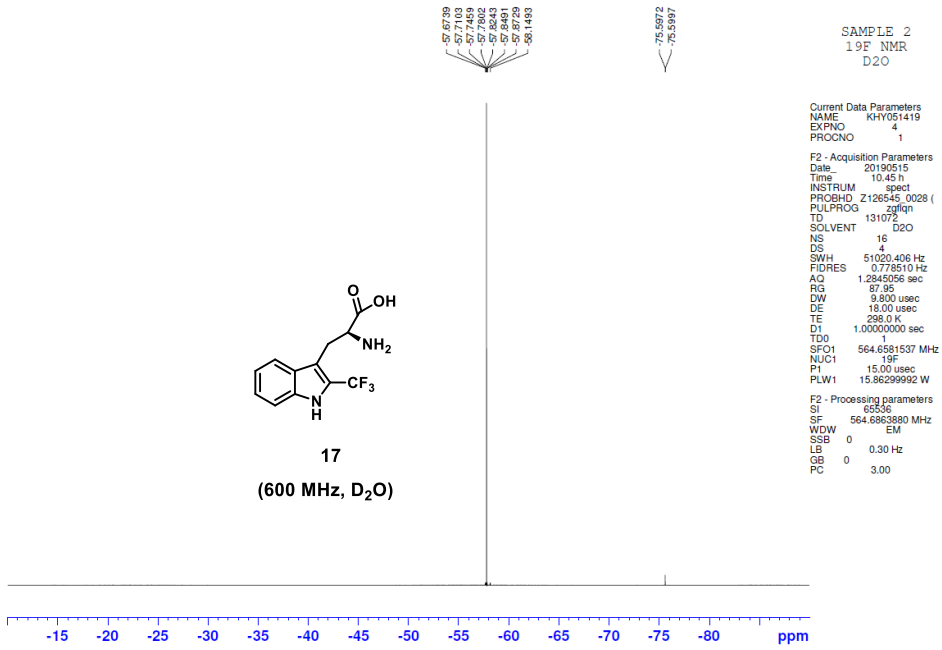
-57.6739
-57.7103
-57.7459
-57.7802
-57.8143
-57.8491
-57.8729
-58.1493
-75.5972
-75.5997
SAMPLE 2
19F NMR
D2O
Current Data Parameters
NAME KHY051419
EXPNO 4
PROCNO 1
F2 - Acquisition Parameters
Date_ 20190515
Time 10.45 h
INSTRUM spect
PROBHD Z126545_0028 (
PULPROG zgflqn
TD 131072
SOLVENT D2O
NS 16
DS 4
SWH 51020.406 Hz
FIDRES 0.778510 Hz
AQ 1.2845056 sec
RG 87.95
DW 9.800 usec
DE 18.00 usec
TE 298.0 K
D1 1.00000000 sec
TD0 1
SFO1 564.6581537 MHz
NUC1 19F
P1 15.00 usec
PLW1 15.86299992 W
F2 - Processing parameters
SI 65536
SF 564.6863880 MHz
WDW EM
SSB 0
LB 0.30 Hz
GB 0
PC 3.00
O
OH
NH2
CF3
N
H
17
(600 MHz, D2O)
-15
-20
-25
-30
-35
-40
-45
-50
-55
-60
-65
-70
-75
-80
ppm

SPECTRAL ANALYSIS RESULTS

Mass Spectra

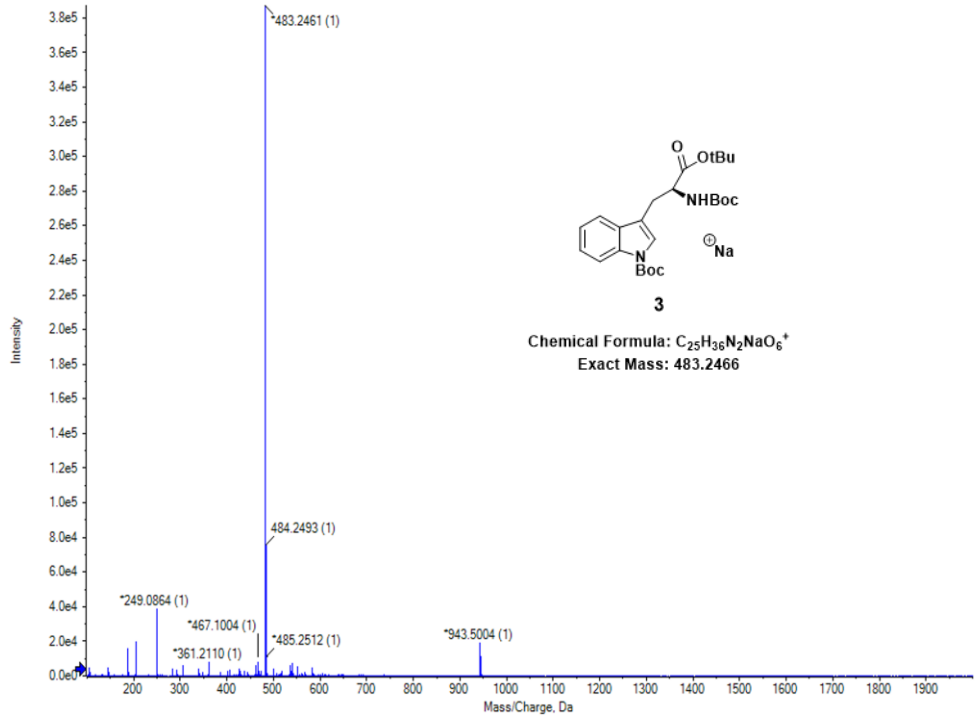
*483.2461 (1)
484.2493 (1)
*249.0864 (1)
*467.1004 (1)
*485.2512 (1)
*361.2110 (1)
*943.5004 (1)
Intensity
Mass/Charge, Da
OtBu
NHBoc
Na
Boc
3
Chemical Formula: C25H36N2NaO6+
Exact Mass: 483.2466

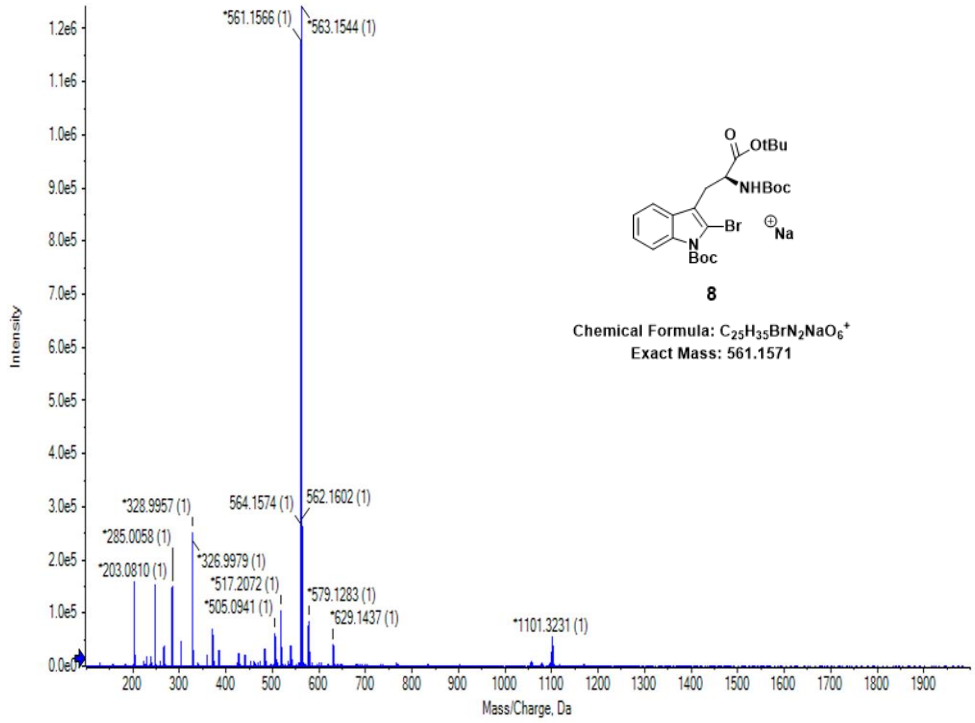
*561.1566 (1)
*563.1544 (1)
*328.9957 (1)
564.1574 (1)
562.1602 (1)
*285.0058 (1)
*326.9979 (1)
*203.0810 (1)
*517.2072 (1)
*505.0941 (1)
*579.1283 (1)
*629.1437 (1)
*1101.3231 (1)
Intensity
Mass/Charge, Da
OtBu
NHBoc
Br
Na
N
Boc
8
Chemical Formula: C25H35BrN2NaO6+
Exact Mass: 561.1571

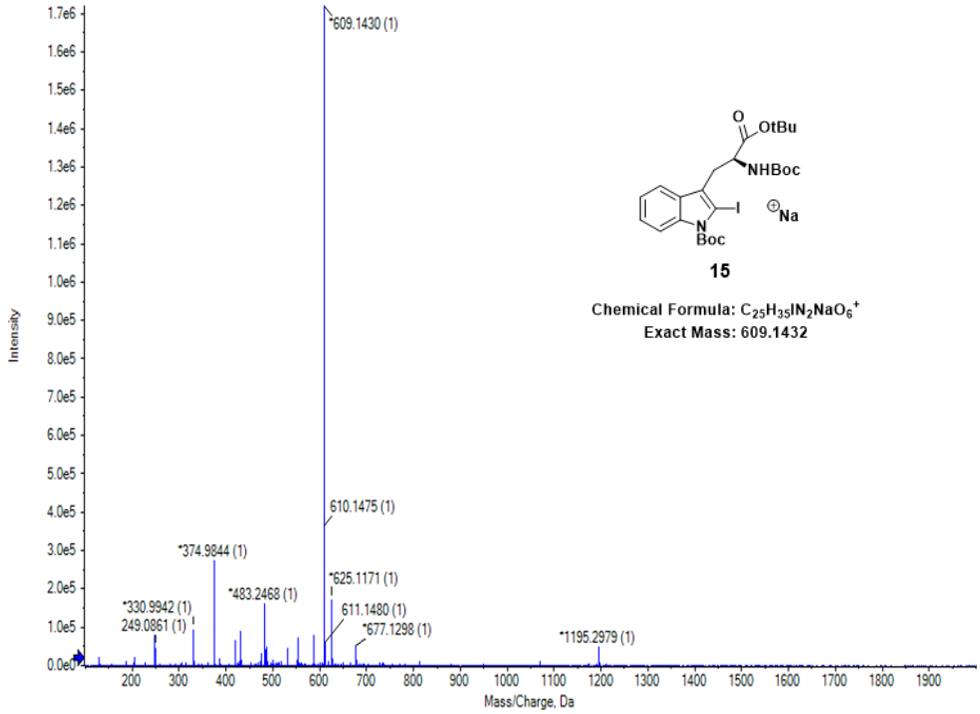
*609.1430 (1)
610.1475 (1)
*374.9844 (1)
*625.1171 (1)
*483.2468 (1)
*330.9942 (1)
249.0861 (1)
611.1480 (1)
*677.1298 (1)
*1195.2979 (1)
Intensity
Mass/Charge, Da
O
OtBu
NHBoc
I
Na
N
Boc
15
Chemical Formula: C25H35IN2NaO6+
Exact Mass: 609.1432

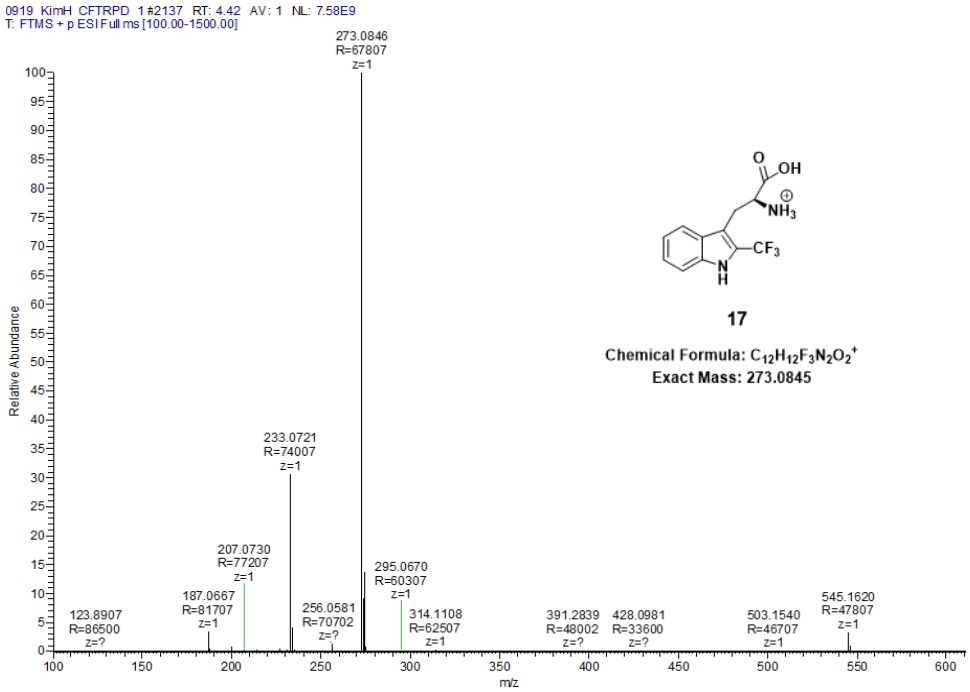

17

Chemical Formula: $C_{12}H_{12}F_3N_2O_2^+$

Exact Mass: 273.0845

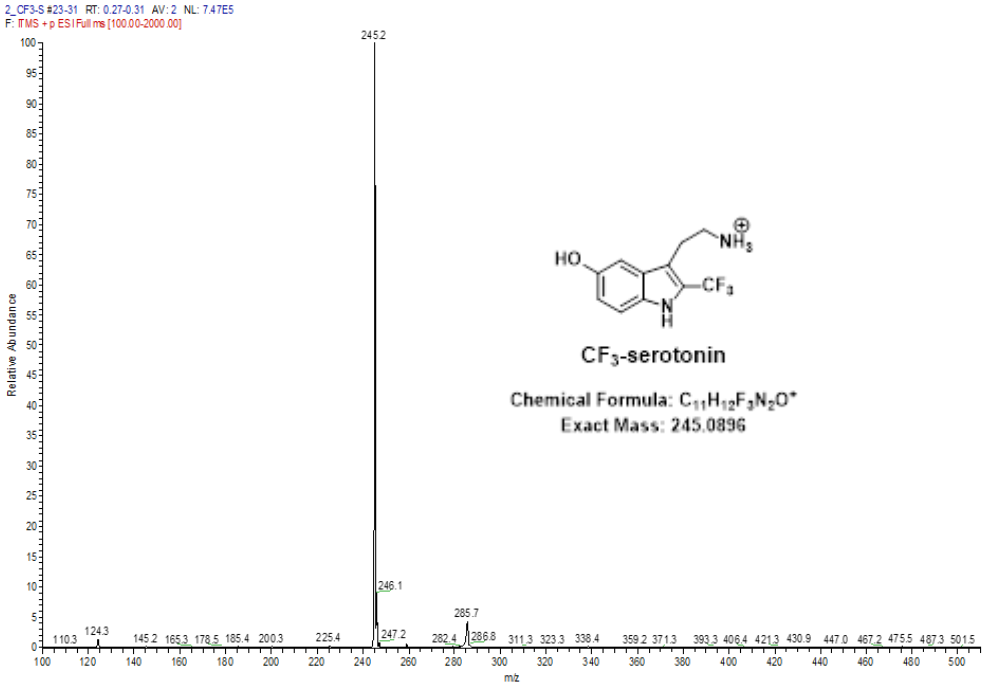
2_CF3-S #23-31 RT: 0.27-0.31 AV: 2 NL: 7.47E5
F: ITMS + p ESI Full ms [100.00-2000.00]
Relative Abundance
m/z
245.2
246.1
285.7
HO
NH3
CF3
N
H
CF3-serotonin
Chemical Formula: C11H12F3N2O+
Exact Mass: 245.0896

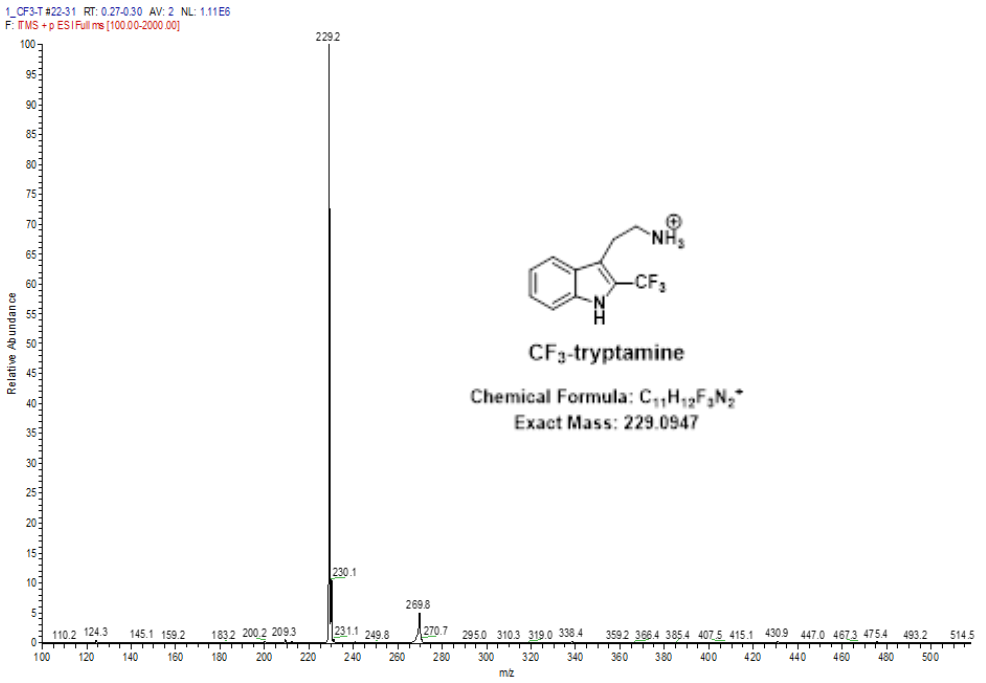
1_CF3-T #22-31 RT: 0.27-0.30 AV: 2 NL: 1.11E6
F: ITMS + p ESI Full ms [100.00-2000.00]
Relative Abundance
m/z
229.2
230.1
269.8
NH3
CF3
N
H
CF3-tryptamine
Chemical Formula: C11H12F3N2+
Exact Mass: 229.0947

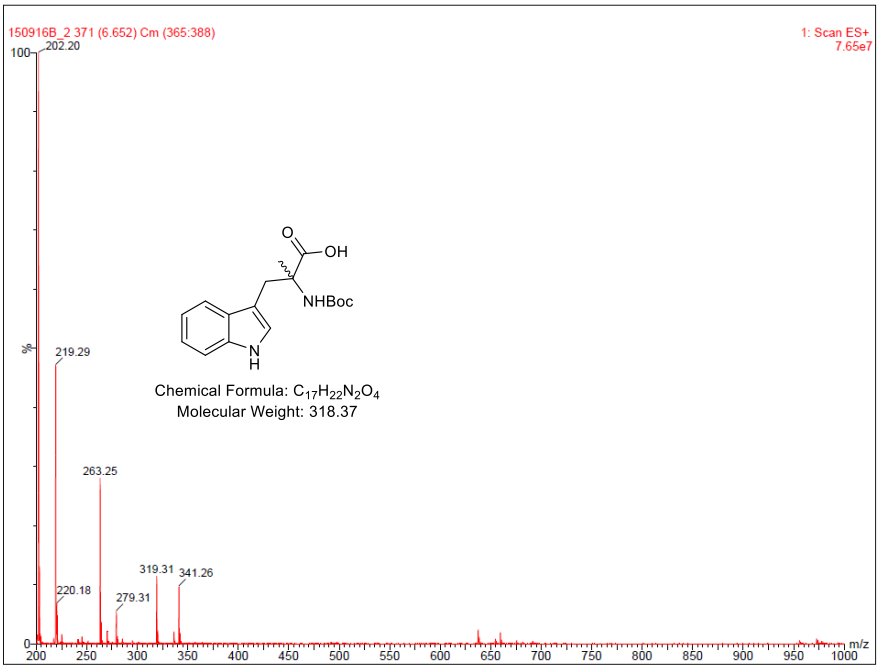
150916B_2 371 (6.652) Cm (365:388)
1: Scan ES+
7.65e7
100
%
0
202.20
219.29
263.25
319.31
341.26
220.18
279.31
O
OH
NHBoc
N
H
Chemical Formula: $C_{17}H_{22}N_2O_4$
Molecular Weight: 318.37
200 250 300 350 400 450 500 550 600 650 700 750 800 850 900 950 1000
m/z

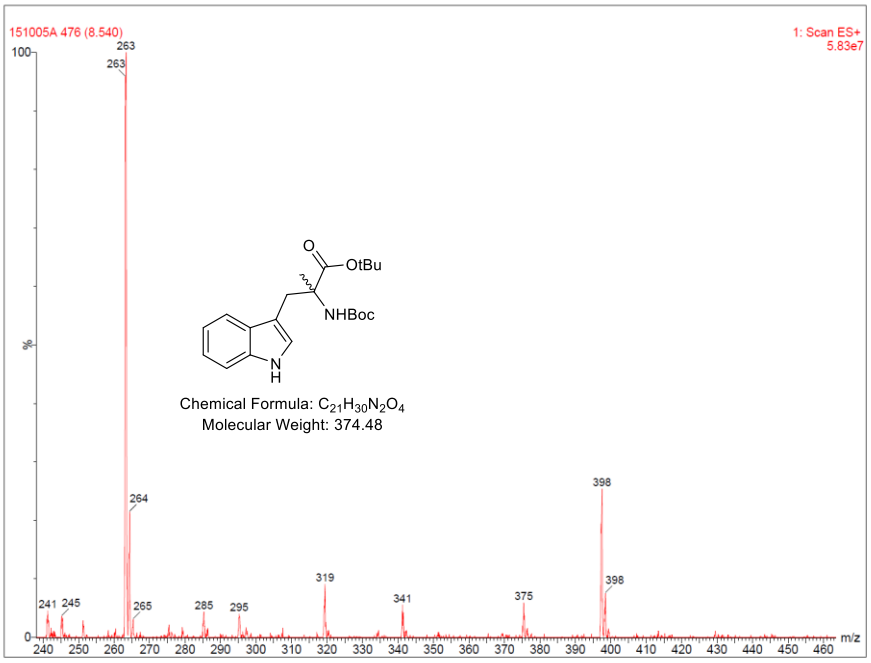
151005A 476 (8.540)
1: Scan ES+
5.83e7
100
%
0
263
263
264
398
398
319
341
375
241
245
265
285
295
O
OtBu
NHBoc
N
H
Chemical Formula: $C_{21}H_{30}N_2O_4$
Molecular Weight: 374.48
240 250 260 270 280 290 300 310 320 330 340 350 360 370 380 390 400 410 420 430 440 450 460
m/z

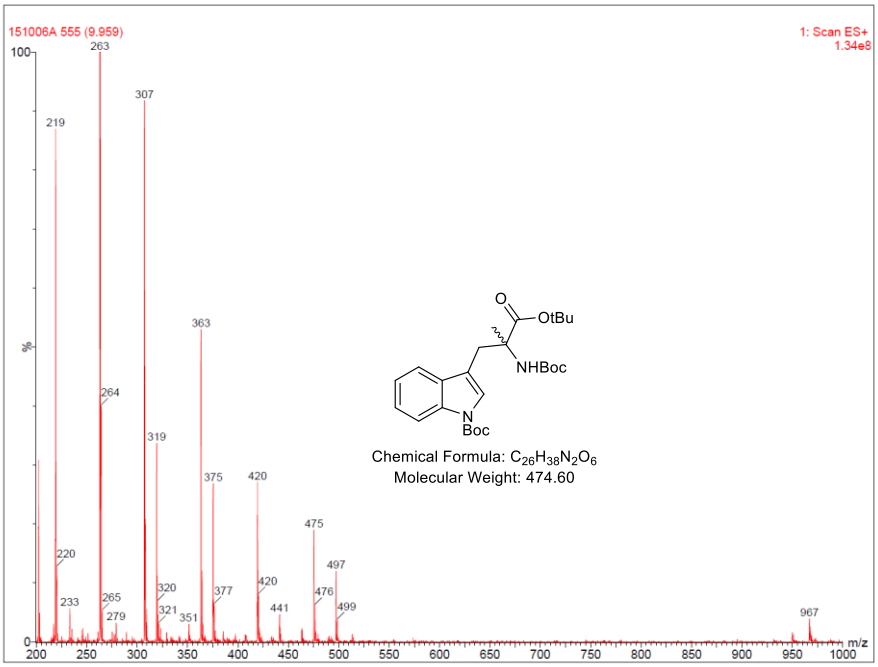
151006A 555 (9.959)
1: Scan ES+
1.34e8
100
%
0
263
307
219
363
264
319
375
420
475
497
220
420
476
233
265
320
377
441
499
279
321
351
967
200 250 300 350 400 450 500 550 600 650 700 750 800 850 900 950 1000
m/z
O
OtBu
NHBoc
N
Boc
Chemical Formula: C26H38N2O6
Molecular Weight: 474.60

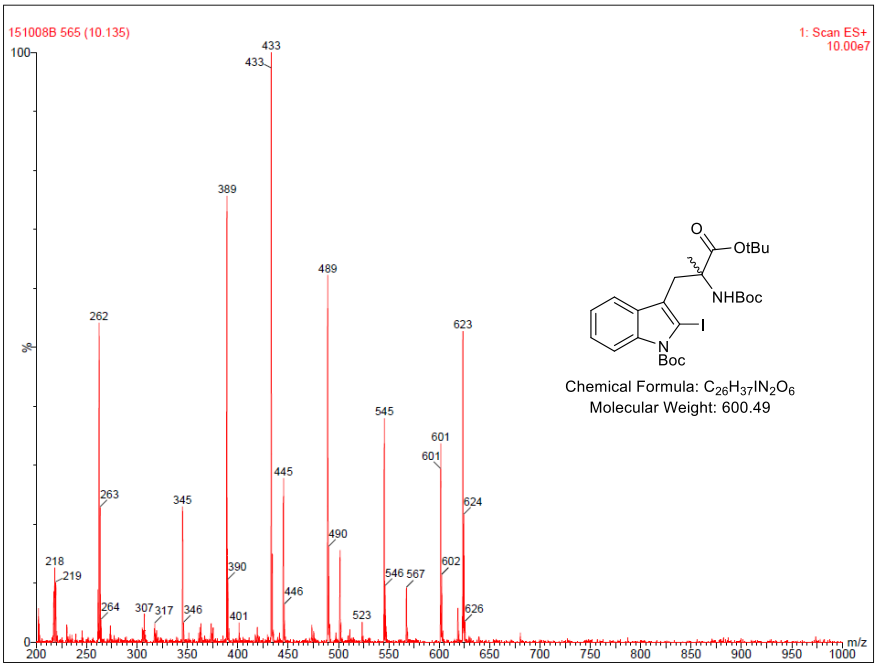
151008B 565 (10.135)
1: Scan ES+
10.00e7
100
%
0
433
433
389
489
262
623
545
601
601
445
624
263
345
490
218
390
546 567
602
219
446
264
307
317
346
401
523
626
200 250 300 350 400 450 500 550 600 650 700 750 800 850 900 950 1000
m/z
O
OtBu
NHBoc
I
N
Boc
Chemical Formula: C26H37IN2O6
Molecular Weight: 600.49

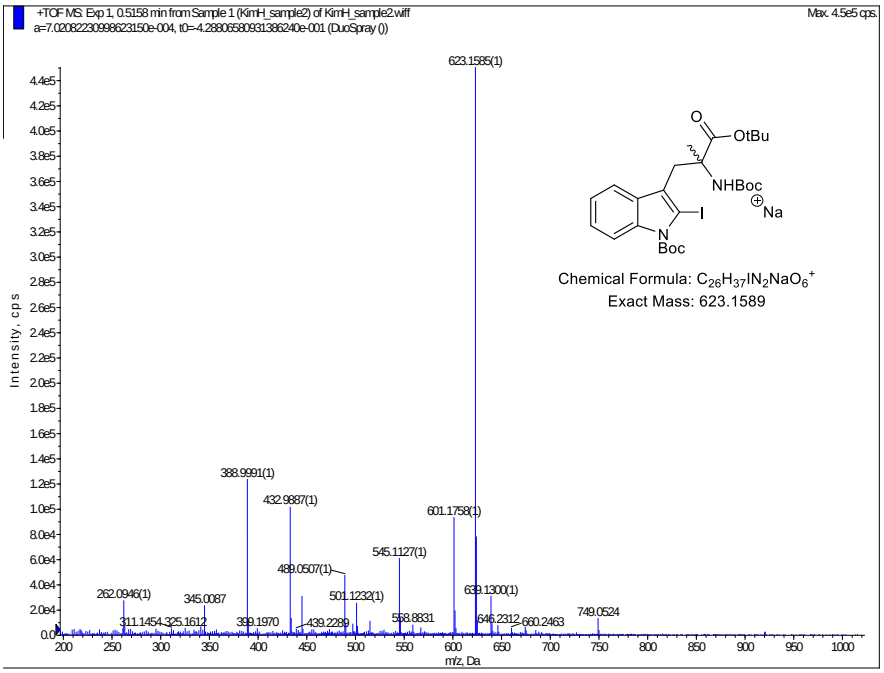
+TOF MS: Exp 1, 0.5158 min from Sample 1 (KimH_sample2) of KimH_sample2.wiff
a=7.020822309982315 0e-004, t0=-4.288065809313862 40e-001 (DuoSpray ())
Max. 4.5e5 cps.
Intensity, cps
m/z, Da
623.1585(1)
388.9991(1)
432.9887(1)
601.1758(1)
545.1127(1)
489.0507(1)
501.1232(1)
639.1300(1)
262.0946(1)
345.0087
311.1454
325.1612
399.1970
439.2289
568.8831
646.2312
660.2463
749.0524
OtBu
NHBoc
Na
I
N
Boc
Chemical Formula: C26H37IN2NaO6+
Exact Mass: 623.1589

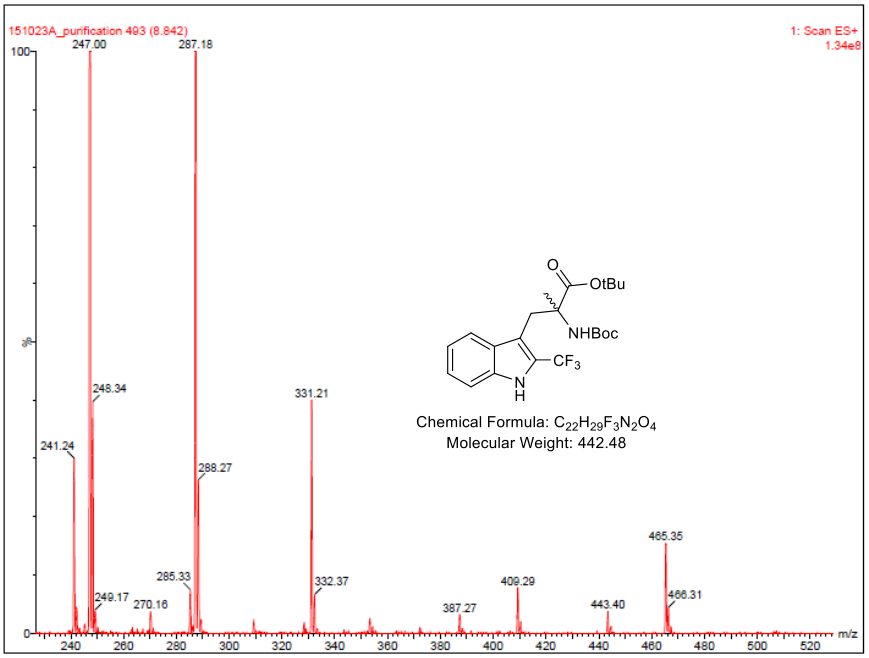
151023A_purification 493 (8.842)
1: Scan ES+
1.34e8
%
m/z
247.00
287.18
248.34
241.24
331.21
288.27
285.33
249.17
270.16
332.37
387.27
409.29
443.40
465.35
466.31
OtBu
NHBoc
CF3
N
H
Chemical Formula: C22H29F3N2O4
Molecular Weight: 442.48

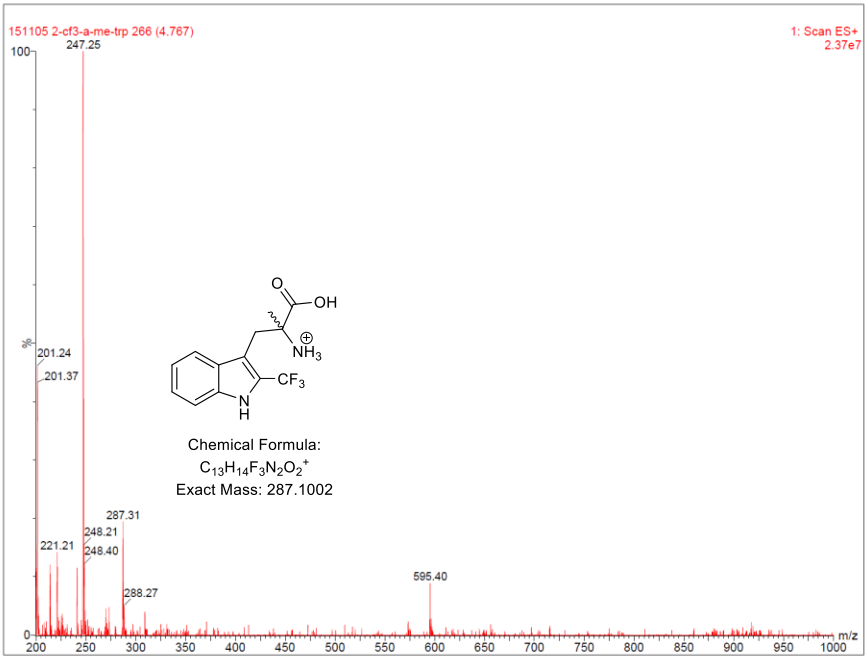
151105 2-cf3-a-me-trp 266 (4.767)
1: Scan ES+
2.37e7
247.25
201.24
201.37
287.31
248.21
248.40
221.21
288.27
595.40
m/z
Chemical Formula:
$C_{13}H_{14}F_3N_2O_2^+$
Exact Mass: 287.1002

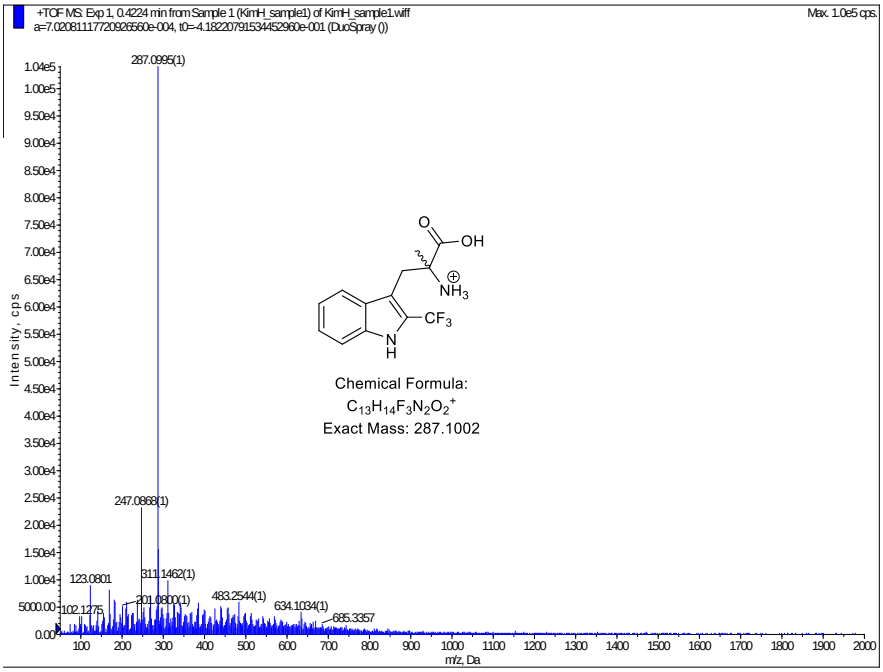
+TOF MS: Exp 1, 0.4224 min from Sample 1 (KimH_sample1) of KimH_sample1.wiff
a=7.020811177209265 60e-004, t0=-4.182207915344529 60e-001 (DuoSpray ())
Max. 1.0e5 cps.
Intensity, cps
287.0995(1)
247.0868(1)
123.0801
311.1462(1)
201.0800(1)
483.2544(1)
634.1034(1)
685.3357
102.1275
m/z, Da
Chemical Formula:
$C_{13}H_{14}F_3N_2O_2^+$
Exact Mass: 287.1002

국 문 초 록

^{18}F-표지 트립토판 유도체를 이용한 세로토닌 대사 PET 영상제 개발

김 호 영

서울대학교대학원

의학과 핵의학전공

목적:

세로토닌 신경계는 우울증, 사회적 불안 장애 및 간질과 같은 중추 신경계의 다양한 기능 장애와 연관이 있다. 그러므로 세로토닌의 합성을 영상화할 수 있는 방사성 프로브의 개발은 그러한 질병의 진단에 중요하다. α-[^{11}C]메틸트립토판 ([^{11}C]AMT)은 세로토닌 합성 영상에 이용

가능한다. 그러나 [^{11}C]AMT 의 뇌 내 섭취는 세로토닌 대사 뿐만 아니라 키뉴레닌 대사 또한 반영할 수 있으므로 잘못된 정보를 제공할 수 있다. 또한 트립토판은 뇌에서 빠르게 제거되기 때문에 뇌에서의 머무름 시간을 연장시키고 모노 아민 산화 효소 (MAO)에 의한 대사를 감소시키기 위해 α-메틸화가 필요하다. 본 연구에서는 구리(I)를 매개로 한 [^{18}F]트리플루오로메틸화를 이용해 인돌 고리의 2 번 위치에 ^{18}F을 표지하여 세로토닌 대사만을 반영할 수 있는 [^{18}F]트리플루오로메틸-L-트립토판 ([^{18}F]CF_3-L-Trp)과 [^{18}F]트리플루오로메틸-L-α-메틸트립토판 ([^{18}F]CF_3-L-AMT)을 설계하고 개발하려고 하였다. 또한 세로토닌 영상화를 위한 표지된 트립토판 유도체의 가능성을 평가하기 위하여 쥐의 뇌 내 분포와 대사를 조사하였다.

방법:

[^{18}F]CF_3-L-Trp 또는 [^{18}F]CF_3-L-AMT의 전구체는 팔라듐 또는 수은 촉매를 이용한 위치 선택적 요오드화를 통해 합성하였다. [^{18}F]트리플로오로 메틸기는 methyl chlorodifluoroacetate와 tetramethylethylenediamine를 넣고 구리 촉매 하에서 150°C에서 15 분간 반응하여 도입할 수 있었고, 이 후 보호기는 1 N 염산 수용액을 넣고 100°C에서 10 분간 반응하여 제거하였다. 반응 혼합물은 HPLC를 이용하여 정제하였고, 분리된 [^{18}F]CF_3-L-Trp의 방사화학적 확인 및 순도와 이성질체 확인 및 순도는 분석용 HPLC로 확인하였다. 생체 내 분포는 정상 BALB/c 마우스에서 마취 없이 [^{18}F]CF_3-L-Trp를 주사한 후 10, 60 및 120 분에 확인하였고, 자가방사기록은 SD 랫에서 주사 후 10 분째에 확인하였다. PET 영상 역시 SD 랫에서 얻었으며, 마취 없이 [^{18}F]CF_3-L-

Trp를 주사한 후 5, 10, 20, 40 및 80 분에 쥐를 희생시키고 뇌를 추출하여 영상을 얻었다. 대사체 연구는 비방사성 CF_3-L-Trp를 BALB/c 마우스에 투여한 후 10 분 및 60 분째에 뇌, 혈액, 및 소변에서 샘플을 얻어 HPLC와 LC/MS를 이용해 분석하였다. 세로토닌 대사가 증진된 SD 랫에서 [^{18}F]CF_3-L-AMT의 뇌 분포 및 대사를 평가하기 위해 염화 리튬을 하루 2 회 5일간 85 mg/kg을 복강주사로 SD 랫에 투여하였다.

결과:

보호된 L-Trp및 브롬화와 요오드화 유도체를 이용해 [^{18}F]트리플루오로메틸화 반응을 수행하였고, 요오드화 유도체가 가장 높을 표지 효율을 보였다. 표지 후, 산에 불안정한 보호기를 1 N 염산 수용액을 사용하여 동시에 제거하였고, 반응 혼합물은 HPLC로 정제하였다. 방사 화학적 수율을 분리된 생성물을 기준으로 6±1.5%였으며, 방사 화학적 순도는 99% 이상이었고 [^{18}F]CF_3-L-Trp의 머무름 시간은 합성한 표준물질과 동일하였다. 몰당 비방사능은 [^{18}F]CF_3-L-Trp가 0.44–0.76 GBq/μmol이고 [^{18}F]CF_3-L-AMT가 0.94–1.46 GBq/μmol으로 친핵성 치환반응으로 합성한 ^{18}F−표지된 화합물보다는 비교적 낮지만 생체 내 적용을 하기에는 충분하였다. 거울상 이성질체 확인 및 순도는 키랄 HPLC에 의해 측정되었고 다른 이성질체는 발견되지 않았다. 10 분에 생체 분포에서 [^{18}F]CF_3-L-AMT와 [^{18}F]CF_3-L-Trp의 뇌 섭취량은 각각 2.27 ± 0.14%ID/g와 2.06 ± 0.22%ID/g 이었고 [^{18}F]CF_3-L-AMT의 뇌 섭취 (0.73 ± 0.08%ID/g)는 [^{18}F]CF_3-L-Trp (0.43 ± 0.08%ID/g)보다 60 분에서 유의하게 높았다. 이 결과는 α−메틸화가 MAO에 의한 대사를 감소시킴으로써 두뇌의 보유를 증가 시킨다는 것을 나타냈다. 60 분

(4.50 ± 0.47%ID/g)에서 [^{18}F]CF_3-L-AMT의 골 흡수는 [^{18}F]CF_3-L-Trp (9.34 ± 0.62%ID/g)의 골 흡수보다 현저히 낮았으며 두 화합물 모두 신장에서 높은 섭취를 보였다. PET 및 자가방사기록에서, 솔기핵 (지느러미 및 내측)의 섭취는 비교적 매우 낮았다. 대신 송과선, 시상, 시상 하부 및 중뇌는 특히 높은 섭취량을 보였다. [^{18}F]CF_3-L-Trp는 L형 아미노산 수송체를 통해 혈뇌장벽을 투과하였고 [^{18}F]CF_3-D-Trp는 투과하지 못하였다. 대사체 연구에서는 60 분에 뇌와 혈액에서 CF_3-serotonin의 피크가 검출되었고, LC-MS를 통해 CF_3-serotonin의 질량 값을 확인함으로써 뇌 및 혈액 내에서 CF_3-L-Trp이 CF_3-serotonin로 대사되는 것을 증명하였다. 리튬 처리 한 SD 래트 뇌에서의 [^{18}F]CF_3-L-AMT의 분포 패턴은 정상 SD 랫 뇌와 유사하였다. 그러나 리튬 처리한 SD 래트에서 [^{18}F]CF_3-L-AMT 의 뇌 흡수율은 정상 SD 랫보다 약 10 분 더 빨리 최고 농도에 도달하였고, 리튬 처리된 SD 랫트에서의 뇌 섭취는 정상 SD 랫보다 더 오래 지속되었다.

결론:

본 연구에서, 구리를 촉매로 한 [^{18}F]트리플루오로메틸화를 이용해 성공적으로 [^{18}F]CF_3-L-Trp를 합성할 수 있었고 2 번 위치의 ^{18}F은 이 물질이 세로토닌 대사에 특이적으로 작용할 수 있도록 하였다. 하지만 뇌에서의 빠른 배출과 높은 생체 내 탈 불소화는 [^{18}F]CF_3-L-Trp가 세로토닌을 영상화하는데 적합하지 않음을 보여 주었다. 트립토판의 α-메틸화는 대사를 줄임으로써 뇌의 머무름 시간을 증가시켰으며 생체 내 탈 불소화를 감소시켰다. 하지만 낮은 솔기핵 섭취는 [^{18}F]CF_3-L-AMT의 PET 영상이 세로토닌 대사를 반영하는 지를 불분명하게 하였다. 또한

뇌에서의 [^{18}F]CF_3-L-AMT가 대사되지 않은 채 남아있음으로써 대사된 것과 대사되지 않을 것을 구분하기 어렵게 하여 절대적인 세로토닌 합성 속도 얻는 것을 어렵게 하였다. 그럼에도 불구하고 실험 결과들은 정상 및 리튬 처리된 SD 랫에서 [^{18}F]CF_3-L-AMT의 분포 패턴이 세로토닌 작용 및 대사와 관련이 있음을 시사하였다. 따라서 [^{18}F]CF_3-L-AMT는 세로토닌 대사를 영상화할 수 있는 PET 영상제로 사용될 가능성이 있으나 더 많은 검증이 필요하다.

주요어: [^{18}F]트리플루오로메틸화; CF_3-L-Trp; 세로토닌; 5-HT; 트립토판; 아미노산; 모노 아민 산화 효소; α-메틸트립토판.

학번: 2011-31118